A MORPHOLOGICAL AND SEDIMENTOLOGICAL ANALYSIS OF ROGEN MORAINE ON THE AVALON PENINSULA, NEWFOUNDLAND

ANDREA S. MARICH

A MORPHOLOGICAL AND SEDIMENTOLOGICAL ANALYSIS OF ROGEN MORAINE ON THE AVALON PENINSULA, NEWFOUNDLAND

by

Andrea S. Marich

A thesis submitted to the

School of Graduate Studies

in partial fulfillment of the

requirements for the degree of

Master of Science

Department of Geography
Memorial University of Newfoundland

September 2006

St. John's Newfoundland

Abstract

This thesis re-examines the glacial landscape of the central Avalon Peninsula, Newfoundland, Canada. Specifically, it focuses on an area of moraine ridges, previous studies of which have generated conflicting interpretation of genesis and deglacial significance. For instance, it has been interpreted as a series of recessional moraines, and as a field of Rogen moraines. In light of new developments in our understanding of subglacial landscape processes, and in the available technology for mapping and analysis of digital topographic data, it is an appropriate time to re-analyse this landscape and evaluate past interpretations.

Several methods of data acquisition were employed for this study; air photo interpretation of black and white photos at the 1:50 000 scale and colour photos at the 1:12 500 scale, field research including a review of the sedimentology of the moraine ridges, the construction of a Digital Elevation Model (DEM) for a portion of the study area, and the calculation of moraine ridge orientation within a GIS.

The moraine ridges of the central Avalon Peninsula are considered to be classical examples of Rogen moraine. An examination of the moraine field using the 1: 5000 scale digital elevation model (DEM) with an elevation resolution between 5 and 10 m revealed a suite of glacial landforms, including Rogen moraine, hummocky moraine, flutes, meltwater channels and large streamlined bedrock ridges. Rogen and hummocky moraine were found in close association with each other and represent end members of a transitional landform assemblage, with neither landform overprinting the other. An examination of the internal composition of both Rogen and hummocky moraine revealed

similar sediments and structures that suggest deposition via melt-out and sediment gravity flows. The sediment within Rogen moraines and hummocky moraines was transported and deposited subglacially, and later melted out of stagnating ice.

The timing of glacial events on the Avalon Peninsula are difficult to constrain, but the internal composition and morphology of the Rogen moraines suggest that they were formed during deglaciation. During this phase the ice centre shifted from over the central Avalon Peninsula to the head of St. Mary's Bay. Ice flow out of St. Mary's Bay was radial, with the dominant ice flow direction being in the northeastward direction, and a secondary ice flow northwards into Trinity Bay. The final deglaciation of the Avalon Peninsula is constrained by the C^{14} date of 10 100 +/- 250 y BP, from pollen in basal pond sediments.

The predominant hypotheses of Rogen moraine formation found in the literature were examined in the context of the Avalon Rogen moraines, but currently it is difficult to use any of these previous developed ideas to explain the formation of Rogen moraine on the Avalon Peninsula.

Acknowledgements

Although this thesis bears only my name, it is only with the help of many individuals was I able to complete it. Firstly, thanks goes to my field assistants, Christa Quilty, Heather Hickman, Stacy Campbell, Mariana Trindade, Jennifer Bose, Tim Hollis and Zack Bartlett, all with the Department of Geography, Memorial University of Newfoundland, whose hard work, and long hours spent clearing sections and measuring clast fabrics is greatly appreciated. Jeff Wood, Surveys and Mapping Division, Department of Environment and Conservation, provided the digital data for the DEM, while Larry Nolan and Dave Taylor, Geochemistry, Geophysics and Terrain Sciences Section, Department of Natural Resources, provided additional digital data. Thanks also go to Dave Liverman and Shirley McCuaig of the Geochemistry, Geophysics and Terrain Sciences Section for their discussion of Rogen moraine and related glacial processes.

The funding for this project was provided by a Natural Sciences and Engineering Research Council of Canada (NSERC) grant to Dr. Trevor Bell. Field assistance was funded through the Summer Career Placement Program of Human Resources and Skills Development Canada. I would also like to acknowledge receipt of a Memorial University of Newfoundland graduate student fellowship.

I would like to thank my supervisor, Dr. Trevor Bell, for his support and guidance, I appreciate that he let me go off and reach my "state of most confusion" before reeling me back in. I have learned so much because of it. Thanks to Dr. Martin Batterson, with whom I have spent many hours discussing glacial processes within and outside the realm of Rogen moraine, and who was always available to lend an ear when I was confused, or frustrated with the project. I always left his office feeling excited about the work I was

doing. Thanks also go out to the third member of my supervisory committee, Dr. Alvin Simms. Dr. Simms's GIS expertise and sense of humour made what could have been extremely tedious work with digital data, much more bearable.

Beyond this, I have received much emotional support from my friends and family. Fellow graduate students in the Department of Geography at MUN have been great friends, and have helped guide me through the rough spots. I'm sure there isn't a single geography grad that doesn't know at least a little about Rogen moraines, and for that I apologize profusely. Heartfelt thanks for the support I have received from my parents, David and Karen, and my brother Michael, who have always encouraged me in everything I do, even if it involves moving half way across the country. Without their help I'm not sure I could have made it this far.

TABLE OF CONTENTS

LIST OF TABLES

LIST OF FIGURES

Chapter 1 Introduction

This thesis re-examines the glacial landscape of the central Avalon Peninsula, Newfoundland. Of particular interest is a field of distinctive moraine ridges that occupy much of the area. Previous work has lead researchers to classify the moraines as recessional moraines (Henderson, 1972), and as Rogen moraines (Rogerson and Tucker, 1972; Fisher and Shaw, 1992). It has been discovered that Rogen moraines occupy large areas of previously glaciated terrain, but to date the community of researchers involved are divided as to how these landforms should be interpreted. Although it is unclear how Rogen moraines may be used to reconstruct the glacial events that occurred in a particular area, they are generally thought to form subglacially, and likely indicate a melted-bed or a poly-thermal basal ice regime (Carl, 1978; Shaw, 1979; Aario, 1987; Aylsworth and Shilts, 1989; Bouchard, 1989; Hättestrand, 1997; Knight and McCabe, 1997; Knight, 2002; Dunlop, 2004, Möller, 2005).

The understanding of the subglacial environment has progressed substantially over the past decade or so and one major advancement has been the discovery that many glaciers are situated upon a bed of sediment that can be deformed and mobilized. This is in contrast to the previous idea that glaciers form directly upon the underlying bedrock. The catalyst for this change in ideas was the discovery of extremely high flow velocities (up to 825 m/year) along low surface slopes from Ice Stream B of the West Antarctic ice sheet onto the Ross Ice Shelf (Murray, 1997). With this new discovery regarding the subglacial environment, much emphasis has been placed on research concerning

subglacial landforms, and the importance of such landforms to the interpretation of glacial events.

The field of moraines on the central Avalon Peninsula is considered to be a classic example of well-developed Rogen moraines (Fisher and Shaw, 1992; c.f. Hättestrand, 1997;) and recently new data for the area has been acquired. Digital topographic data as well as increased access to the sediments within the Rogen moraine ridges has allowed for the re-examination of this field of Rogen moraines, and the results have been used to assess the validity of the conflicting ideas of Rogen moraine formation found in the literature.

There are several groups of ideas concerning the formation of Rogen moraine; 1) Lundqvist (1969, 1981, 1989) and Hättestrand (1997) have suggested that Rogen moraines were formed as debris was squeezed into subglacial crevasses. Crevassing occurs in similar wavelengths to Rogen moraine spacing and it was postulated that the weight of the overlying ice would cause sediment to flow into the crevasses (Lundqvist, 1969). Hättestrand (1997), in an attempt to explain the wide range of Rogen moraine characteristics, has suggested that basal crevassing can lead to the break up of the subglacial debris rich horizon as basal ice thaws, and melt-out preserves ridges of debris. 2) A second group of ideas suggests that Rogen moraines are formed as slabs of debris rich basal ice that are thrust up onto one another, followed by regional stagnation (Shaw, 1979; Bouchard, 1989; Ayslworth and Shilts, 1989). 3) Rogen moraine formation resulting from an instability within the subglacial environment (such as factors that alter the flow, erosion, and deposition of subglacial till) has also been suggested (Carl, 1978; Aario, 1987; Dunlop, 2004). As with any natural system, the processes within the

subglacial environment respond to disturbances to restore the systems equilibrium. In the subglacial environment anything that alters the flow, erosion and deposition of subglacial till can be considered an instability. Within the subglacial environment an instability was proposed as a general model of Rogen moraine formation because instabilities create the same patterns repeatedly over large areas (Dunlop, 2004). 4) Massive subglacial meltwater floods have also been theorized to form a range of subglacial landforms including Rogen moraine (Fisher and Shaw, 1992; Shaw, 2002). In this hypothesis a massive subglacial sheet flood erodes cavities into the underside of a glacier and subsequently deposits sediments into these cavities. 5) Finally, Boulton (1996) described the transition of Rogen moraine to drumlins as a result of the deformation and reworking of previously deposited sediments by a change in ice flow direction.

In order to address these hypotheses of Rogen moraine formation as well as the newly acquired data for the study area, several research goals were devised and they include: 1) the completion of an in-depth assessment of the morphological characteristics of the Rogen moraine ridges of the central Avalon Peninsula; 2) an examination of the glacial landform associations present in the study area; 3) an inspection of the potential processes and environments involved in the development of the Rogen moraines; and 4) a discussion of the timing of glacial events related to the formation of landforms in the central Avalon peninsula, to develop a relative chronology, and, if possible, to attach relative dates to the events.

This study consists of several research methods including: an in-depth interpretation of aerial photographs; a review of the sedimentology of the Rogen

moraines; as well as the construction and interpretation of a digital elevation model (DEM) created from the newly acquired digital topographic data.

The thesis is therefore organized to reflect the research goals as well as the results of the research methods. It begins with an introduction to Rogen moraines including descriptions from previous work, and summaries of the leading hypotheses of Rogen moraine formation.

The following sections describe the glacial history of the Avalon Peninsula as well as the links between it and the main portion of the island of Newfoundland. The description of the study area includes a brief overview of the bedrock and surficial geologies. The research goals or questions are then listed in detail, followed by a description of the methodologies and rationale for choosing them. The results obtained from each of the methods are described and discussed, and discussions and interpretations are made. The final section of the thesis re-evaluates the hypotheses of Rogen moraine formation in the context of this new data and makes suggestions as to which hypotheses may be applicable to the Avalon Peninsula.

To conclude, the purpose of this study was to add new information to the breadth of knowledge concerning Rogen moraines, as well as to increase the understanding of the glacial processes that occurred on the central Avalon Peninsula.

Chapter 2 Introduction to Rogen moraines

2.1 Introduction

This chapter serves as an introduction to Rogen moraines, and to the central Avalon Peninsula, which is the focus of this research. It begins with a description of Rogen moraines, their global distribution, and discusses the conflicting ideas of Rogen moraine formation. A discussion of Rogen moraine in Newfoundland and Labrador follows, as well as a brief review of the ideas concerning glaciation of the island and the Avalon Peninsula. The bedrock and surficial geology of the study area is described in detail. Finally the research aims and rationale are listed.

2.2 Rogen moraines

The term Rogen moraine was first applied by Hoppe (1959) to describe the set of transverse ridges in the Lake Rogen area of Sweden. Lundqvist (1969, 1981) has since proposed that the term "Rogen" only be used to describe fields of moraines that exhibit drumlinization of ridges, and/or a transition to drumlins. This transition does not always occur, and therefore other terminology has been proposed for landforms that are similar to Rogen moraines, but lack the transitional forms. Hughes (1964), for example, used the term "ribbed" moraine to describe a set of ridges near Nichicun-Kaniapiskau Québec, which in plan view looked similar to a rib cage (Hughes, 1964; Carl, 1978; Bouchard *et al.*, 1989; Dunlop, 2004). Another term includes washboard moraines (Mawdsley, 1936).

The classic form of Rogen moraine is a set of evenly spaced ridges oriented transverse to glacial flow. Individual Rogen moraine ridges are sinuous, commonly

anastomosing and branching (Lundqvist 1969, 1981, 1987, 1997). They are concave down-ice and asymmetrical with steeper distal slopes. Rogen moraine ridges within a tract are generally the same height (Aylsworth and Shilts, 1989; Hättestrand, 1997, Hättestrand and Kleman, 1999). The moraines range from 10 to 30 m high, 50 to 200 m wide, 300 to 1200 m long, and are spaced 100 to 300 m apart (Lundqvist, 1989; Hättestrand, 1997). The largest Rogen moraines discovered to date are in Ireland, and they range from 0.5 to 2.5 km long, 15 to 35 m high, and 100 to 450 m wide (Knight and McCabe, 1997, Knight, 2002; Dunlop, 2004).

2.2.1 Global distribution of Rogen moraine

Rogen moraine is a conspicuous landform that occurs within glaciated terrain throughout the Northern Hemisphere. Rogen moraines occur as a group of ridges organized into fields or tracts, commonly located within several hundred kilometres of former ice divides (Lundqvist, 1969, 1989, 1997; Aario, 1987; Hättestrand, 1997). They have been identified in Scandinavia, (Lundqvist 1969, 1981, 1987, 1997; Shaw, 1979; Hättestrand, 1997, Hättestrand and Kleman, 1999) Canada (Hughes, 1964; Aylsworth and Shilts, 1989; Bouchard, 1989; Fisher and Shaw, 1992), the United States (Carl, 1978), and Ireland (Knight and McCabe, 1997; Dunlop, 2004) (Figure 2.1). The Irish examples were identified from satellite imagery, where a previously unrecognized distinct pattern of ridge alignment was observed (Knight and McCabe, 1997).

Rogen moraines have been most commonly observed within topographic depressions (Hughes, 1964; Lundqvist, 1969; Carl, 1978; Bouchard, 1989; Fisher and Shaw, 1992). Hättestrand and Kleman (1999) have also observed Rogen moraines on

plains and wide upland plateaus, whereas Aylsworth and Shilts (1989) observed that in some areas Rogen moraines appear to have developed independent of topography.

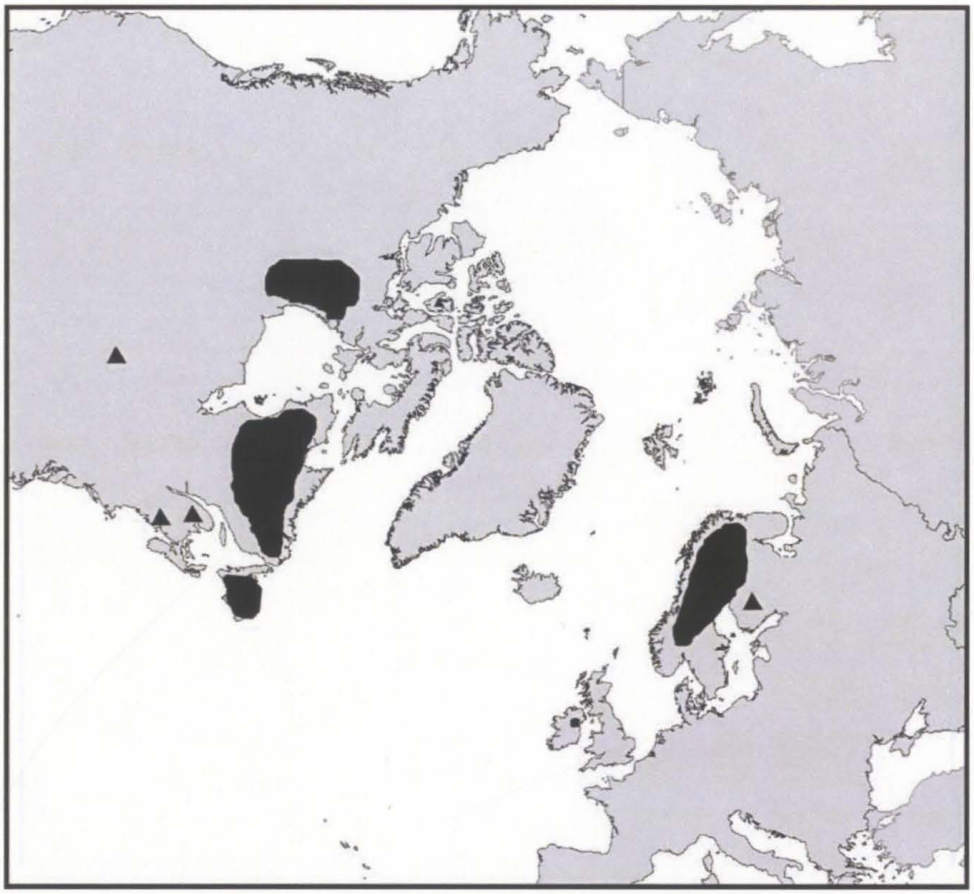

Figure 2.1 Global distribution of Rogen moraine. Dark shaded areas outline where Rogen moraine commonly occur. Dark triangles denote outliers of Rogen moraine found beyond the core areas (after Dunlop, 2004).

2.2.2 Subglacial landform continuum

In his definition of Rogen moraines, Lundqvist (1969, 1981) required that a transition to drumlins be observed. Although this does not occur within every Rogen moraine field, it is a commonly observed characteristic of Rogen moraines. Rogen moraines and drumlins are part of a sediment landform association, with Rogen moraines occurring in areas of

compressive flow over a concave glacial bed, and drumlins in areas of extending flow over convex beds (e.g., Lundqvist, 1969; Burgess and Shaw, 2003) (Figure 2.2). When drumlins are found aligned perpendicular to Rogen moraines, the drumlins and Rogen moraines were likely formed at the same time by a similar ice flow direction (Hättestrand and Kleman, 1999). An anomaly in this pattern was described from Keewatin, Canada, by Aylsworth and Shilts (1989) who observed a lateral transition from Rogen moraines to drumlins, with the drumlins being oriented parallel to the Rogen moraines. They explained this lateral transition as being the result of two different ice flow events.

Sedimentological research has revealed a wide range of internal compositions and sedimentary structures associated with Rogen moraine. Sediment matrices are of varying texture from clay to coarse sand, and clasts range in size from pebble to large boulders (Lundqvist, 1969, 1989, 1997; Bouchard, 1989). Sediments commonly exhibit minor sorting, and are commonly deformed (Carl, 1978; Shaw, 1979; Aario, 1987; Bouchard, 1989; Lundqvist, 1997). Materials that comprise the ridges are generally locally derived, representing the underlying bedrock and are similar to materials found in landforms of the surrounding area. These sediments also exhibit a wide range of fabric orientations (Lundqvist, 1969, 1989; Fisher and Shaw, 1992). Sediments found within Rogen moraine have been variously classified as: basal melt-out till (Lundqvist, 1969), lodgement till, Kalix till (Shaw, 1979), glaciofluvial sediments, and debris flow deposits (Fisher and Shaw, 1992).

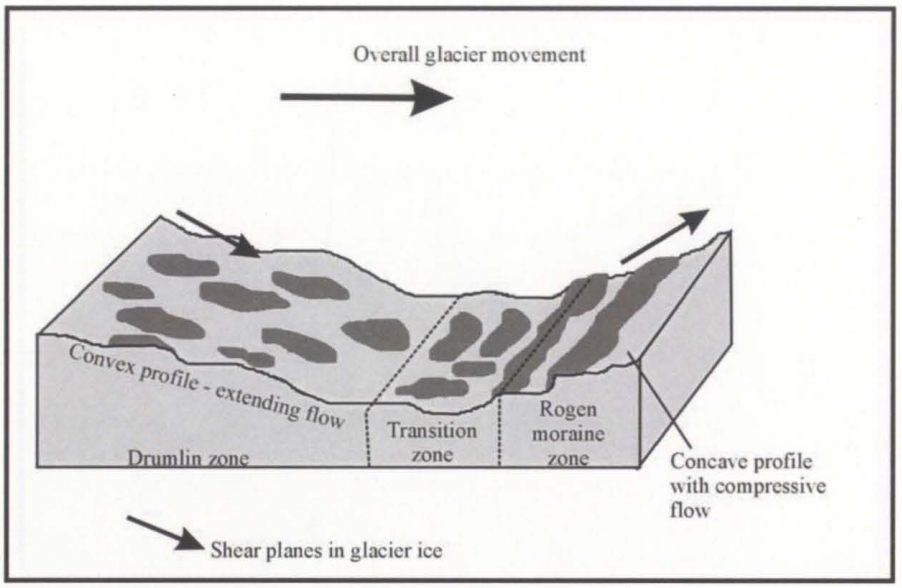

Figure 2.2 Diagrammatic representation of the continuum of subglacial landforms. Rogen moraines form in area of slow, compressive ice flow, over a concave glacial bed. Drumlins form in areas of faster moving ice undergoing extension, above a convex glacial bed (Burgess and Shaw, 2003).

2.2.3 Rogen moraines versus other morainic forms

Correctly identifying Rogen moraines can be difficult. Several landforms that resemble Rogen moraines include: recessional end moraines, De Geer moraines, and hummocky moraine.

2.2.3.1 Recessional end moraines

Recessional end moraines are linear to curvilinear ridges that outline the shape of the retreating glacier. They may be narrow, only a few dozen metres wide, but occasionally reach up to a kilometre wide, and hundreds of kilometres long (Menzies, 2002; Batterson, 1980) that mark standstills or readvances in glacial retreat. These moraines are generally between 100 and 200 m long, generally no more than 5 m high, and are irregularly spaced (Sharp, 1984; Krüger, 1995). The shape of recessional moraines is

similar to Rogen moraines but they are generally smaller and more irregularly spaced. Also, fabrics within recessional moraines are generally perpendicular to ridge crests, while there is no apparent relationship between fabric orientation and ridge alignment in Rogen moraines (Aario, 1987; Aylsworth and Shilts, 1987; Lundqvist, 1997).

2.2.3.2 De Geer moraine

De Geer moraine consists of a series of parallel ridges that develop in former pro-glacial lakes or shallow marine basins. These ridges can be straight or sinuous, and may bifurcate (Beaudry and Prichonnet, 1995; Bennett and Glasser, 1996; Benn and Evans, 1998). De Geer moraines are 1-10 m high, 5-150 m wide, 50–1500 m long, and are asymmetrical in profile, with a steeper proximal side. The sediments within De Geer moraines may consist of till or sorted sediments (Beaudry and Prichonnet, 1995).

Several hypotheses exist for the formation of De Geer moraines including; formation as a result of glaciofluvial deposition into crevasses at the base of the ice (Beaudry and Prichonnet, 1995), deposition at the grounding line on a seasonal or periodic basis (Bennett and Glasser, 1996), and infilling of basal crevasses behind the glacial margin following the let-down of the floating ice margin into the underlying sediments as a result of a decreased water level (Benn and Evans, 1998). De Geer moraines are distinguished from Rogen moraines since they commonly possess fine sorting and organic sediments linked to deposition within a marine or lacustrine environment, which are lacking in Rogen moraine ridges.

2.2.3.3 Hummocky moraine

Hummocky moraine is a grouping of irregular to circular-shaped hills and knobs, and localized depressions, with the occasional elongate ridge (Johnson *et al.*, 1995; Hambrey *et al.*, 1997; Munro and Shaw, 1997; Fisher *et al.*, 2003). The topographical relief in hummocky moraine can vary from a few metres to as much as 25 m (Eyles *et al.*, 1999) and the summits of neighbouring hummocks are at similar heights. The crests of elongated features within hummocky terrain are generally weakly oriented, either parallel or transverse to glacial flow (Eyles *et al.*, 1999). Some depressions within tracts of hummocky moraine have been filled with glaciolacustrine sediment forming flat-topped plateaus (Eyles *et al.*, 1999), and others may be filled with ponds or wetlands (Johnson *et al.*, 1995). The internal composition of hummocky moraine is variable and several models have been proposed to explain their formation (Johnson *et al.*, 1995; Munro and Shaw, 1997; Benn and Evans, 1998; Eyles *et al.*, 1999; Fisher *et al.*, 2003).

(1) It is a result of overall glacial stagnation, following the thrusting of sediments at the glacial margin, or as ice presses into fine-grained deformation till (Johnson *et al.*, 1995; Hambrey *et al.*, 1997; Andersson, 1998; Eyles *et al.*, 1999), (2) It is due to the erosion of sediments by a subglacial meltwater flood (Munro and Shaw, 1997; Fisher *et al.*, 2003). Hummocky moraine consists of much more irregularly arranged landform structures than Rogen moraine. Some linear features do occur in hummocky moraine, although they are not grouped together in evenly spaced tracts, and there is no relationship between the alignment of these features and the ice flow direction.

Although Rogen moraine morphology resembles that of marginal recessional moraines, De Geer moraines, and hummocky moraine, it is possible to distinguish Rogen moraines. Typically, Rogen moraines are larger and more evenly spaced than recessional moraines, they lack the fine-grained sediments and organic remains commonly found in De Geer moraines, and their sets of parallel ridges differentiate them from the randomly oriented hills and knobs of hummocky moraine.

2.2.4 Rogen moraine formation

2.2.4.1 Introduction

Most research on Rogen moraines has been concerned with describing their morphology, sedimentology, and relationship with other glacial landforms in order to develop models for their formation (e.g. Lundqvist, 1969, 1997; Hättestrand, 1997; Dunlop, 2004). The most popular and commonly cited hypotheses of Rogen moraine formation can be subdivided into five main groups; they are discussed in the following sections.

2.2.4.2 Shattered till sheet hypothesis

Hättestrand (1997) developed the shattered till sheet hypothesis to explain the wide range of morphological and sedimentological characteristics of Rogen moraines. He notes that the sediments within Rogen moraines are commonly similar to sediments making up areas surrounding the moraines. He also emphasizes the idea that adjacent Rogen moraine ridges fit together like a jigsaw puzzle. These observations led him to suggest that the sediments within Rogen moraines and surrounding landforms were part of a pre-existing frozen till sheet beneath the glacier, and overlying bedrock. At the onset of

deglaciation the glacier margin becomes warm-based as the phase change surface (PCS) (the boundary between frozen and non-frozen material) migrates upwards allowing the base to melt (Figure 2.3). The central portion of the glacier is cold-based. The ice and till sheet undergo extension at the margin, and fractures within the till sheet develop perpendicular to the ice flow direction. With continual advance of the margin the fractures expand and blocks of frozen till become detached from the remainder of the till sheet. The weight of the overlying ice causes deformation of ice into the fractures, which leaves alternating blocks of the till sheet interspersed with blocks of cleaner ice. Advancement of the glacier margin can cause the blocks of shattered till sheet to deform, because of frictional drag, bending the ends of the blocks to reflect the shape of some Rogen moraines. Eventually the ice mass stagnates and melts out leaving behind evenly spaced till ridges.

Although this hypothesis was developed in order to explain the wide range of morphological and sedimentological characteristics of Rogen moraine, it is not a physically-based model, or one that has been tested using principles of ice mechanics, and it is difficult to determine if fractures the size of Rogen moraines could be sustained through deglaciation. Also, this hypothesis was developed primarily because Hättestrand observed that adjacent Rogen moraine ridges fit together like a jigsaw puzzle. This idea is similar to the pattern used to explain plate tectonics. It was observed that outside edges of neighbouring Rogen moraine ridges mirrored one another, not unlike Africa's west coast roughly mirroring South America's east coast. This jigsaw-fit was not observed by Dunlop (2004) nor Catto (2005, Memorial University of Newfoundland, personal communication). Adjacent ridges, they found, fit together as well or as badly as two non-

adjacent ridges (Dunlop, 2004; Catto, 2005, Memorial University of Newfoundland, personal communication).

Another argument opposing Hättestrand's model is proposed by Möller (2005) who states that there is currently no evidence to indicate that the shear strength of the till sheet would decrease as it thaws. He was unsure that the stress induced by the overlying ice would be strong enough to overcome the shear strength of the till, thus leading to its fracturing. Möller (2005) also states that the areas between the shattered blocks of ice would eventually close as the ice becomes compressed near the margin.

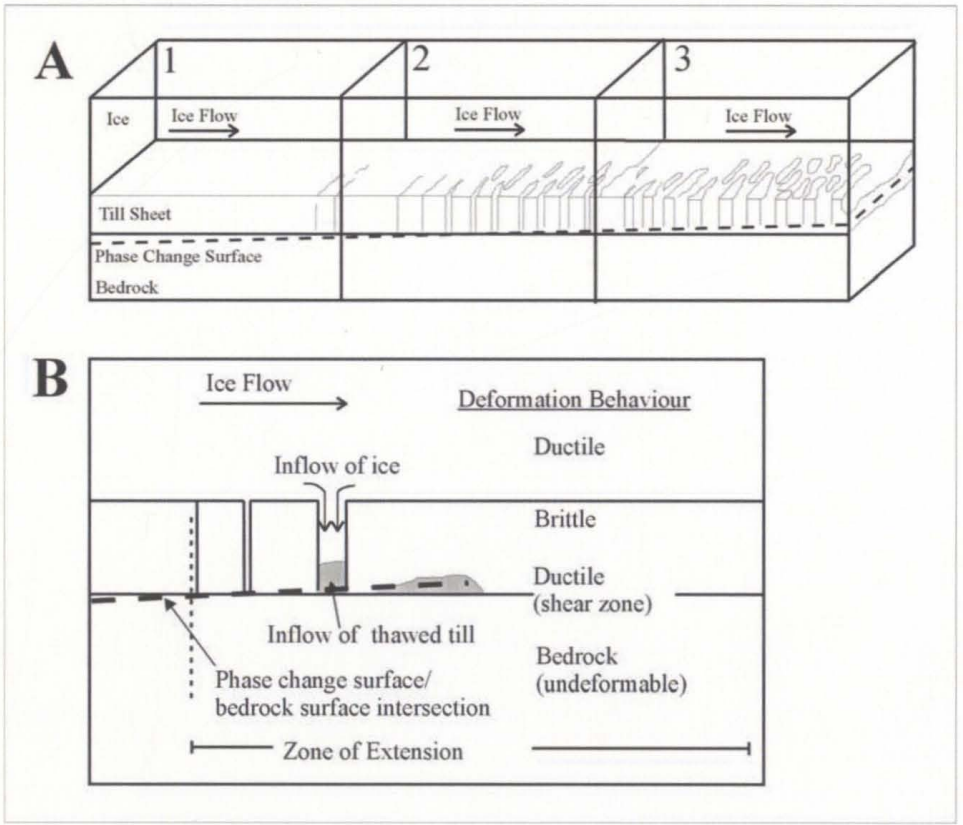

Figure 2.3 Shattered till sheet hypothesis for Rogen moraine formation. A) Time slice boxes (1-3) showing the evolution of Rogen moraine as a result of the upward migration of the pressure melting isotherm (Phase Change Surface (PCS)). Once the PCS intersects the bedrock surface frozen slabs of overlying till are detached. B) Close-up diagram of the zone where the till sheet begins to detach and extend as a result of increased ice flow velocity. During and after deglaciation mass movement processes may decrease the slope angles of the ridges and degrade the tabular morphology (Modified from Hättestrand, 1997).

2.2.4.3 Subglacial meltout and basal thrusting

Several studies have explained Rogen moraines as being the product of shearing and stacking of slabs of debris-rich basal ice (Shaw, 1979; Aylsworth and Shilts, 1989; Bouchard, 1989). This hypothesis attempts to explain the formation of Rogen moraine within topographic basins and its relationship to hummocky moraine. Ice flowing into basins slows as it encounters the down-ice slope. Compressional forces lead to the formation of shear planes and slabs of debris-rich ice are thrust up onto one another englacially. As the glacier continues to flow into the basin, compressional forces reach a threshold leading to the development of a décollement plane. Along this plane the glacier shears across the top of the stacked ice wedges, levelling the sediment and ice in the ridges. As the glacier flows over its new effective bed, fluting, grooving, and drumlinization of the ridges may occur. The final deposition occurs as the glacier stagnates and melts, preserving englacial structures.

In this hypothesis Rogen moraines are well developed along the down-ice edge of the basin and hummocky terrain occurs farther up ice (Figure 2.4). This hypothesis has been used to explain the accordant summits of Rogen moraine ridges, deformation of sediment layers within ridges, and their common occurrence within basins (Shaw, 1979; Aylsworth and Shilts, 1989; Bouchard, 1989). Objections to this hypothesis have been made based on the evidence that not all Rogen moraine fields are located within basins, and it is difficult to determine how such large shear planes could develop without a

substantial obstacle to glacial flow (Dunlop, 2004; Shaw, 2005, University of Alberta, personal communication).

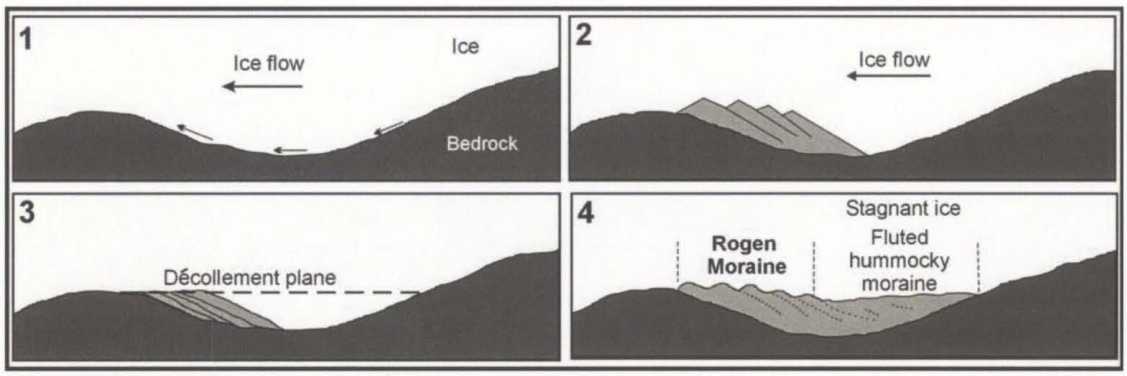

Figure 2.4. Subglacial meltout and basal thrusting: glacial ice flows against the down-ice slope of the basin, the ice slows down and compresses forming shear planes. Rogen moraines form on the up ice edge of the basin while hummocky and fluted moraine form in the centre of the basin (after Shaw, 1979).

2.2.4.4 Subglacial meltwater hypothesis

Shaw (1983) developed the subglacial meltwater hypothesis as a means to explain the formation of drumlins. This hypothesis began as a form analogy between subglacial erosional and depositional features and those produced by turbidity currents in non-glacial environments. Shaw (1983) hypothesized that drumlins may be deposited or eroded by large and turbulent subglacial floods. He also suggested that related landforms such as Rogen moraines, eskers, and hummocky moraine could also be described by the same hypothesis (Shaw *et al.*, 1989; Shoemaker, 1995, 1999; Fisher, 1994). Rogen moraine and drumlins are explained as infilling of scours eroded out of the base of an ice sheet. Shaw *et al.* (1989) postulated that Rogen moraines develop at the centre of a topographic basin where sheet flow is much thicker and more turbulent. The heavily

debris-laden meltwater scours grooves in the base of the overlying ice and as the grooves increase in size the sheet flow moving through them is able to expand, decrease in velocity, and deposit debris into the cavities. The cavities may continue to increase in size through ablation, resulting in meltout of subglacial sediment from the cavity roof. Towards the edges of the basin, sheet flow is much thinner and less turbulent, and therefore landforms developed at the basin edge are more subdued (Figure 2.5). The velocity and thickness of the flood sheet is variable over time, and therefore sediments initially deposited as the floodwaters wane may later be reworked by minor increases in velocity.

A second form analogy has been used to explain the formation of the continuum of subglacial bedforms. Shaw *et al.*, (1989), found similarities in form between the subglacial bedforms and the forms found in the fluvially eroded loessic hills of the Missoula Scablands, U.S.A. They explain the formation of these landforms as a result of the erosion of the substrates between the landforms by a meltwater flood, therefore suggesting that Rogen moraines, drumlins and the associated landforms were the remnants of pre-existing sediments (Shaw *et al.*, 1989).

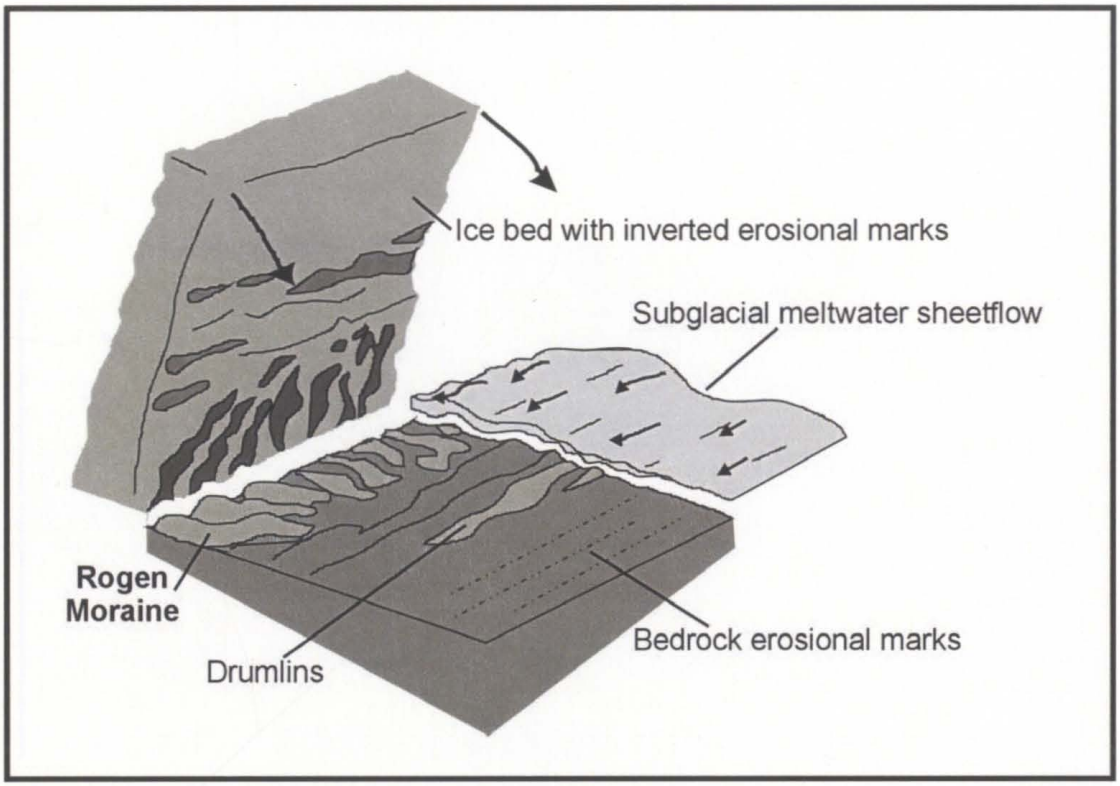

Figure 2.5 Diagrammatic representation of the subglacial meltwater flood hypothesis. A massive meltwater sheet flood scours out the base of the overlying ice producing grooves that are subsequently in filled with glacial debris. Rogen moraines are located well within the ice margin, and in the area of thickest sheet flow (after Fisher and Shaw, 1992).

Several pieces of sedimentological evidence have been used to support the meltwater flood hypothesis. Shaw (1983, 2004) suggested that horizontal sorted beds of sand and gravel that conform to the shape of the landform indicate direct deposition of sediment into cavities. Concentrations of boulders that show evidence of rounding and percussion marks are also interpreted to be consistent with deposition by subglacial meltwater floods (Kor and Cowell, 1998).

Shaw (2002) also interpreted small- and large-scale flutings and S-forms as meltwater eroded features. In addition, Kor and Cowell (1998) suggest that when

potholes are found in association with S-forms and are located in the lee of bedrock knolls or ridges they may be indicative of catastrophic subglacial meltwater events. .

An association between drumlins, tunnel channels and eskers is interpreted by Shaw (2002) to represent a transition from sheet flow to channelized flow. Explanation of such landform transitions should be a requirement of any hypothesis that attempts to explain the formation of any single landform according to Lundqvist (1969, 1981), Aylsworth and Shilts (1989), and Hättestrand and Kleman (1999).

Fisher and Shaw (1992) concluded that catastrophic subglacial meltwater floods formed the Rogen moraines on the central Avalon Peninsula. They cited several pieces of sedimentological evidence in support of their conclusion, including sorted sediment beds beneath perched clasts, undisturbed horizontally stratified beds of sands and gravels, and relatively few striated clasts. Clast fabric studies suggested that sediments were deposited by fluvial and debris flow processes.

The meltwater flood hypothesis for subglacial landforms has met with much criticism. Benn and Evans (1998) suggest that using sole marks beneath turbidites as analogues for drumlins is problematic because of the large difference in scale of features. They also state that different mechanisms can form similar landforms, and until the physics behind the meltwater flood hypothesis can be adequately modeled it is inappropriate to use the hypothesis in genetic interpretations.

The most common argument against the meltwater flood hypothesis is the question of where was the floodwater stored (Benn and Evans, 1998; Hättestrand, 1997; Dunlop, 2004; Clarke *et al.*, 2005) A very large volume of water is required to produce landforms of 10 to 30 m in height, and if an outburst flood is to be sustained the water

must be held in a reservoir. Clarke *et al.* (2005) discuss the physics involved in a glacier storing large quantities of subglacial water, and they concluded that a substantial difference in glacial surface slope and bed slope must be present. This must occur because a glacier expels water much easier than it stores it; therefore reservoirs of this magnitude are rare. Clarke *et al.* (2005) did concede that a large store of meltwater can occur subglacially, and used subglacial Lake Vostok in Antarctica as an example, but they were careful to state that the lake is situated in a tectonic basin, which prevents much of the meltwater from escaping the subglacial environment.

2.2.4.5 Bed deformation hypothesis

According to this hypothesis Rogen moraines are the precursors to the drumlinization of transverse ridges (Boulton, 1982). There are two main requirements for this hypothesis: landforms produced by a previous glacial event must possess alternating sections of weak and resistant sediment, and there must be a change in glacial flow direction. The change in ice flow direction leads to the reworking of the previously deposited sediment, moving the weak sediment down ice, and leaving the more resistant components behind (Boulton, 1982) (Figure 2.6). Eventually the parent landform will be almost completely reworked and the sediment will be realigned to reflect the new ice flow direction. Lundqvist (1989) used this model to explain the formation of Rogen moraines at the type-site near Lake Rogen, Sweden, where he observed a transition between Rogen moraines and drumlins.

Boulton (1982) did not consider the internal composition in his initial work, but there is now sufficient published work pertaining to deformation of subglacial sediments

(e.g., Boulton, 1982; Hart, 1994, 1994a, 1997; Hindmarsh, 1997; Murray, 1997; Boulton *et al.*, 2001; Möller, 2005) to test this hypothesis. Building on the ideas of Boulton (1982), Möller (2005) described a similar hypothesis to explain the external morphology of ridges and their highly deformed internal sediments in Dalarna, Sweden.

A limitation of the bed deformation hypothesis is that it does not explain the origin of the parent landforms, nor does it apply in areas where there was only one dominant ice flow direction (Catto, 1998; Hättestrand, 1997, 1998). Dunlop (2004) found that Rogen moraines exist over large areas, irrespective of topography, and concluded that the bed deformation model does not readily explain the large-scale, regional distribution of Rogen moraines. Finally, the requirement that beds of resistant and non-resistant sediments are evenly distributed along the long axis of the parent landform is inconsistent with the published sedimentology of Rogen moraines.

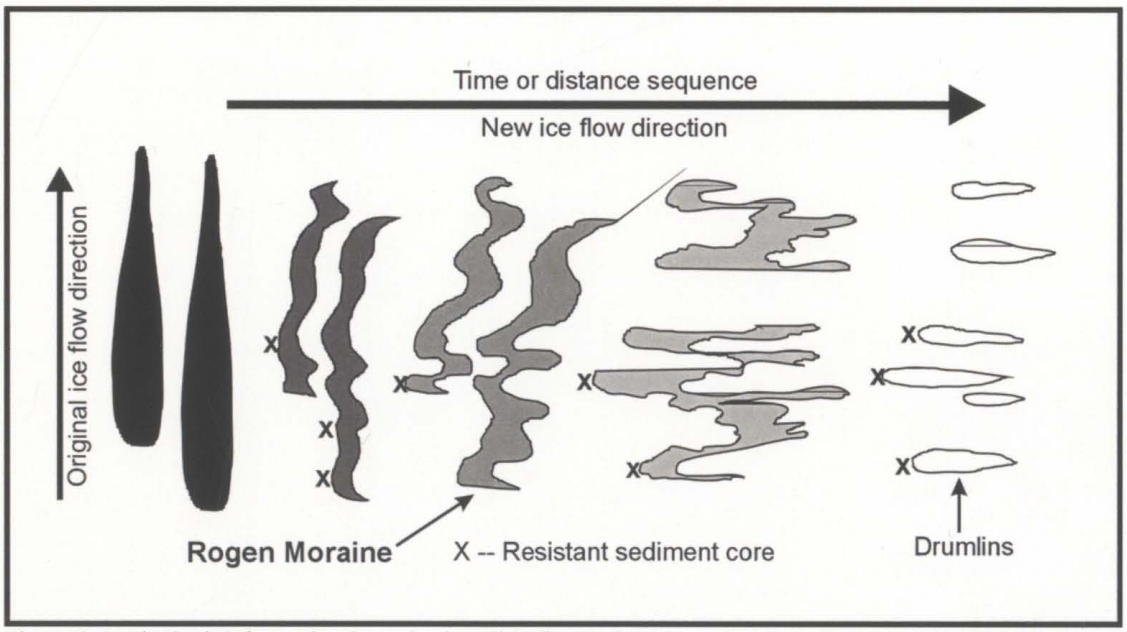

Figure 2.6. The bed deformation hypothesis. This figure shows two ice flow directions; one that deposited the linear ridges, and a second that deforms the ridge into secondary landforms including Rogen moraines and drumlins (after Boulton, 1982).

2.2.4.6 Bed Ribbing Instability Explanation (BRIE)

Deformation of the subglacial sediment layer has been attributed to an instability within the subglacial environment (Hindmarsh, 1998, 1998a, 1998b; Dunlop, 2004). The Bed Ribbing Instability Explanation (BRIE) model predicts the expected wavelengths for instabilities within the subglacial environment that are thought to initiate the formation of subglacial bedforms. Natural systems constantly move towards equilibrium, and when the equilibrium is interfered with an instability occurs. The BRIE is based on the observation that fields of Rogen moraines look like waves in the topography. Wave patterns are frequently observed in natural systems and these patterns are commonly driven by instabilities. Dunlop (2004) refers to the Kelvin Helmholtz instability that is key to the development of many cloud formations, the Bénard Instability for convection plumes, and the ripples in sand produced by a shear flow instability as examples of these instabilities occurring in natural systems. There are various processes occurring within the subglacial environment and the alteration of any of these processes can destabilize other processes, and then an instability is created.

The BRIE models the interaction of viscously deforming ice overlying viscously deforming till situated on bedrock. Sliding also occurs at the ice-till interface as well as at the bedrock surface. The model examines how deformation processes in the subglacial environment vary. If the surface of the till is uneven, the coupled flow of ice and till is unstable. As a result the ice begins to slide over the till and small undulations in the till thickness are increased as the till deforms, causing abrupt development of relief.

Therefore, if the flow of ice and till is unstable, variations in erosion and deposition of subglacial till can affect the equilibrium of the subglacial system. In order to overcome the instability, various other processes within the subglacial environment may be amplified. If there is a large disturbance in the process, the instability is large and therefore the wavelength of sediment deformation increases. Another example is that if erosion in one part of the subglacial environment is increased, the amount of deposition in another part of the subglacial environment will increase to compensate for the increase in erosion.

Therefore, the height of individual Rogen moraine ridges and the spacing between them are dictated by the size of the wave caused by the instability. This model uses effective pressure at the ice surface, shear stress, ice velocity, till thickness, and proportion of slip due to till deformation as parameters for calculating wavelengths. The BRIE has predicted Rogen moraine formation at wavelengths between 100 and 1000 m, similar to measurements of actual Rogen moraine wavelengths (Hindmarsh, 1998,1998a, 1998b; Dunlop, 2004). Dunlop (2004) has concluded that the BRIE is a good general model of Rogen moraine formation because it predicts naturally occurring wavelengths, it does not require specific localized conditions for the formation of Rogen moraine, and it can be used to explain the general characteristics of Rogen moraine that are consistent throughout large areas. This is a fairly new hypothesis and it has yet to be tested by researchers other than Hindmarsh (1998 a,b,) and Dunlop (2004).

2.3 Rogen moraine in Newfoundland and Labrador

Surficial geology maps of Newfoundland and Labrador show that parallel ridges aligned perpendicular to glacial flow are common in many areas of the province (Figure 2.7). These ridges usually have been interpreted as Rogen moraines because of their similar morphologies to Rogen moraine described in the literature (e.g. Fisher and Shaw, 1992; Munro, 1994; Catto, 1998; Batterson and Taylor, 2004). Within the province these moraines are most commonly located within topographic basins (Figure 2.7). Rogen moraines are located adjacent to the Nouveau-Québec Ice divide (Bouchard, 1989) (Figure 2.7); on Newfoundland they are situated in patches throughout the island, with the largest field being located within the central Avalon Peninsula. The moraines are generally 150 to 200 m wide, 10 to 25 m high and up to 1000 m long (Ives, 1956; Henderson, 1959, 1962; Hughes, 1964; Rogerson and Tucker, 1972; Bouchard, 1989; Fisher and Shaw, 1992).

Figure 2.7 Areas of ridged till in Newfoundland and Labrador. These areas have been interpreted from surficial geology mapping of the province. These landforms are considered similar to Rogen moraine but not all areas have been classified as such. Numbers denote locations of Rogen moraine fields listed in the text, and correspond to Table 2.1.

The internal composition of these moraines is described as generally medium to coarse-grained, locally derived, sandy till with subangular to angular clasts (Ives, 1956;

Henderson, 1959, 1972; Rogerson and Tucker, 1972). There is some minor sorting of the till but it is generally homogeneous. Henderson (1956) noted erratic boulders on the surface of the moraines near Dyke Lake Labrador, and a cover of angular clasts to a depth of about 50 cm. Fisher and Shaw (1992) similarly observed a boulder lag on the moraines of the central Avalon Peninsula. The central Avalon moraines were composed of a coarse diamicton with fine sand to gravelly matrix, and the clasts were predominantly angular with few striations (Fisher and Shaw, 1992).

Rogerson and Tucker (1972) were the first to apply the term Rogen moraine to the set of ridges in the central Avalon Peninsula, and Bouchard (1989) refers to the moraines around the Nouveau-Québec Ice divide as Rogen moraines based on the classification on the Glacial Map of Canada (Prest *et al.*, 1969).

Several formative mechanisms have been suggested for Rogen moraine in Newfoundland and Labrador. Henderson (1959, 1972) suggested that the moraines south of Dyke Lake, Labrador as well as the moraines of the central Avalon Peninsula were formed as glaciers retreated because they are perpendicular to ice flow, and are curved down-ice. Bouchard (1989) hypothesized that the moraines in Labrador were formed through the shear and stack hypothesis described previously. Rogerson and Tucker (1972) suggested the moraines on the central Avalon Peninsula were formed at the margin as the Avalon Peninsula ice cap grew. Fisher and Shaw (1992) have used the subglacial meltwater flood hypothesis to explain the formation of the same moraines on the central Avalon Peninsula. Munro (1994) argued for the meltwater erosion of similar landforms near Carmanville (The * on Figure 2.7).

Table 2.1 Summary of observations on Rogen moraine in Newfoundland and Labrador.

Location	Topographic Setting	Description	Dimensions	Internal Composition	Formative Theory	Data Source
Central Labrador (#1)					Downwasting of glacial ice	Ives, 1956
Nichicun_Kaniapiskau, Quebec (#2)	Ridges occupy minor depressions	Fluted on sides and crests		Fabrics parallel to flow Compact sandy till with abundant pebbles and cobbles Predominantly sub-angular	Unknown, may be related to proglacial lakes (deltas in the area show lake levels above crests)	Hughes, 1964
Avalon Peninsula (#3)	Broad basin	Ridges are concave up ice			Recessional features	Henderson, 1972
Avalon Peninsula (#3)			10-30 m high 200-400 m apart Several hundred metres long	Fabrics are sub-parallel to ice flow and ridge crest orientation	Moraines formed subglacial during glacier advance followed by stagnation	Rogerson and Tucker, 1972
Northwestern Labrador and Eastern Quebec (#4)	Topographic lows	Broad arcuate ridges Concave down ice Jig saw fit Surface lineations	50-100 m wide 5-20 m high 20-200 m apart	Massive to stratified, matrix supported, fine-grained diamicton Varying provenance Layers of poorly sorted diamicton beds and thin layers of better-sorted sandy to gravel sediments with gradational boundaries Some deformation of layers around and above clasts	Shear and stack of subglacial ice	Bouchard, 1989
Avalon Peninsula (#3)	Broad basin	Ridges are curved, convex down ice		Cross-bedded gravels Poorly sorted sand/muddy gravel Clast supported pebble and cobble beds Diamicton bed overlying gravel beds Sand and silt stringers Laminated lenses Openwork lenses Angular or sub-rounded clasts Weak clast alignment Sediment debris flows	Subglacial meltwater flood	Fisher and Shaw, 1992

2.4 Glacial History of the Avalon Peninsula

2.4.1 Last Glaciation of the Island of Newfoundland

During the last glacial maximum (LGM) the island of Newfoundland supported an ice complex broadly independent of the Laurentide Ice Sheet (LIS), except where ice from southern Labrador flowed across the tip of the Great Northern Peninsula (Grant 1989) (Figure 2.8). The maximum ice extent occurred roughly at 21 ka BP (all dates in 14 C yr BP) and the eastern and southern margins of the Newfoundland ice cap were located near the continental shelf edge (Shaw *et al.*, in press). The western margin coalesced with ice in the Laurentian Channel. At the LGM, the Newfoundland Ice Complex consisted of a main ice divide extending south (from Labrador) along the axis of the Great Northern Peninsula and east through central Newfoundland and onto the Avalon Peninsula (Figure 2.9). Second-order divides extended over southwest Newfoundland, Cape Freels peninsula and the Burin Peninsula. By 18 ka BP, the ice margins started to retreat from the continental shelves. Ice occupying Notre Dame Bay had retreated allowing sedimentation to occur on the ocean floor (Shaw *et al.*, in press). The development of a large calving embayment in the Gulf of St. Lawrence (at approximately 14 ka BP; Shaw *et al.*, in press) initiated the deglaciation of Newfoundland, beginning with the southwest coast (Bell *et al.*, 2001). Ice retreated rapidly to the modern coast, but once on land, retreat was much slower (Shaw *et al.*, in press). Deglacial ice dispersal centres were located over the Long Range Mountains, The Topsails, Middle Ridge and the Avalon Peninsula (Grant 1977).

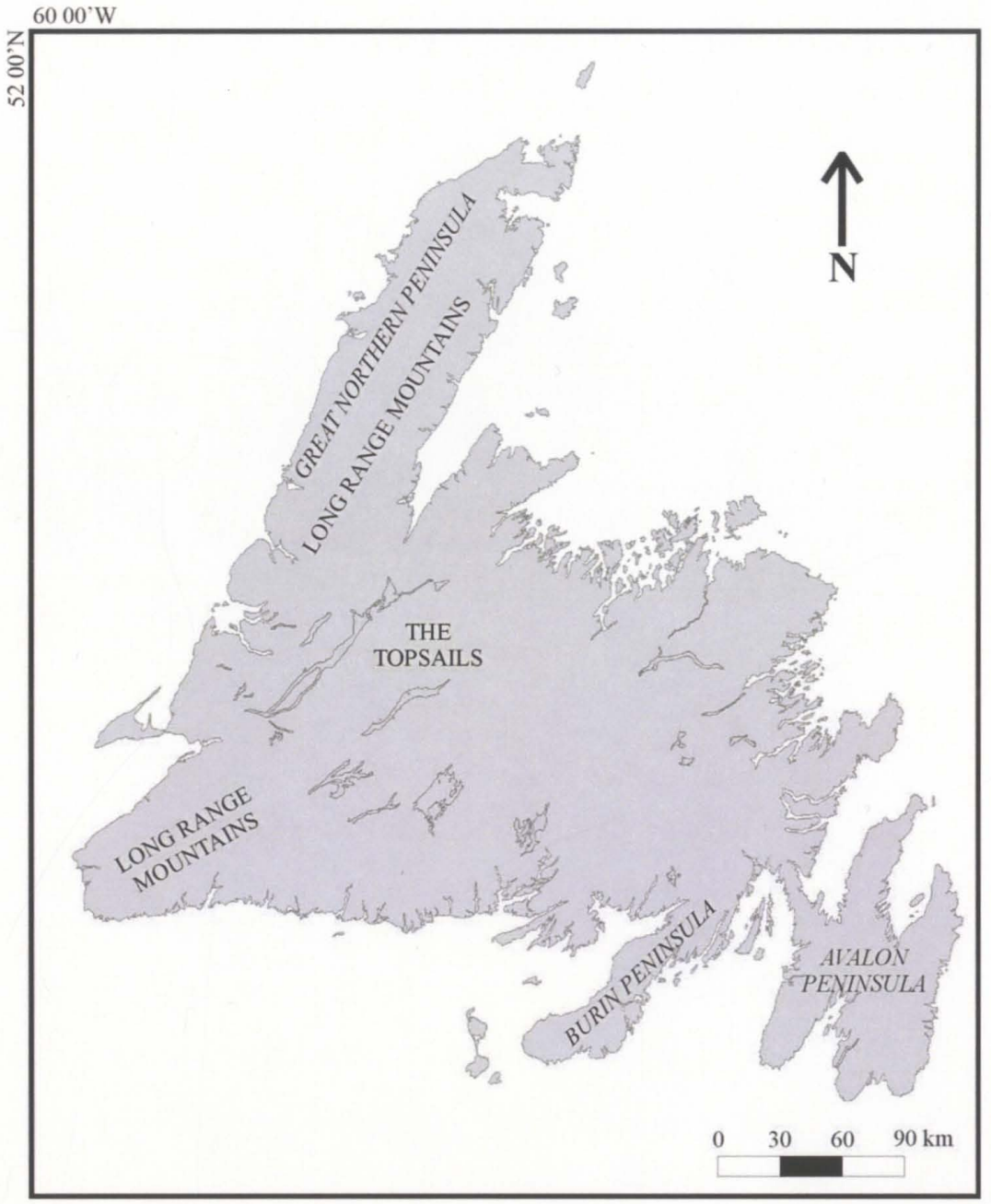

Figure 2.8 Location map of Newfoundland, including place names mentioned in the text.

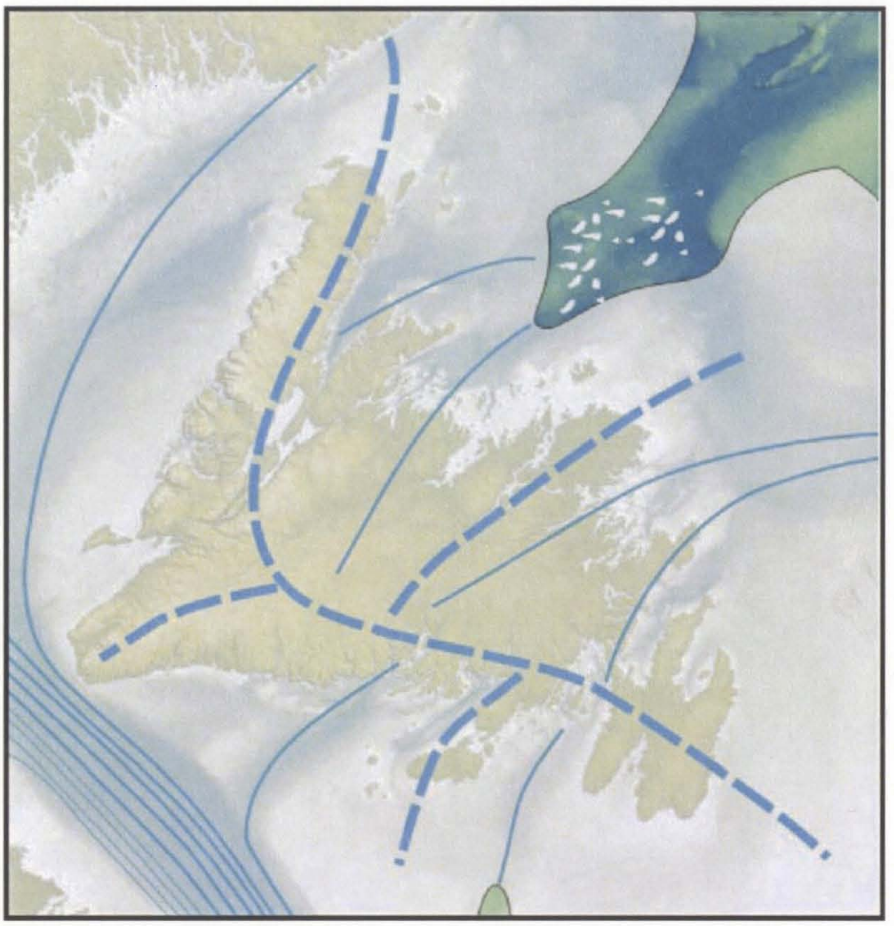

Figure 2.9 Conceptual drawing of ice coverage and the major ice divides over Newfoundland at the LGM. Thick dashed lines represent ice divides. Thin lines represent flow lines. (Modified from Shaw *et al.*, in press).

2.4.2 Ice on the Avalon Peninsula

Early work on the glacial history of the Avalon Peninsula by Murray (1883), Colman (1926), and MacClintock and Twenhofel (1940) suggested that ice flowed across the peninsula from the main part of the island, based primarily on clast provenance data. Evidence for this flow was presented by Summers (1949) who found serpentinite clasts in the St. John's area, which he interpreted as being derived from bedrock in central Newfoundland. This has since been discounted because similar looking rocks are derived

from Avalon Peninsula bedrock. Chamberlin (1895) was the first to propose that the Avalon Peninsula supported an independent ice cap during the Late Wisconsinan, and Henderson (1972) indicated that the main ice dispersal centre was likely located over St. Mary's Bay (See Figure 2.8 for locations of place names mentioned). Striations and clast provenance data support the idea of an independent ice cap over the Avalon Peninsula which deflected ice from the main part of the island into Trinity and Placentia bays (Henderson, 1972; Catto, 1998; Batterson and Taylor, 2004). During glacial maximum a main ice divide extended out across the central Avalon Peninsula originating on the Great Northern Peninsula (Figure 2.9) (Shaw *et. al.*, in press).

The history of glaciation on the Avalon Peninsula has been reconstructed primarily through the analysis of striation data, as well as streamlined landforms (Henderson, 1972; Rogerson and Tucker; Catto, 1998; Batterson and Taylor, 2004). The main centre at the LGM was located over the head of St. Mary's Bay, with smaller centres being located over sub-peninsulas. Ice flowed radially from these centres into adjacent bays (Figure 2.10). The dominant flow direction over the central Avalon Peninsula was north to northeastward into Trinity and Conception bays respectively.

Trinity and Conception bays acted as calving embayments which caused draw-down of local ice caps over the Carbonear and St. John's sub-peninsulas (Henderson, 1972; Catto 1998). This ice movement dominated the glacial maximum configuration and is considered to be the formative ice direction for the moraines that occupy much of the central Avalon Peninsula (Rogerson and Tucker, 1972; Catto, 1998).

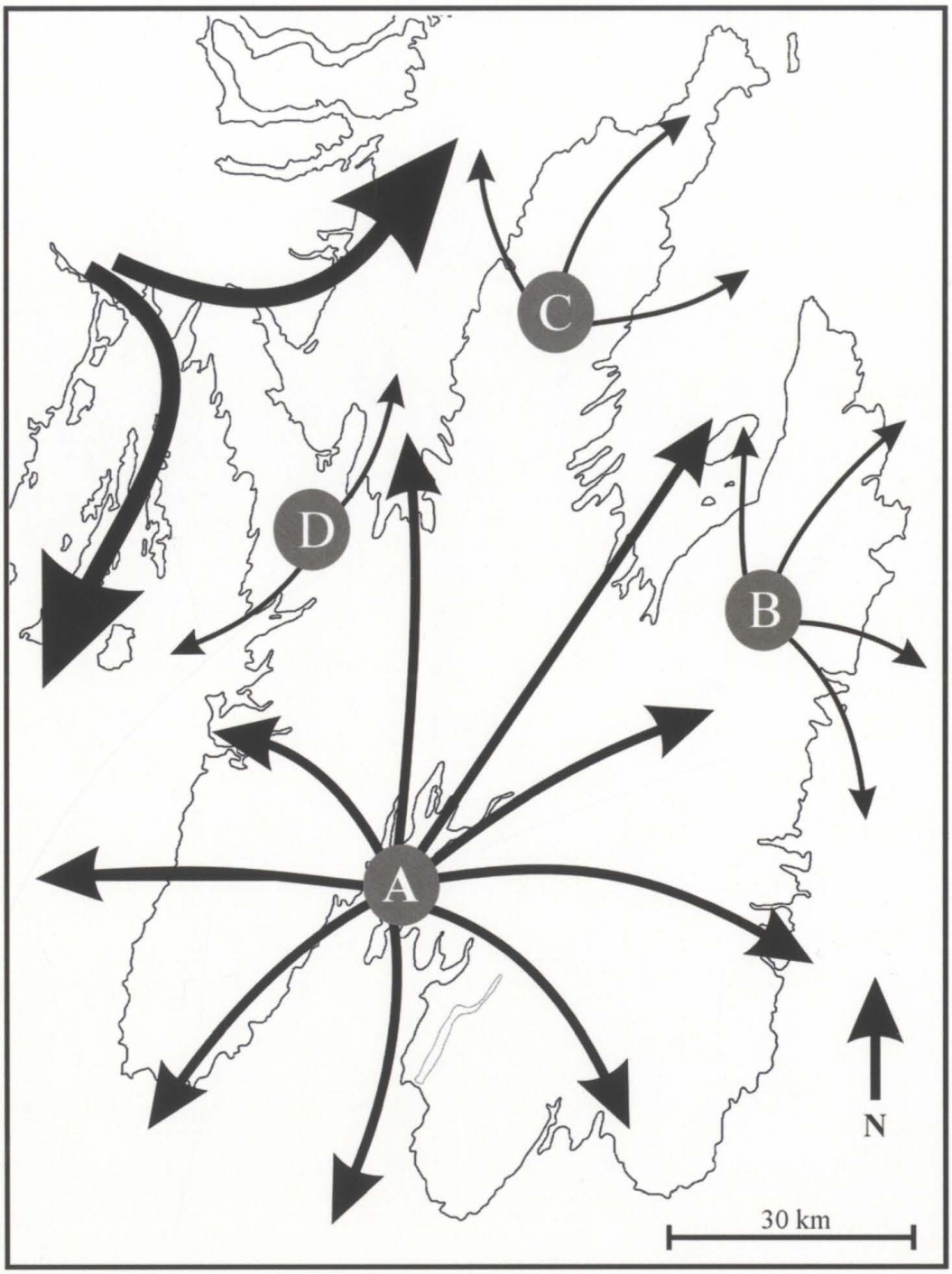

Figure 2.10 Potential ice dispersal centres and ice flow directions, during the glacial maximum on the Avalon Peninsula. A large ice dispersal centre with radial ice flow was located over St. Mary's Bay (A). Smaller ice dispersal centres were also located over the St. John's, and Carbonear sub-peninsulas (B and C), and D) the Isthmus of Avalon. (Modified from Catto, 1998)

The timing of deglacial events on the Avalon Peninsula is poorly constrained, and the mode of deglaciation is not completely understood; downwasting has been suggested by several authors based on the presence of hummocky moraine (Rogerson and Tucker 1972; Catto 1998; Batterson and Taylor, 2004) and by the sequence of radiocarbon dates from basal lake sediments (Macpherson, 1996). Catto (1998) indicates that the St. Mary's Bay ice cap became destabilized due to rising sea level. Subsequently, several small stagnating ice centres developed over sub-peninsulas and the Isthmus of Avalon. He also proposed that the field of moraines on the central Avalon formed during the LGM, by a pervasive ice flow into Conception Bay and that later ice stagnation preserved them during final deglaciation. Surficial geology maps of the Avalon Peninsula by Batterson and Taylor (2004) identify patches of hummocky moraine throughout the field of ridged moraines, which may support the idea of final ice stagnation.

2.5 Study Area

2.5.1 Location and access

The study area covers an area of approximately 1000 km^2 on the central Avalon Peninsula roughly south of Conception Bay, west of the Hawke Hills, east of Whitbourne, and north of St. Mary's Bay (Figure 2.11). The dimensions are approximately 37 km from north to south and 33 km from east to west. The study area is situated within a broad topographic basin, the floor of which rises from approximately 115 to 170 m above sea level (a.s.l).

Access to the area is through a network of gravel logging roads, which can be reached from the Trans Canada Highway, Route 81 or Route 90 (Salmonier Line) (Figure

2.11). Forestry road construction and cabin development is ongoing in the area, expanding access to the central portion of the study area.

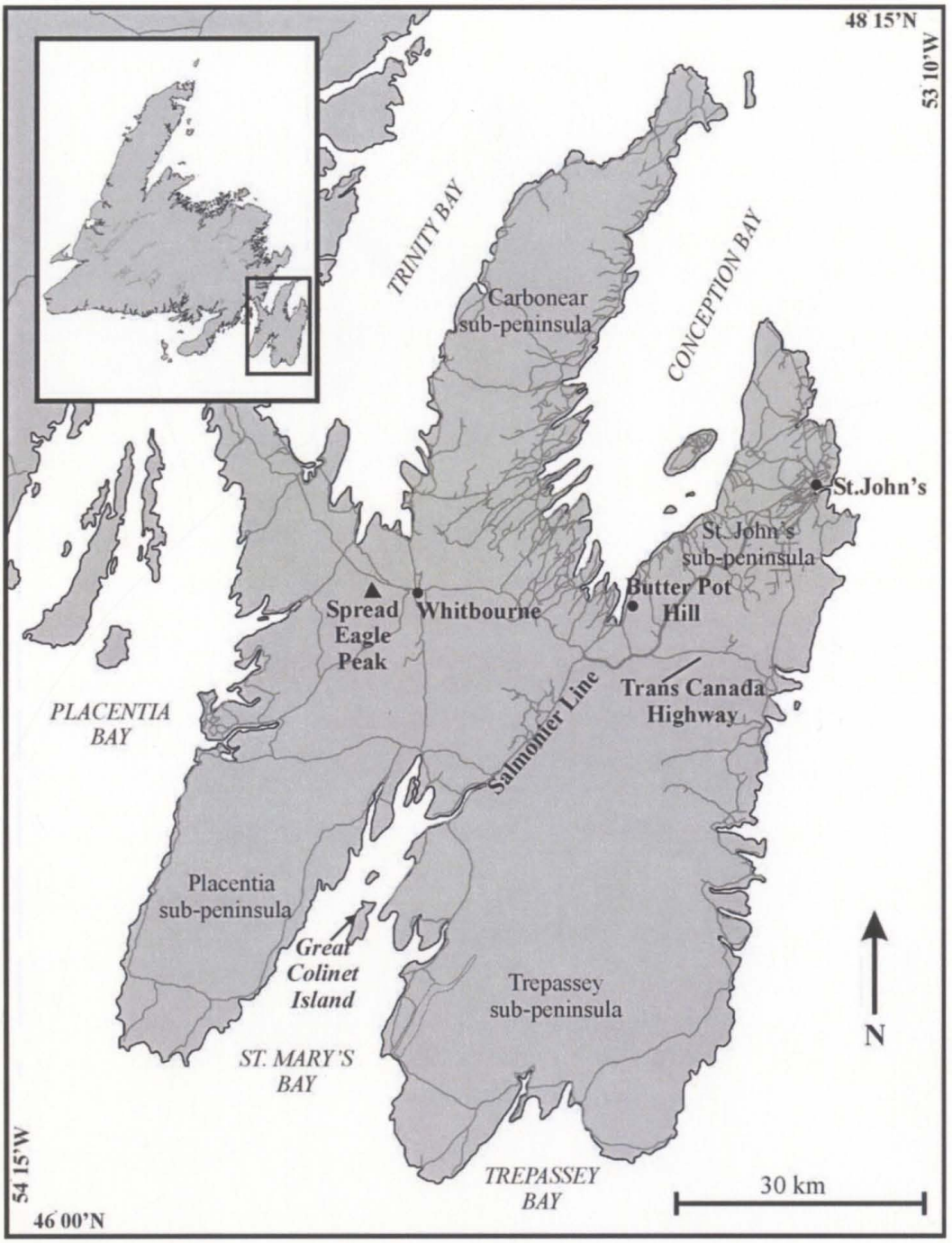

Figure 2.11 Location map of the Avalon Peninsula, including place names mentioned in the text.

2.5.2 Bedrock geology

Between 570 and 650 million years ago, the Avalon Peninsula was folded and faulted during the Appalachian Orogeny, and several large structural domes and basins were formed. The large bays (Conception, St. Mary's, Trinity, and Placentia) are the result of water infilling the structural basins, whereas the sub-peninsulas (St. John's, Trepassey, Placentia and Carbonear) are domes (King, 1988, 1990). The northeast-southwest structural trend reflects the location of these large domes and basins.

The bedrock of the study area is predominantly marine to fluvial sandstone and siltstone (with minor volcanic components) of the Conception and Signal Hill groups. (King, 1988, 1989)(Figure 2.12). The Harbour Main Group of volcanics is fault-bounded on the western margin by the Peak Pond Fault. The Drook Formation of the Conception Group is the oldest of the sedimentary rocks. These are green silicious sandstone and siltstone that extend through the centre of the study area, northward from Salmonier Arm into Bay de Grave in Conception Bay, and eastward from Harricott Bay and Stony Ridge. Other exposures of this formation are located in the southwest section of the Hawke Hills, underlying and surrounding Franks Pond. A linear exposure of Drook Formation rocks extends southeastward from Colliers Point into the central part of the Hawke Hills (King, 1989). The Mistaken Point Formation of the Conception Group consists of red, green, and grey to pink tuffaceous siltstone and sandstones and is located in linear bands near the eastern and western margins of the study area. The Trepassey Formation of the St. John's Group is a medium to thinly bedded sandstone and shale with minor tuffaceous rocks. It outcrops as two linear bands that extend between the northern tip of Harricott

Bay and the southern shore of Bay Roberts, as well as between Murphy's Pond and Hawcos Pond (King, 1989).

Provenance studies of clasts derived from within the central Avalon Peninsula are of limited use because bedrock in the area is predominantly sandstone and siltstone. The Harbour Main Group of volcanics may prove useful because of their limited exposure on the Avalon Peninsula.

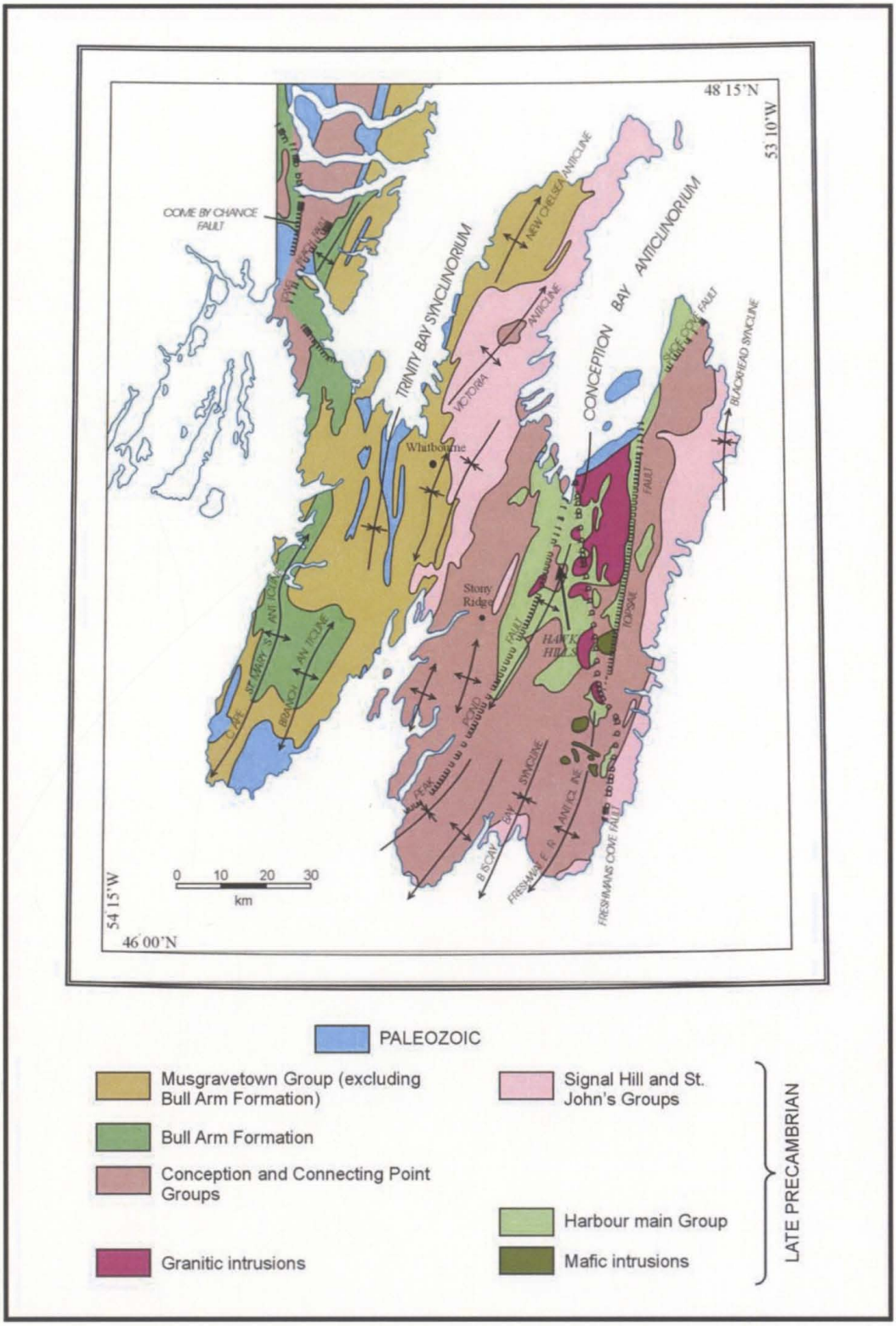

Figure 2.12 Simplified bedrock geology of the central Avalon Peninsula.

2.5.3 Surficial geology

Catto and Taylor (1998) recently mapped the surficial geology of the Avalon Peninsula and the following section draws on these maps for a description of the surficial geology of the study area. The terminology follows the legend for surficial materials and landforms on provincial geological maps (Figure 2.14).

The surficial geology of the central portion of the Avalon Peninsula is dominated by large patches of ridged and hummocky till (> 1.5 m thick). Ridged till commonly occurs in sub-parallel ridges up to 30 m high (Catto and Taylor, 1998), between which peatlands and ponds are common. Hummocky till is located in patches between bands of ridged till, and consists of a random assemblage of knobs, mounds, ridges and depressions (Catto and Taylor, 1998). Till thins (to less than 1.5 m) towards Conception Bay, St. Mary's Bay and to the east and west of the central lowland. Bedrock is exposed in areas of extremely thin till, most notably along the southern shore of Conception Bay, where bedrock is exposed as elongate ridges parallel to the bedrock structural trends. Pond and bog orientation also reflect this northeast-southwest trend. Minor glaciofluvial sediments occur near St. Mary's Bay, as well as west of Rocky River (south of Whitbourne). It commonly consists of fine sand to cobble gravel generally >1 m thick, occurs as plains, ridges, hummocks, and terraces (Catto and Taylor, 1998).

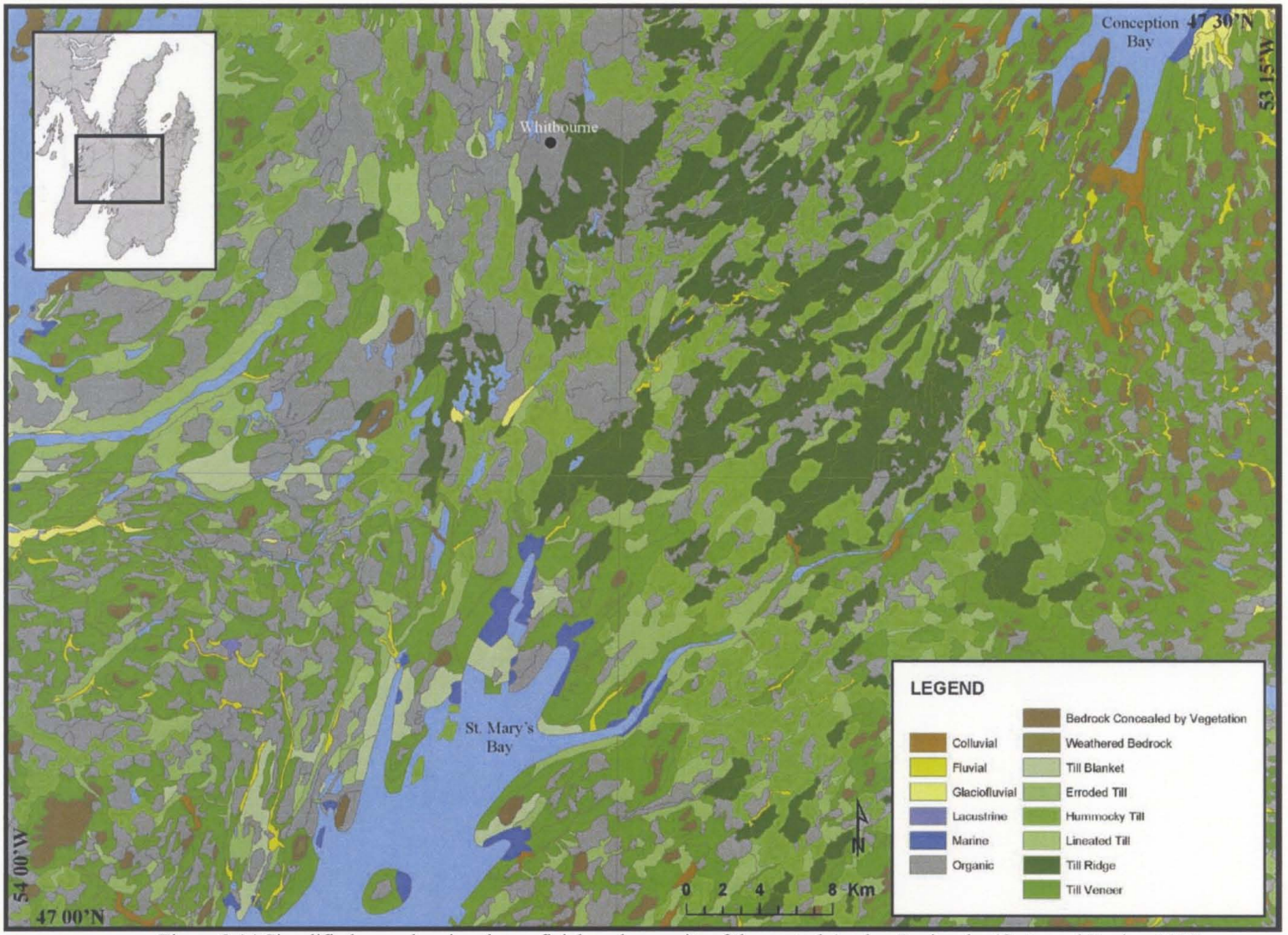

Figure 2.14 Simplified map showing the surficial geology units of the central Avalon Peninsula. (Catto and Taylor, 1998)

2.6 Research Aims

There are several goals for this study. 1. An in-depth examination of the morphological characteristics of the moraine ridges of the central Avalon Peninsula. This includes a detailed description of glacial landforms as well as a re-evaluation of their classification as Rogen moraine. Data were collected in order to address the following question:

1. What is the morphology, orientation, and spatial pattern of moraine ridges on the central Avalon Peninsula?

2. What are the landform associations observed in the central Avalon Peninsula?
Glacial landform associations in the study area will be examined. Rogen moraine are part of a subglacial landform continuum, and it was important to determine if these same types of landform associations could be observed on the central Avalon Peninsula.

3. How were these moraine ridges developed?
Potential processes and environments involved in the development of the moraine ridges were evaluated.

4. What was the relative timing of events during landform deposition on the central Avalon Peninsula?
The timing of glacial events related to the formation of landforms in the central Avalon Peninsula is discussed.

The following chapter outlines the methodologies used to address these research questions.

Chapter 3 Methodologies

3.1 Introduction

Data collection and analysis for this research consisted of fieldwork, interpretation of aerial photographs, the production of a Digital Elevation Model (DEM), and analysis of moraine ridge crest orientations. Fieldwork consisted of a sedimentological examination of exposures in moraine ridges to provide information about the depositional environment involved in the formation of the moraine ridges, and to examine the ridge morphology. Aerial photograph interpretation was completed to map out the aerial extent of the field of moraines, and to examine ridge shapes and relationship to other landforms. The DEM was constructed to examine the morphological characteristics of the field of moraines. The DEM provided greater flexibility in viewing the landscape than the aerial photographs; the angle at which the landscape was examined could be altered and shading techniques within the GIS also increased the visualization of the study area. Finally, the moraine ridge crest orientations were calculated in order to determine if there is a relationship between ridge crest orientations and the predominant ice flow direction in the area.

3.2 Fieldwork

As logging is active and cabin development ongoing, all roads, whether paved or gravel, were driven or walked in an exhaustive search for new sediment exposures. Over 150 km of roads were travelled and a total of 26 exposures were examined (Figure 3.1), during an eight-week period between June and August 2004.

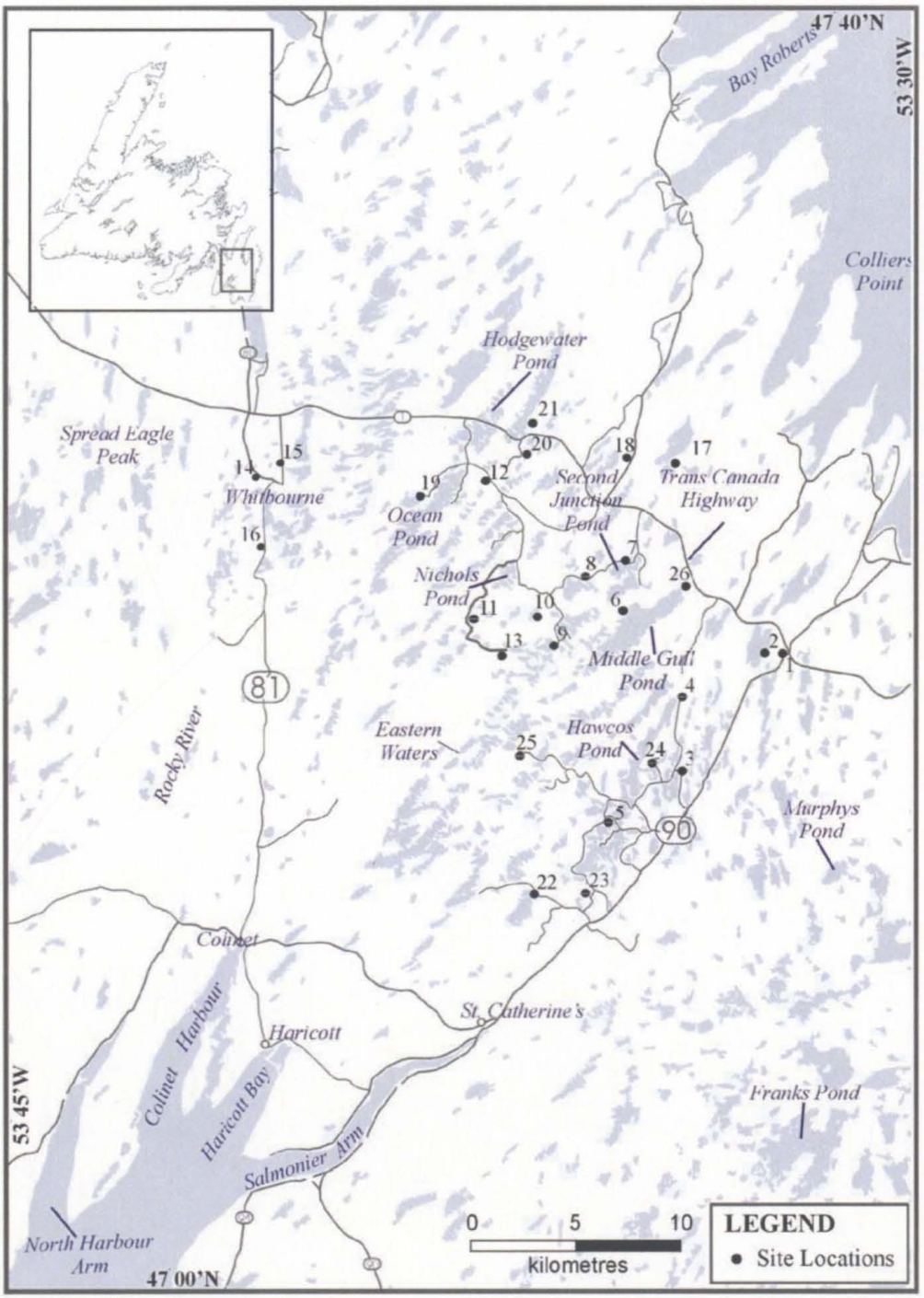

Figure 3.1 The central Avalon Peninsula; site locations and place names mentioned in the text.

The height and width of each site was measured and each exposure was sketched. The location of the exposure, whether within a ridge or a hummock, was identified and recorded using UTM co-ordinates generated from a hand-held GPS. The ridge crest orientation was determined by visual inspection of the surrounding landscape, as well as aerial photographs. Clast lithology was determined through visual inspection, but clasts of uncertain type were collected for later identification.

At least two vertical sections to maximum depths of 1 m were cleared at each of the 26 sites along the exposure face. Observations of sedimentary structures were made, and a sketch of the cleared area was drawn. Sedimentary observations included sediment texture, compactness, sedimentary structures, stoniness, colour, clast lithology, and fabric. Percent stoniness, dominant particle size, and clast angularity were estimated and faceted and striated clasts were noted if present. Within each of these vertical sections at least one clast fabric measurement was completed. Clast fabric measurements in glacial diamictons can be important indicators of ice flow direction, and along with other sedimentological observations may be used to suggest the depositional environment responsible for landform development. For each clast fabric measurement the dip angle and orientation of 25 elongated clasts with a minimum length breadth ratio of 3:2 were measured. Sediment samples were collected within each of the vertical sections for grain size analysis.

3.3 Aerial Photograph Interpretation

Mapping of surficial landforms was completed using 1:50,000 black and white and 1:12,500 colour aerial photographs (Figure 3.2). The latter were used to examine

particular areas in detail, specifically those that exhibited transition in landform type or character. The photographs were interpreted using an 8x magnification mirror stereoscope. Landforms were mapped using standard identification criteria (Wolf, 1983; Blair *et al.*, 1990), but special attention was focused on the outline and crest line of ridged and hummocky moraine elements.

Once interpreted, each aerial photograph was scanned and georectified, using a minimum of 12 ground control points, using the ArcMap component of ArcGIS 8.3. The aerial photographs were rectified to shapefile coverages of water bodies and roads created by the Newfoundland and Labrador Geological Survey. By using the base data from the Geological Survey to rectify the aerial photographs is was possible to ensure that all the data was recorded in the same geographical coordinate system, and with the same initial error incorporated into every file. Consistency in data standards is important in maintaining data quality, and prevents the user from spending extra time correcting data for errors.

The locational accuracy of the aerial photographs following the georectification process was calculated using the accuracy standard of 1/50 inch for map scales greater than 1:20,000 (Eastman, 2003). To convert this accuracy standard into an allowable Root Mean Square (RMS) error (or amount that a single point in the image deviates from its actual location on the earth's surface), it was required that 95% of the accidental errors be equal to or less than 1.96 times the RMS error (Eastman, 2003). Therefore:

Allowable RMS = (Acceptable error on the ground/ z score probability of occurrence)

= (Acceptable error on the ground/1.96)

= (Error on the map * scale conversion * units conversion

= (1/50 inch * 50,000 * 0.0254 metres /inch)/1.96

= 12.96 metres

Therefore the RMS Error for the 1:50,000 aerial photographs must be less than or equal to 12.96 m in order to maintain the 95% accuracy. Thus, for features digitized from the 1:50,000 aerial photographs 95% of the locational errors will not be larger than 1.96 x 12.96 or +/- 25.4 m. It is important to note that although the aerial photographs were scanned at a high resolution the general rule of ½ a pixel for RMS was not practical for the working scale of the photography. Therefore RMS error was calculated using accuracy standards based on scale.

The RMS error for each of the georectified aerial photographs was calculated in the GIS using the following equation:

$$RMS_{error} = \sqrt{\sum_{i=n}^{i} (x' - x_{orig})^2 + (y' - y_{orig})^2 / n}$$

Where x_{orig} and y_{orig} are the actual coordinates for a specific point, and x' and y' are the locations of the same point in the georectified image.

Rectification of the aerial photographs produced an error of ± 4 m, which indicates that there is at most a 4-metre difference between actual distances connecting features on the aerial photographs and those same distances measured within the GIS. This was considered an acceptable error magnitude considering the scale of the aerial photographs and the size of moraine ridges.

Following the georectification process, the interpreted lines drawn on the aerial photographs were digitized on-screen within ArcMap. The interpretation lines could not

be extracted from the scanned photographs to create a separate file; therefore they were digitized from the photographs.

Individual data files were created for each of the landform types interpreted from the aerial photographs; moraine ridges, hummocks, meltwater channels and ridge outlines. Each file was then used to create maps showing the location of the landforms within the study area.

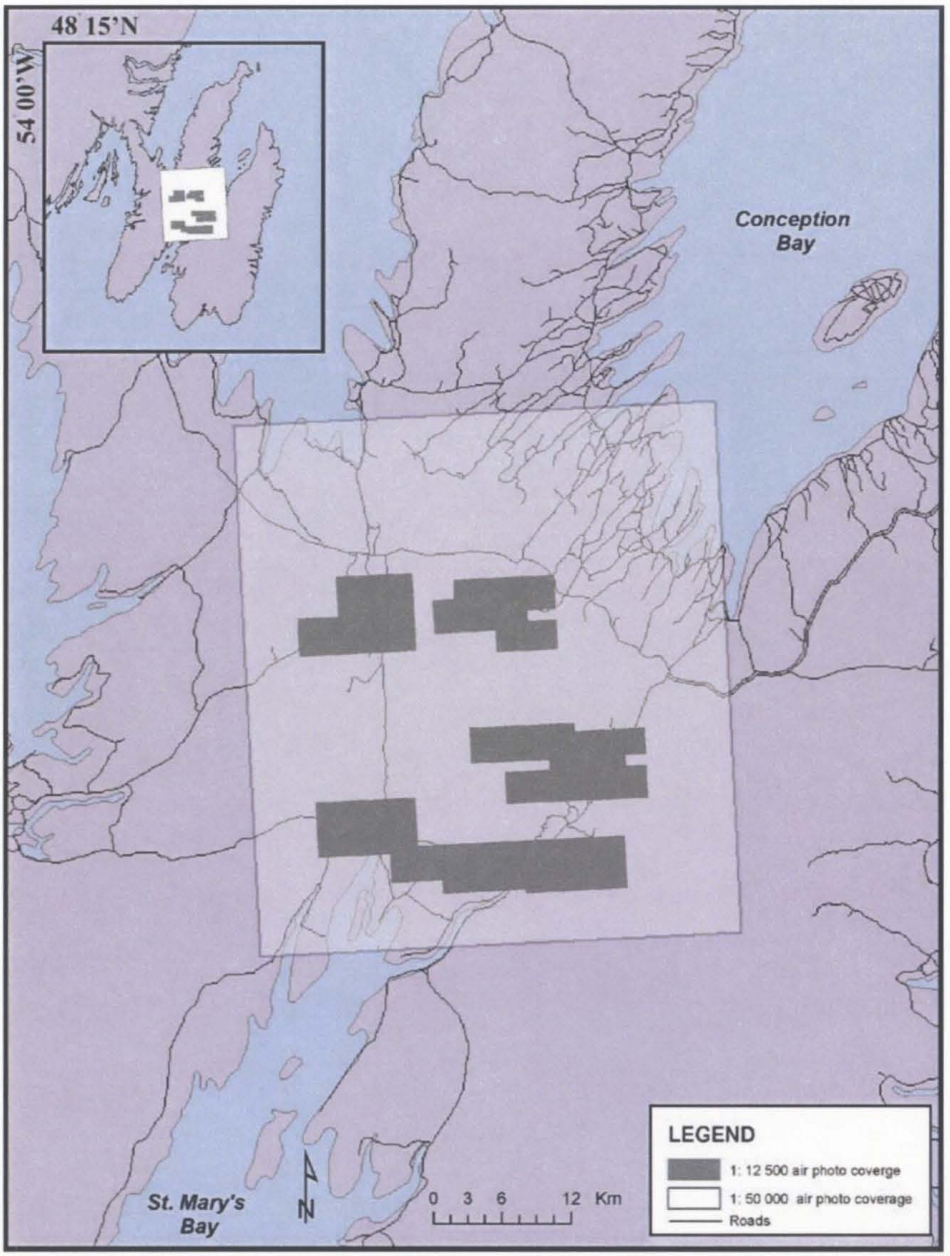

Figure 3.2 Aerial coverage of the 1:50,000 and 1:12, 500 aerial photographs interpreted in this study

3.4 Digital Elevation Model Construction

A digital elevation model (DEM) was created for this study from digital topographic maps at scales of 1:5000 and 1:2500. A total of 59 map sheets were converted to DEMs

covering an area of approximately 40 km^2 in the northeast corner of the study area (Figure 3.3). Digital topographic data was not available for the entire study area, and it was beyond the scope of this project to generate digital topographic maps at the 1:2500 scale. The digital topographic data were acquired as a set of digitized contour maps (5 m contour interval) in ArcView shapefile format from the Surveys and Mapping Division of the Newfoundland Department of Environment and Conservation. Separate shapefile layers included water bodies, road networks, utility lines, contour lines and map annotations. Elevation values were added to each of the contour and lake attribute tables using ArcView 8.3. Two additional layers were created: one containing spot height data, and another the outside boundary of the combined map sheets, which was later used to enclose the DEM, preventing errors of interpolation beyond the boundary.

The DEM was created using ArcMap's 3- D Analyst extension. A triangulated irregular network (TIN) of elevation points was used to model the continuous landscape surface of the map area, because it best preserves the morphology of the landscape (Kumler, 1994). The TIN model uses a continuous series of triangular facets to represent the elevation between contour lines (Burrough and McDonnell, 1998). A slight disadvantage to using a TIN model is that in areas of extremely convoluted contours facets may be created from three points all located on the same contour line thus creating a flat surface where in reality it may be gently sloping (Burrough and McDonnell, 1998). To address this concern, the elevation between two contours was calculated manually then compared to the elevation from the TIN model multiple times, and there was no marked difference in the elevation measures.

In addition to the DEM created for this study, a DEM with 30 m cell size in the USGS format (United States Geological Survey) was acquired from GeoBase to provide increased understanding of the topographic setting of the field of moraines (www.geobase.ca).

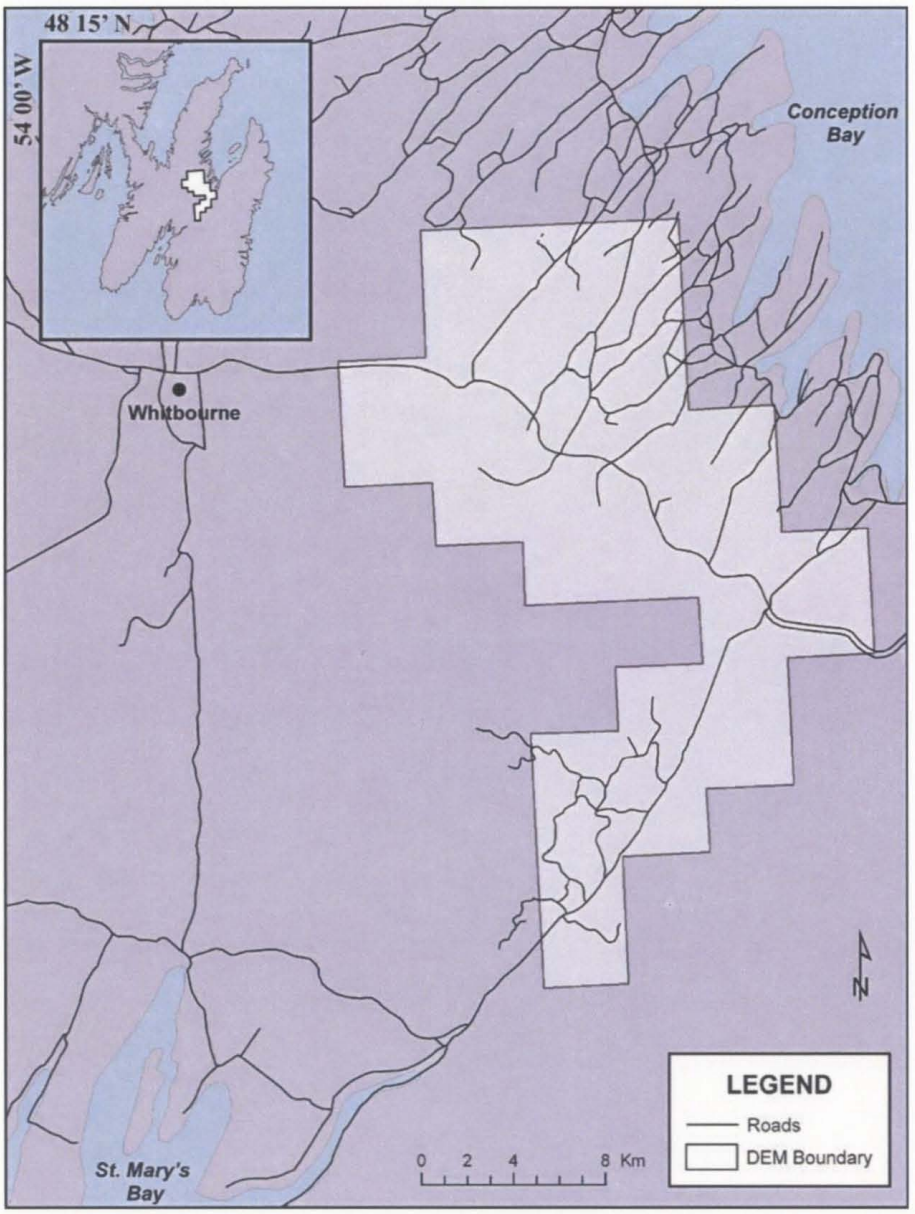

Figure 3.3 Map showing the location of the Digital Elevation Model (DEM) coverage.

To visualize the DEM the ArcScene component of ArcMap 8.3 was used. This program allows the user to alter the display properties of the DEM, such as shading, vertical exaggeration and view angle.

3.5 Data Analysis

3.5.1 Clast fabric statistical analysis

Statistics expressing the shape and strength of the clast fabrics were calculated using Georient 32 v 9, following the methods of Woodcock (1977). Eigenvectors (V_1, V_2, V_3) show the direction in which maximum clustering of clast orientations occur, as well as the planes perpendicular to the preferred fabric orientation. Eigenvalues (S_1, S_2, S_3) describe the degree of clustering around Eigenvectors. The fabric strength parameter is given by $C = \ln(S_1/S_2)$ and is considered weak when <1 and strong when >3 (Woodcock, 1977). The shape parameter is $K = (\text{Ln}(S_1/S_2))/(\text{Ln}\ (S_2/S_3)$. Clusters occur when K>1 and girdles when K<1. Clusters have a narrow range of plunge and trend values, whereas girdles show a broad range in trend values, and a narrow range of plunge values (Woodcock, 1977).

3.5.2 Grain size analysis

Sediment matrix samples were collected from each sediment exposure, and from each diamicton unit, if more than one unit was encountered. Grain size analysis was completed on samples from every site. A total of 31 samples were sieved following the methods of the Newfoundland Geological Survey. Seven sieves with screen sizes of 4 mm (-2Φ), 2 mm, (-1Φ), 1 mm (0Φ), 0.5 mm (1Φ), 0.25 mm (2Φ), 0.125 mm (3Φ), and

0.0625 mm (4Φ), were used. The silt and clay fractions of the matrix samples were not separated, because the grain size analysis was employed primarily to determine if there was a substantial difference in the combined clay and silt fractions of the matrices of different units. The precise percentages of silt and clay were not deemed important for a simple comparison of matrices from different diamicton units, as the research was not concerned with silt and clay proportions simply the total amount. The sediment samples were weighed and all data recorded. Grain size distributions were then graphed using the Microsoft Excel spreadsheet software.

3.5.3 Ridge orientation calculations

The orientations of the moraine ridge crests were calculated within the GIS. Individual ridges were digitized from the aerial photographs, and each ridge consisted of several line segments. Each line segment was treated separately within the GIS; the orientation of which was calculated and an average orientation value was calculated. A simple calculation of average values does not result in the actual average orientation and therefore several calculations had to be performed to determine the mean orientation of the ridge crests (Appendix A).

3.5.4 Ridge wavelength (periodicity) measurement

Ridge wavelength is an important landscape characteristic related to formative process (Dunlop 2004) and therefore calculations were made from the DEM. A "distance coverage" was created from the ridge crest shapefile to aid in the calculation of the distances between ridge crests. This coverage classified the areas around ridge crests

according to the distance it was away from adjacent ridge crests. Transects perpendicular to the ridge crests in individual tracts of moraine were then digitized (Figure 3.4), and profiles showing the distances between ridge crests were created within ArcView 3.2 using the "Easy Profiler" extension. Average wavelength for each transect, as well as the average wavelength amongst all transects, were then calculated.

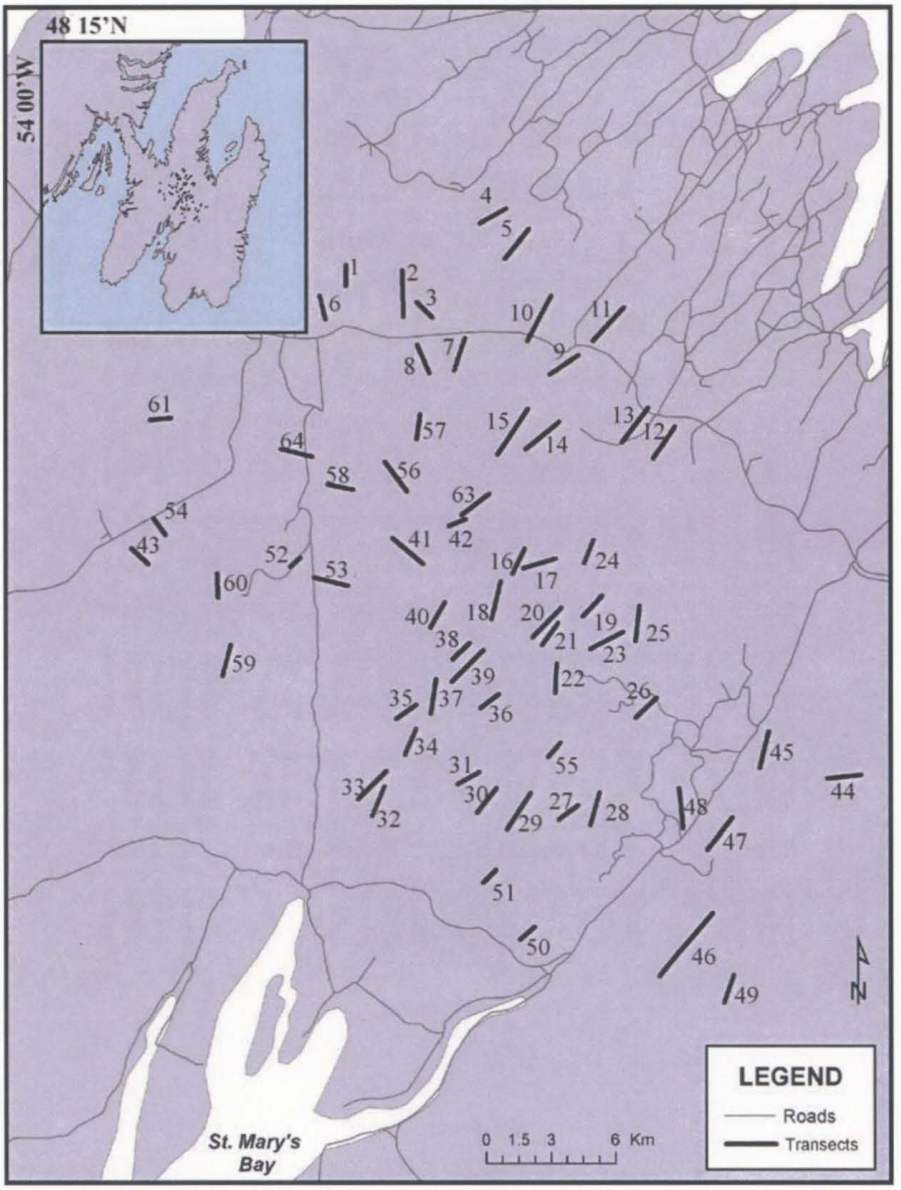

Figure 3.4 Location of transects used for moraine ridge wavelength calculations.

Chapter 4 Results

This chapter presents the study results and is structured according to the research questions posed in Chapter 2.

4.1 Study area description

This research re-examined the field of moraines on the central Avalon Peninsula. Figure 3.1 shows the location of sites examined in this study. The moraine field sits on a broad (~20 km wide), convex bedrock ledge that is bounded to the west by a wide (~8 km), shallow (approximately 25 m deep) north-south trending valley (informally named the Whitbourne trench and approximately 25 m deep) that extends from St. Mary's Bay to Trinity Bay (Figure 4.1). The ledge rises from ~115 to ~170 m a.s.l.

4.2 Morphology, orientation, and spatial patterns of moraine ridges on the central Avalon Peninsula

The moraines ridges are generally well developed, forming continuous, parallel, and evenly spaced ridges (e.g., Figure 4.2). They are best developed in localized, bedrock-controlled linear troughs. Where poorly developed, moraines appear highly dissected, discontinuous, and unevenly spaced (e.g., Figure 4.3). These were observed mostly in the south-eastern part of the moraine field. Moraine ridge shape varies throughout the field, but generally the ridges are linear and sinuous. There is no evidence that any of the moraines in the study area were drumlinised, and no drumlins have been identified within the field of moraines or along its boundaries.

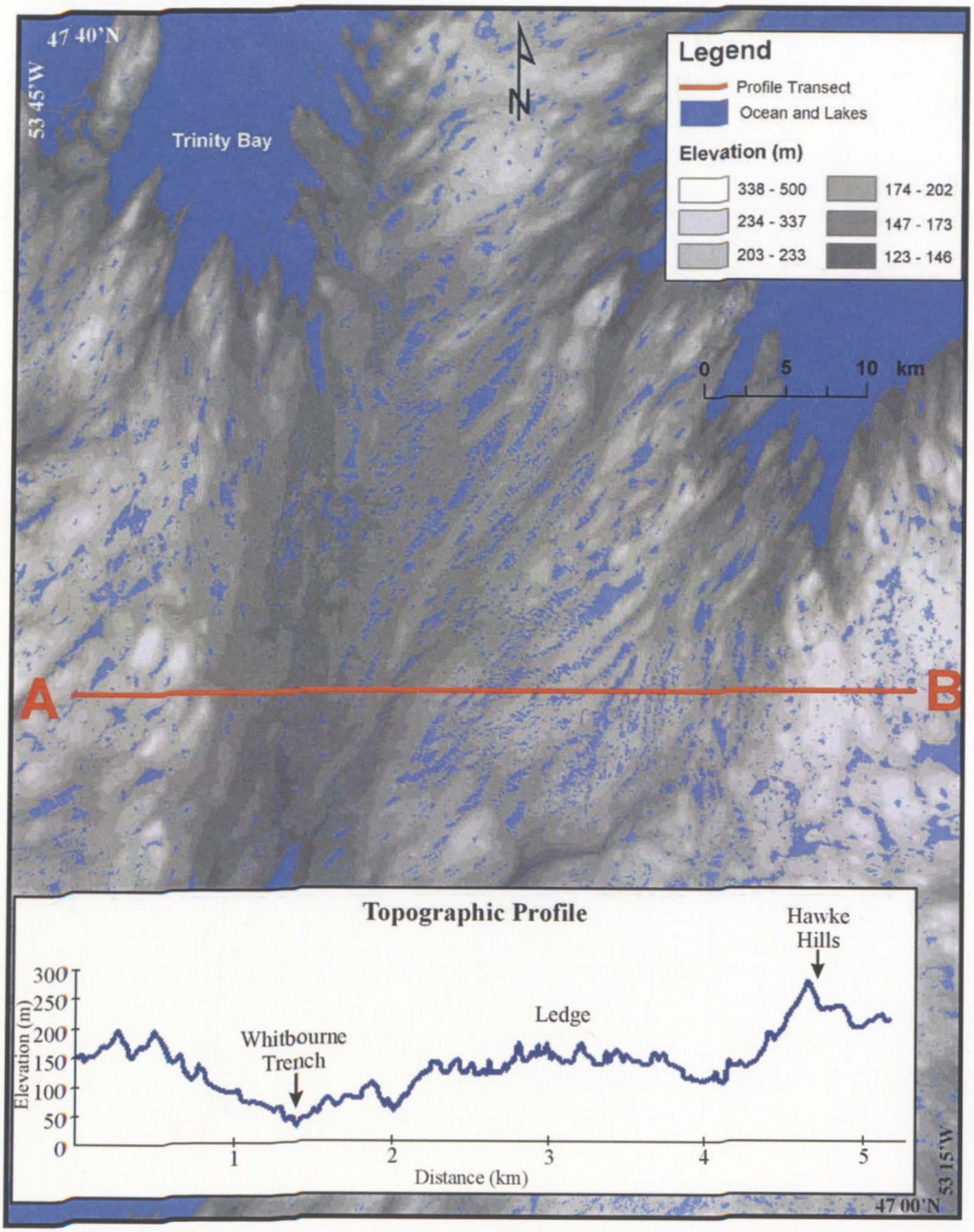

Figure 4.1 Vertical profile across the study area. Note the graph represents a transect between A and B marked on the map. The Whitbourne Trench is easily recognizable in the profile as well as the ledge upon which the majority of moraine ridges are located. Vertical exaggeration equals 20 times.

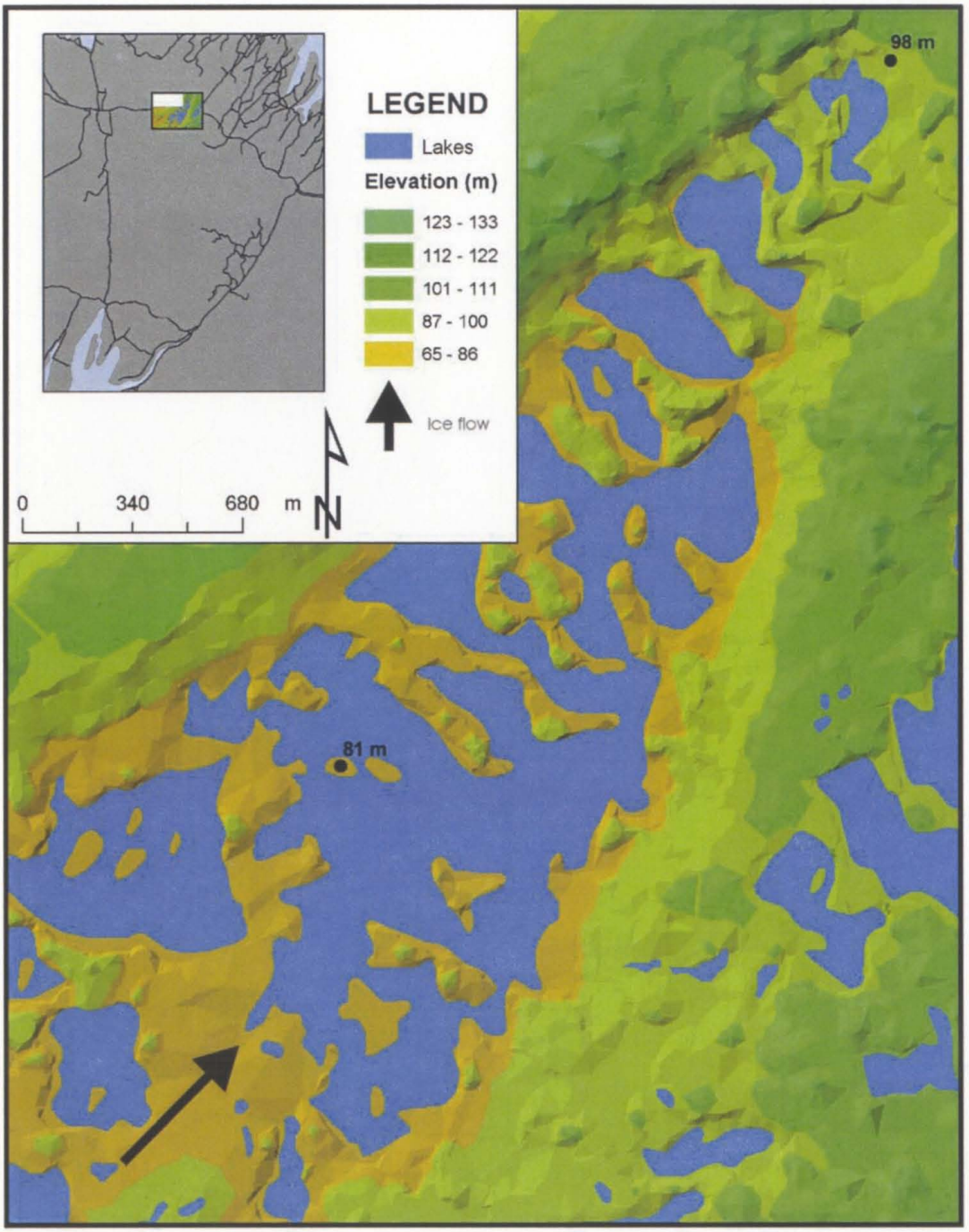

Figure 4.2 Shaded relief map showing well-developed moraine ridges at Hodgewater Pond. Elevation increases from the southwestern corner of the map to the northeast corner.

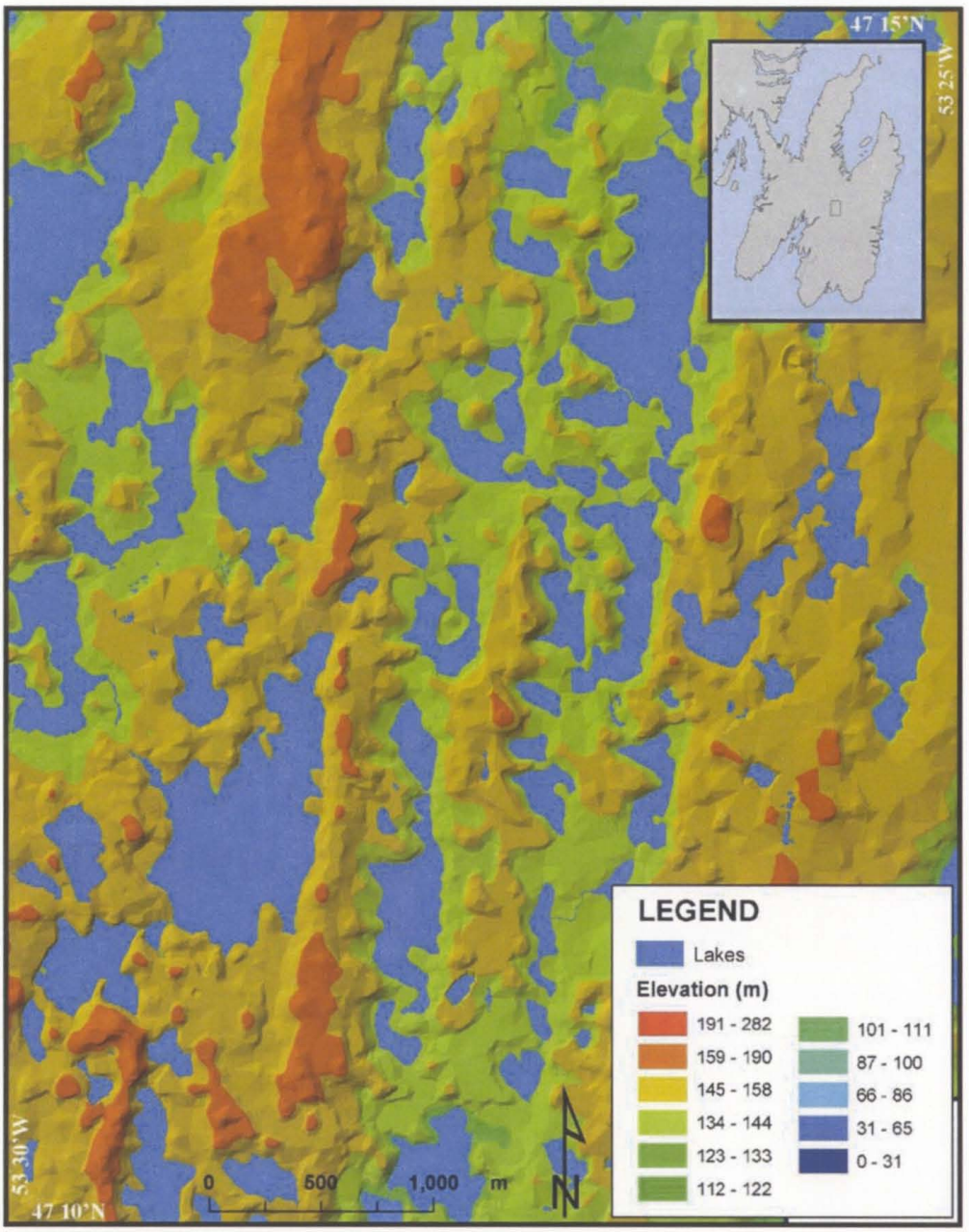

Figure 4.3 Shaded relief image showing poorly-developed moraine ridges. The ridges are short and irregularly-oriented, unlike the well-developed moraine ridges elsewhere.

Mean ridge heights and widths average 25 m and 200 m, respectively as measured from the DEM (Table 4.1). Although, ridge heights estimated from the DEM may be unreliable, elevations are consistent with field observations. Mean ridge length is 400 m,

but ranges from 50 m to 1500 m. The spacing between ridges is generally between 200 and 300 m, based on wavelength measurements along 64 transects of the DEM (the spacing between 292 pairs of ridges) (Table 4.2). Generally, the spacing between ridges within a single transect is fairly uniform, but it does appear to decline as slope gradient increases. For example, at Hodgewater Pond the mean spacing decreases from 350 m to 180 m where the elevation rises by approximately 10 to 15 m and the trough narrows to about 500 m (Figure 4.2). Where there is an abrupt increase in slope gradient, for instance against the steep bedrock slope in the northeast corner of the study area, the moraine field terminates and gives way to streamlined bedrock.

Table 4.1 Moraine ridge dimensions determined from the Digital Elevation Model (DEM).

	Height (m)	**Width (m)**	**Length (m)**	**Spacing/ Wavelength (m)**
Mean	25.0	200.0	400.0	276.0
Median	24.0	199.0	397.0	246.5
Mode	22.0	178.0	340.0	173.0
Standard Deviation	6.9	37.0	157.0	134.6
Standard Error	0.4	2.2	2.7	7.9
Range	25.0	212.0	1450.0	730.0
Minimum	5.0	38.0	50.0	70.0
Maximum	30.0	251.0	1500.0	800.0
Count (n)	292	292	3342	292

Table 4.2 Average wavelength measurements for each of the 64 transects drawn through of the Avalon Peninsula moraine ridges.

Transect No.	Average Wavelength (m)	Transect No.	Average Wavelength (m)	Transect No.	Average Wavelength (m)
1	165.77	22	198.52	43	224.76
2	204.71	23	282.75	44	290.10
3	219.68	24	317.86	45	262.67
4	221.74	25	256.48	46	280.07
5	318.43	26	332.44	47	187.75
6	263.32	27	256.14	48	258.23
7	239.10	28	191.11	49	196.98
8	286.74	29	343.14	50	285.37
9	214.77	30	279.59	51	143.23
10	304.61	31	215.56	52	198.65
11	428.50	32	171.43	53	206.35
12	260.50	33	274.17	54	294.03
13	372.10	34	208.19	55	290.67
14	335.64	35	194.37	56	235.76
15	398.87	36	203.42	57	179.27
16	186.98	37	196.48	58	275.72
17	183.89	38	204.12	59	282.18
18	252.37	39	241.56	60	226.91
19	182.36	40	205.90	61	200.03
20	220.97	41	343.02	63	204.55
21	183.47	42	203.14	64	301.86

Moraine ridges are commonly oriented perpendicular to the northeast-southwest-trending bedrock structure of the study area (Figure 4.4). Only along three transects were ridges observed to roughly parallel the structural trend. Individual ridges may branch at one end (e.g., Eastern Waters, Figure 4.5), or coalesce with one another. Moraine ridges tend to lose their individual morphology at higher elevations between troughs where they coalesce to form hummocky moraine (e.g. Nichols Pond, Figure 4.6).

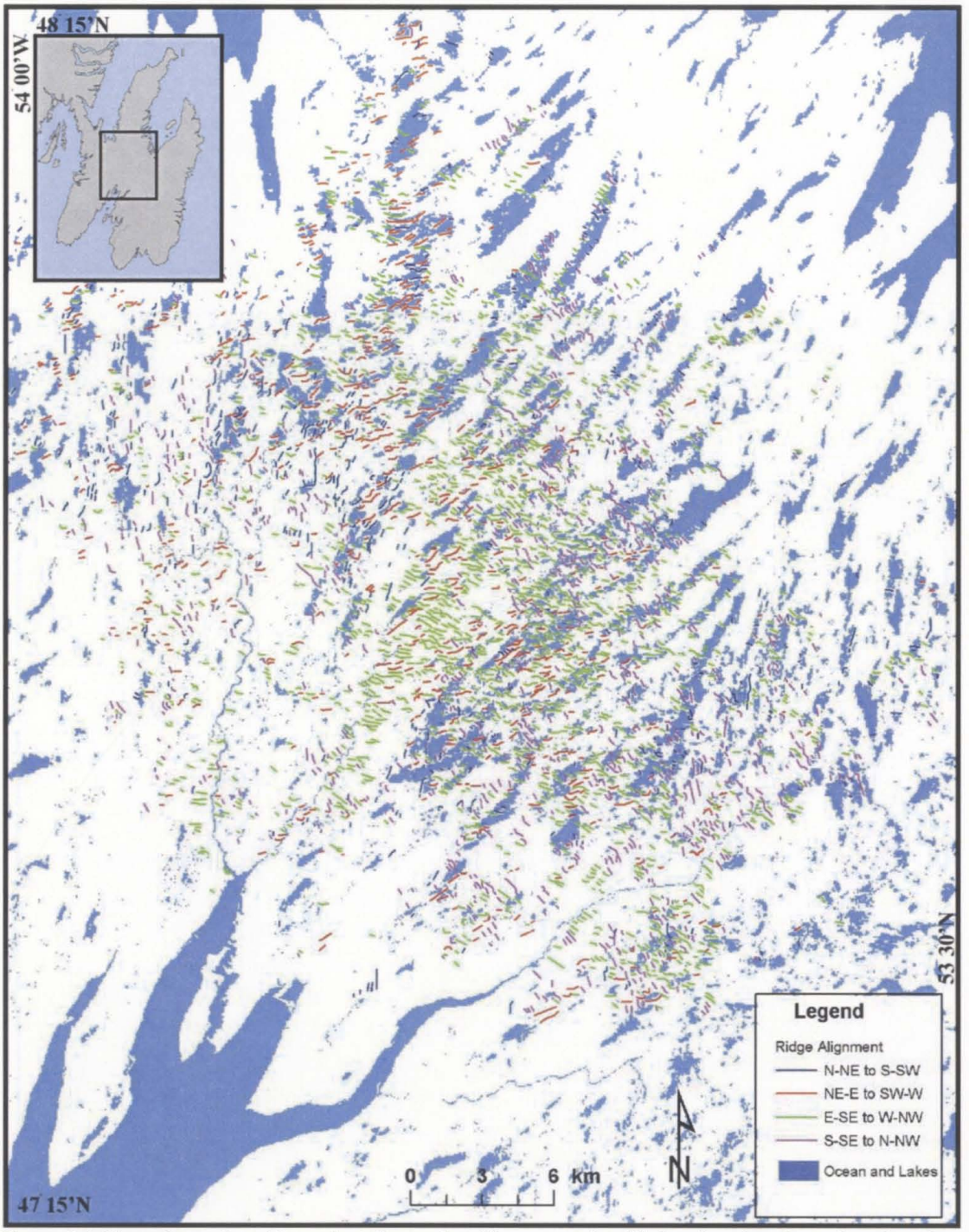

Figure 4.4 Map of moraine ridge orientations. Landforms are classified and assigned a colour based on their average orientation. Notice that a large proportion of the ridge crests are aligned between E-W and NW-SW.

The mean alignment of moraine ridges is northwest-southeast, but there appears to be a gradual progression from northeast-southwest (approximately 20% of the field) to northwest-southeast from west to east across the field. In the western portion of the study area the moraine ridges are aligned predominantly northwest-southeast, in the central portion of the field east-west to northeast-southwest, and northeast-southwest near the eastern edge (Figure 4.4). Calculations of ridge orientations within the GIS support the apparent visual pattern (Figure 4.4). Most of the moraine ridges in the study area are oriented roughly perpendicular to the dominant northeastward ice flow direction on the central Avalon Peninsula as mapped by Henderson (1972), Catto (1998), and Batterson and Taylor (2004).

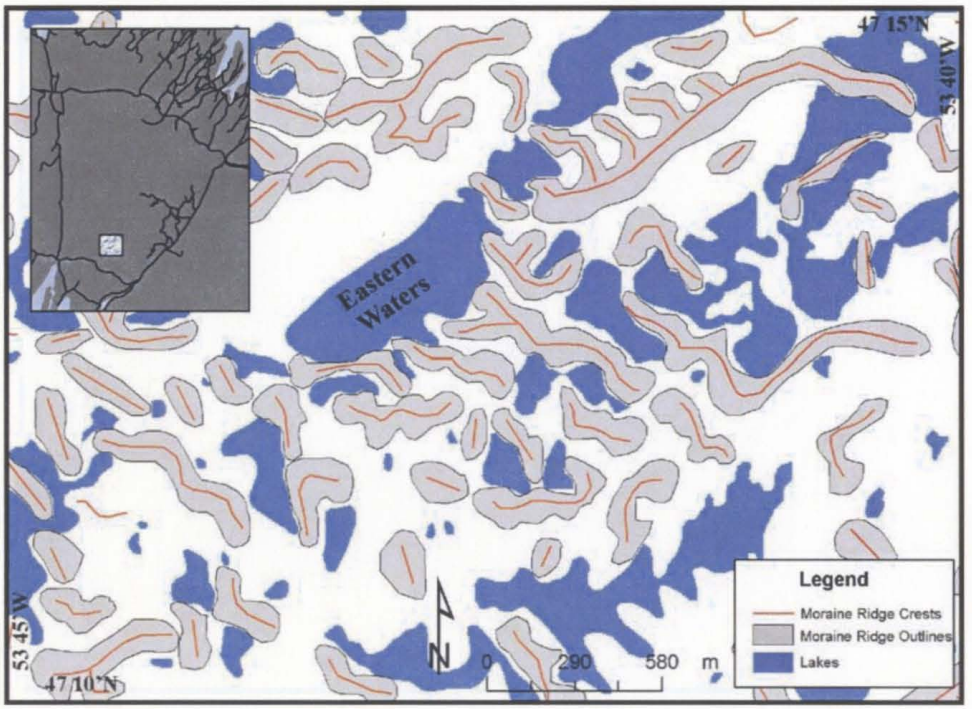

Figure 4.5 Map showing ridge crests (red) and ridge outlines (grey) as interpreted from 1:12,500 colour aerial photographs. This image shows the sinuosity of the ridges, as well as their occasional branching and intersection.

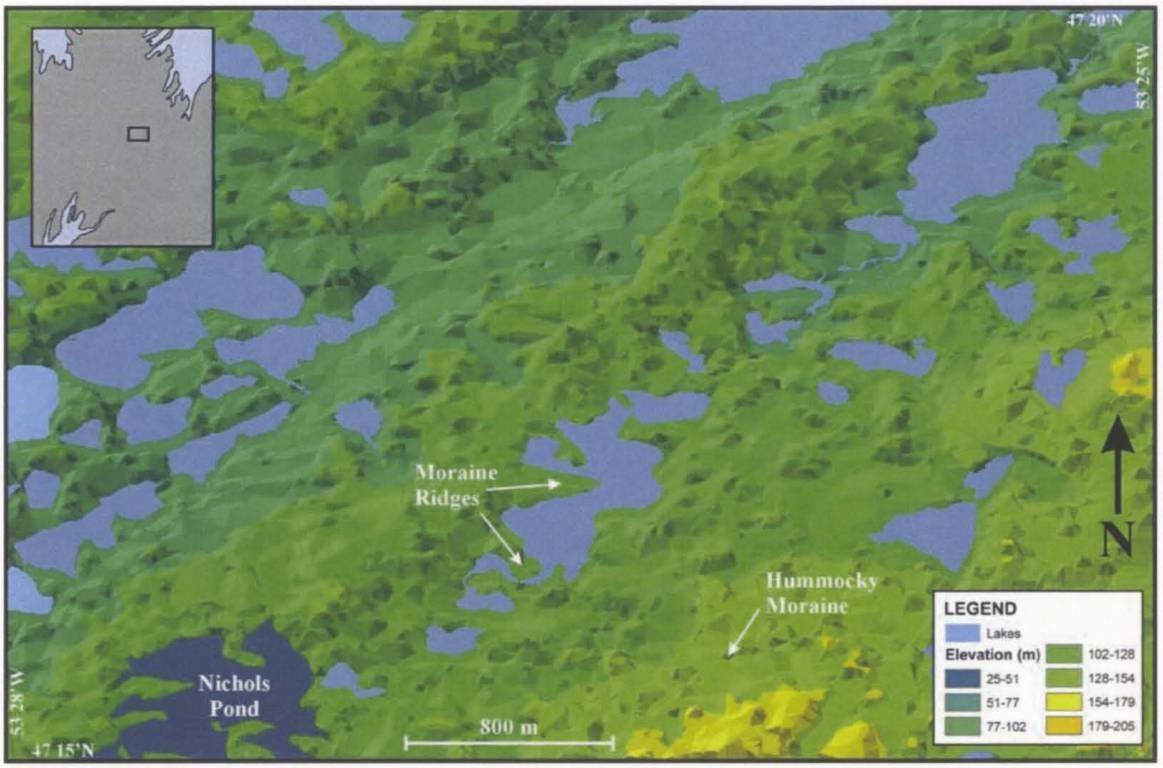

Figure 4.6 Oblique shaded relief image northeast of Nichols Pond.

Although it is typical for multiple moraine ridges to be aligned parallel to one another in sets, some show no such alignment. For example, around Whitbourne some ridges intersect at right angles (Figure 4.7). This is not considered hummocky moraine because the landforms retain their distinct linearity and morphology, and are unlike hummocks mapped elsewhere in the study area.

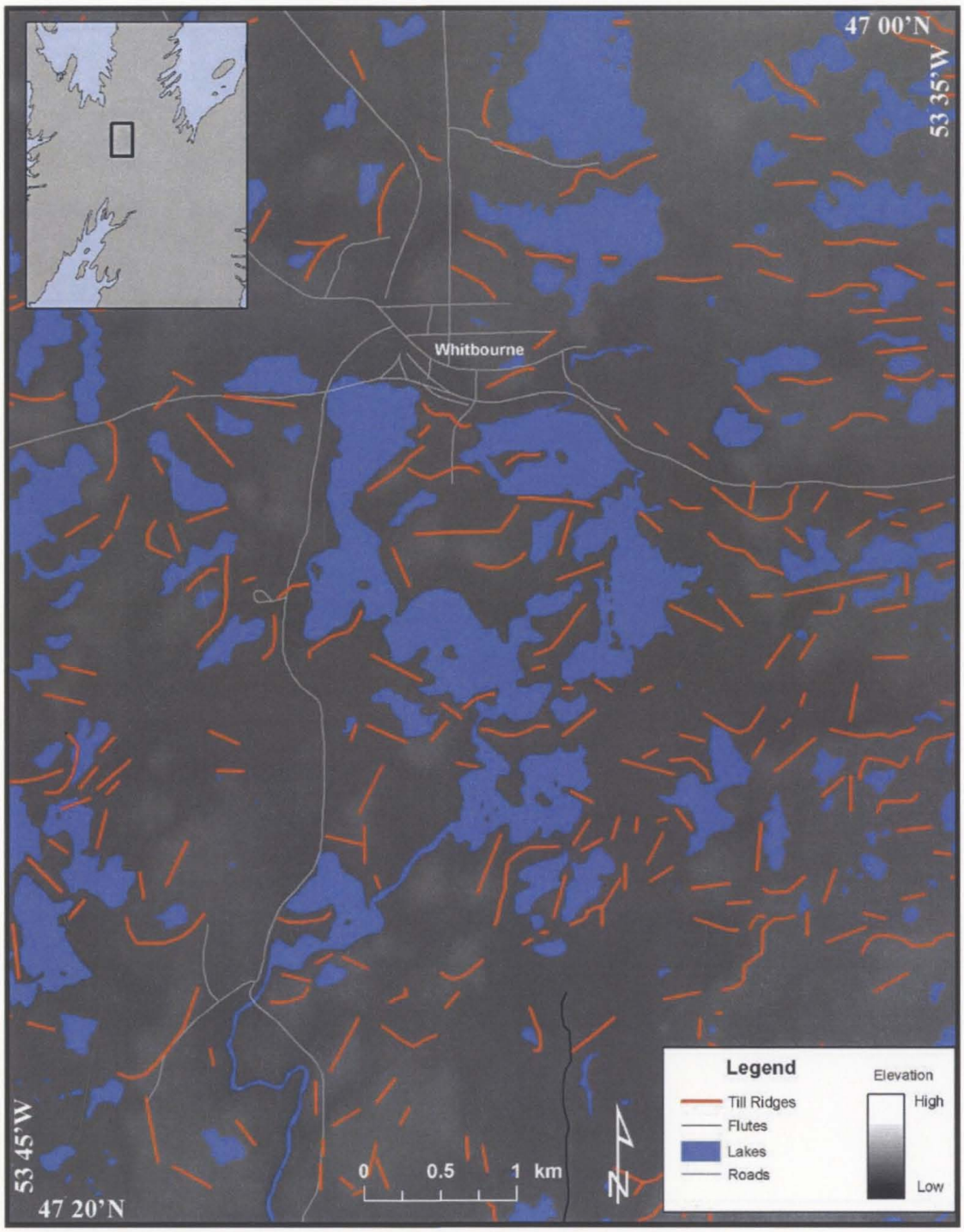

Figure 4.7 Map showing irregularly aligned moraine ridges in the Whitbourne area.

4.3 Relationship of moraine ridges to other glacial landforms

Aerial photograph interpretation, and inspection of the DEM revealed four additional glacial landform types; flutes, hummocky moraine, meltwater channels and streamlined bedrock ridges. The following sections describe these landforms and their relationship to the moraine ridges. (See Appendix B for a map showing the location of moraine ridges, hummocky moraine, and meltwater channels.)

4.3.1 Flutes

Most flutes are located along the western edge of the moraine field, west of the Whitbourne Trench. Less commonly, isolated flutes were also observed within the moraine field, generally oriented perpendicular to moraine ridges. In contrast to moraine ridges, flutes tend to be longer (generally >450 m), straighter, and restricted to higher ground (e.g., Figure 4.8). The height of the flutes could not be calculated but generally they are of lower relief than moraine ridges. The flutes occur in groups and are sub-parallel to one another. Aerial photograph interpretation suggests that they are composed of unconsolidated material, not bedrock, because of surface exposures. There are several instances where moraine ridges appear to grade or drape over a flute, but unfortunately the morphological evidence is unclear.

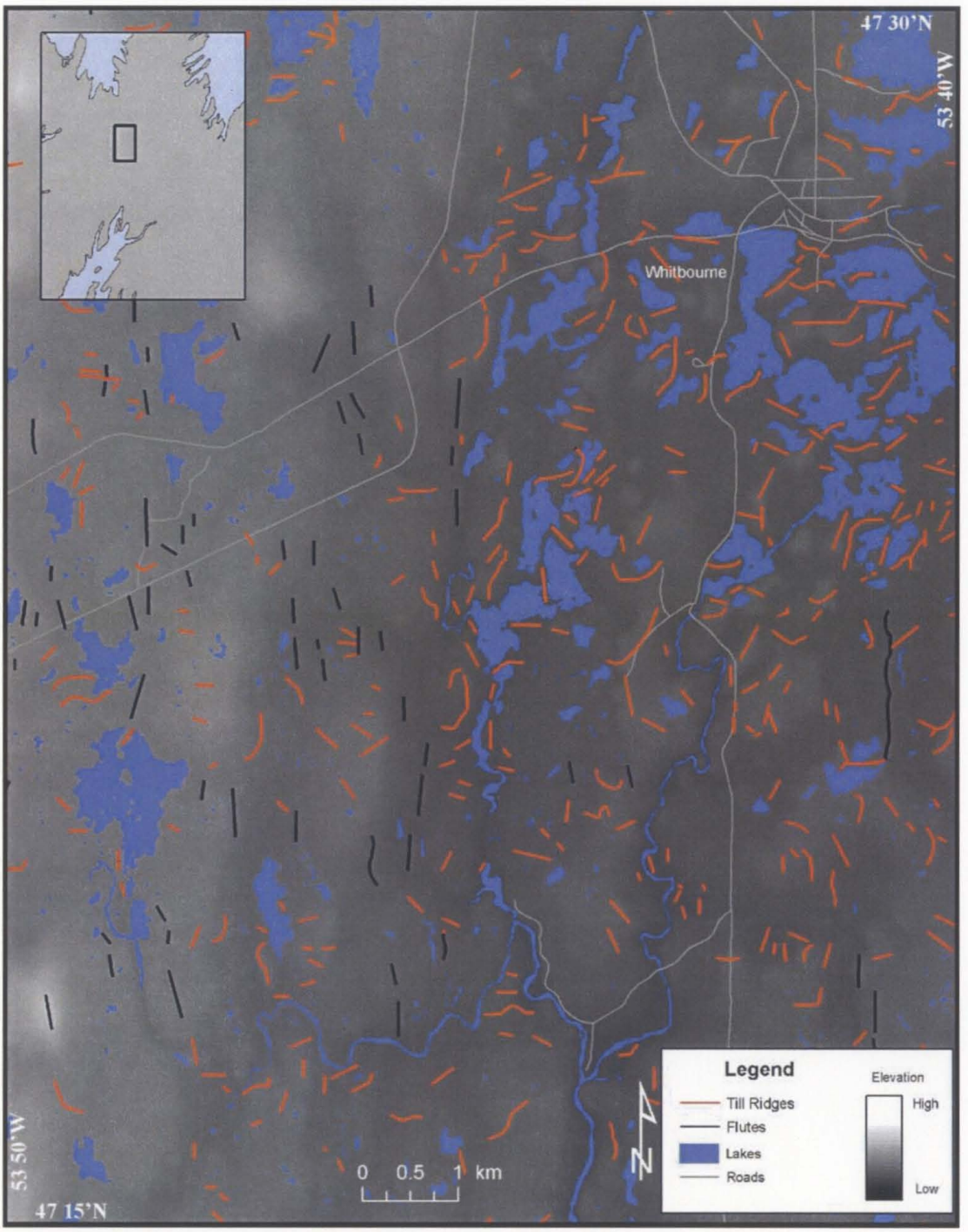

Figure 4.8 Shaded relief map showing moraine ridges in the Whitbourne Trough, and flutes on the uplands to the west.

4.3.2 Hummocky Moraine

Hummocky moraine is generally located on upland surfaces, and on ridges between bedrock troughs (e.g., near Hawcos Pond, Figure 4.9). It consists of rounded knob-like hills, elongate to circular mounds, and short randomly-oriented ridges. Individual hummocks are up to 200 m in diameter. Doughnut-shaped mounds are roughly circular in plan form and have a depression, commonly water-filled, at their centre. In some places, moraine ridges intersect the mounds (e.g., Figure 4.10).

Transition zones occur between the areas of hummocky moraine on the uplands and well-developed moraine ridges on adjacent valley bottoms. In these zones moraine ridges are shorter, more subdued and have a less structured pattern. Hummocks in these zones tend to be spaced farther apart and are longer and more sinuous than elsewhere (e.g., Nichols Pond, Figure 4.6).

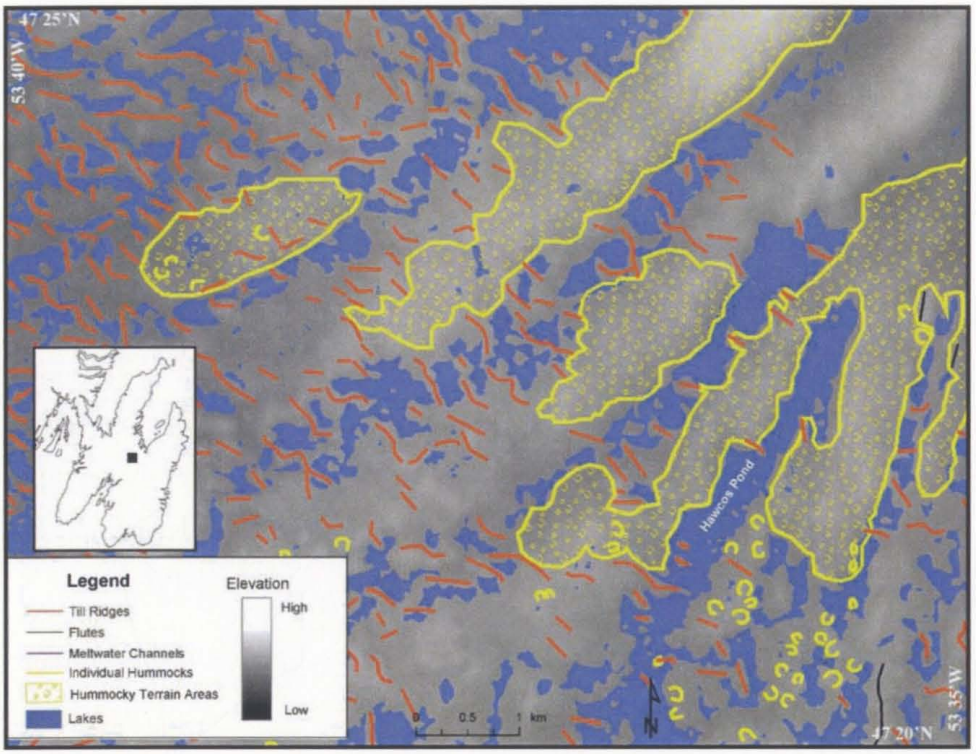

Figure 4.9 Map showing the relationship between ridged moraine, hummocky moraine, and the underlying topography. Hummocky moraine is located on interfluves, whereas moraine ridges occupy the troughs.

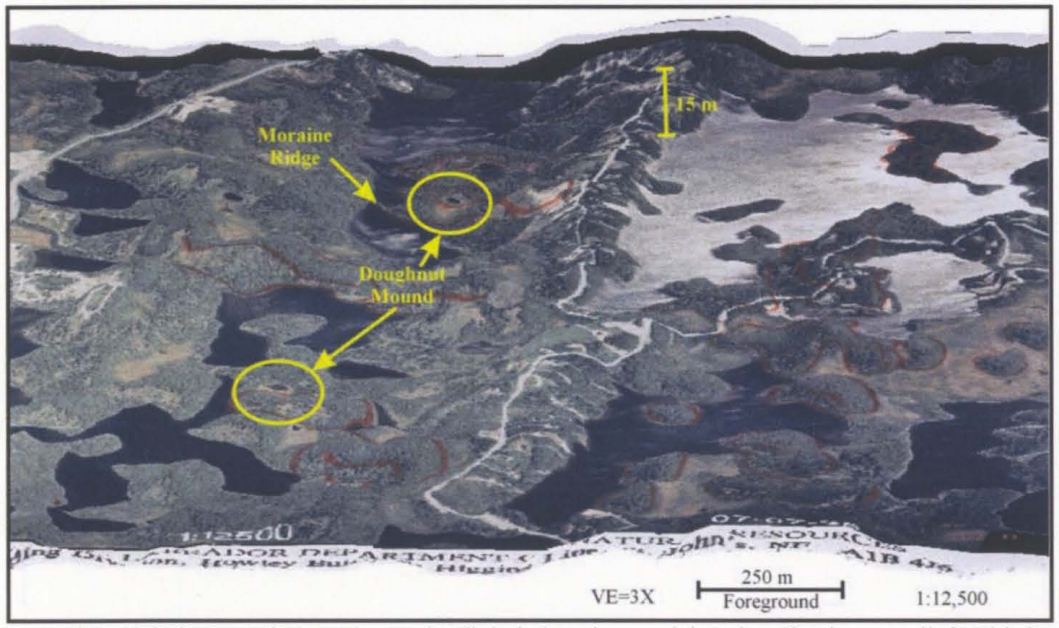

Figure 4.10 Aerial photograph draped over the digital elevation model to show landscape relief. This image shows the doughnut mounds with intersecting moraine ridges (Note, red lines on the photograph were drawn by the author during interpretation).

4.3.3 Streamlined bedrock ridges

Streamlined bedrock ridges are prominent features in the northeast corner of the study area (Figure 4.11). Aerial photograph interpretation indicates that they are eroded in bedrock, predominantly sandstone and siltstone of the Conception and Signal Hill groups. They are between 600 and 3000 m wide - generally widest at their northeast end, between 2 and 7 km long, and between 25 and 100 m above the surrounding landscape. They trend northeast-southwest. A thin, discontinuous till veneer covers their surface.

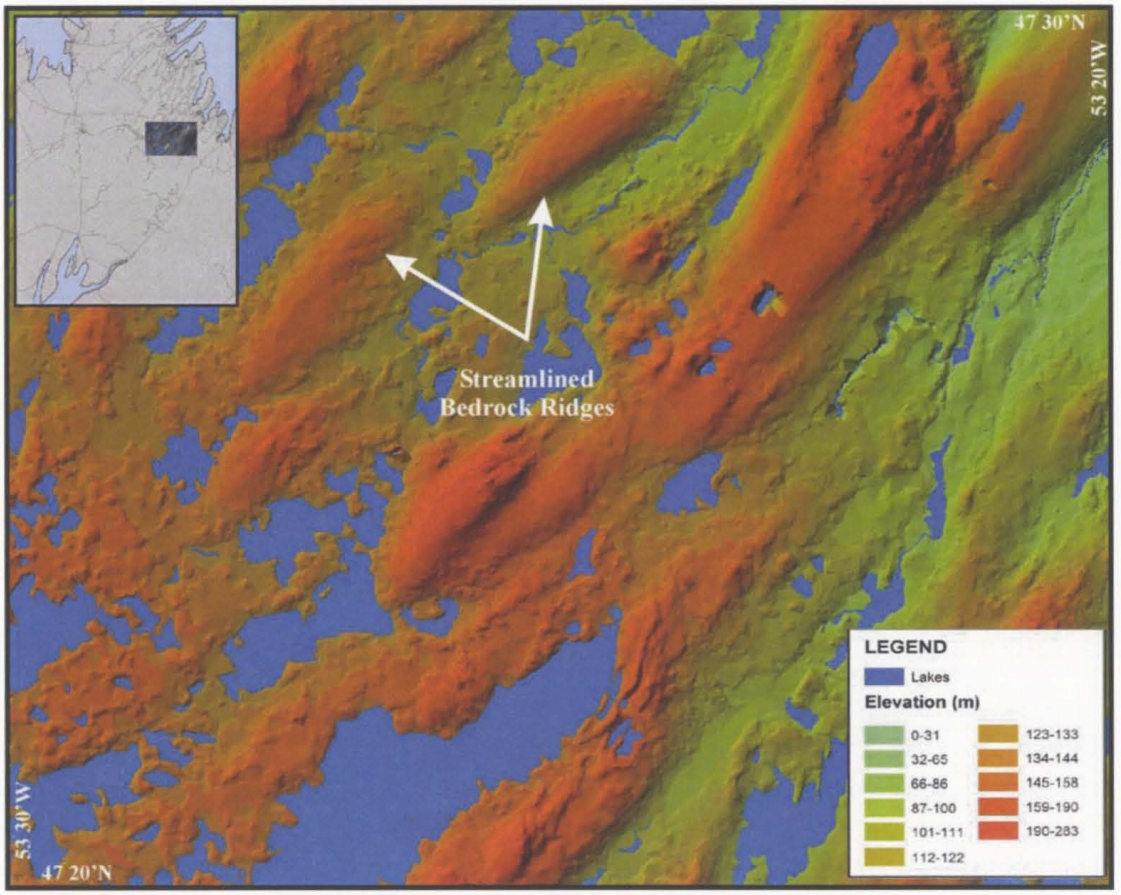

Figure 4.11 Shaded relief showing the streamlined bedrock ridges. Note the dominant northwest-southeast orientation of the features in the landscape. The ridges represent the highest points in the landscape.

4.3.4 Meltwater Channels:

Meltwater channels are confined to valley sides in Salmonier Arm and Colinet Harbour (Figure 4.12). They are relatively short, between 100 and 600 m long, parallel channels eroded into till.

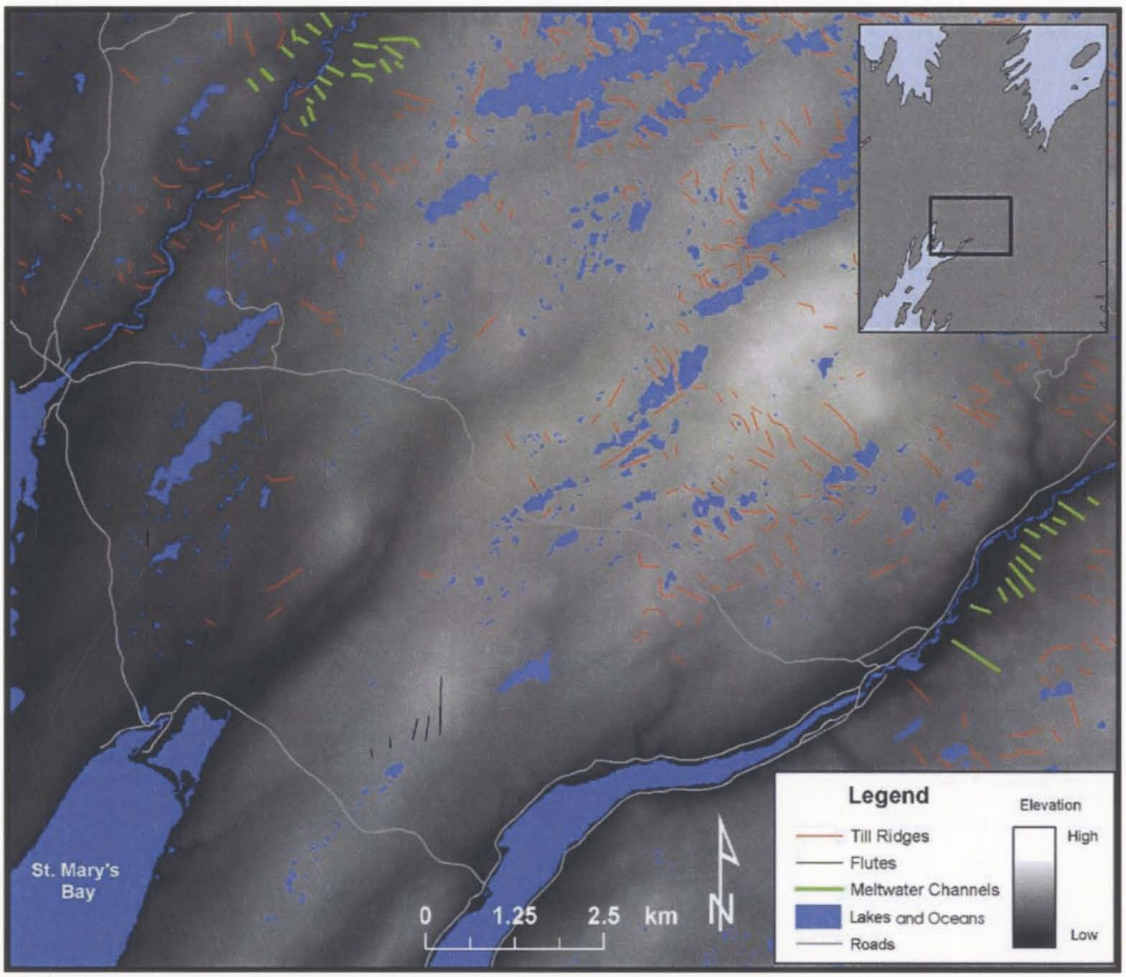

Figure 4.12 Location of side-hill meltwater channels along two valleys draining into St. Mary's Bay.

4.4 Internal composition of ridged and hummocky moraines

4.4.1 General description

A total of 26 exposures were examined, 18 through features interpreted as moraine ridges, and 8 in hummocky moraine. Sedimentary logs are presented for each exposure in Appendix C. Summary descriptions are presented here along with select examples to illustrate important structures and relationships. Exposures were generally located within the upper portion of the ridges and hummocks (Figure 4.13). All of the exposures were either minor aggregate pits, or road cuts. Exposure height ranged from 3 m to 15 m, but were typically 5 to 8 m high.

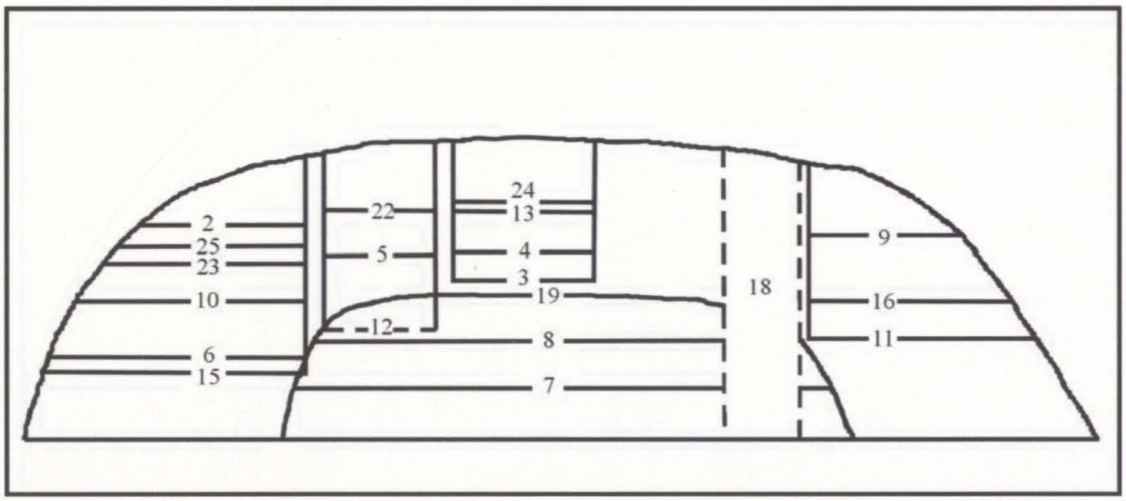

Figure 4.13 Relative position and depth/height of individual exposures recorded in moraine ridges. Numbers refer to the site locations

At 20 of the 26 exposures only a single sedimentary unit was observed. It consisted of an olive grey (5Y 6/1), compact diamicton with a silty sand matrix. Stone content varied from 20 to 80 percent, but was generally greater than 50 percent. Clast lithologies were consistent with the local bedrock, and clasts were predominantly angular

to subangular. Clast diameter averaged 10 cm but ranged up to several metres. Faceted and striated clasts were observed in half to three-quarters of the exposures.

Grain size analysis was carried out on 31 samples of diamicton matrix (the fraction of material sand sized and smaller) (Appendix D). For the most part they were bimodally distributed, with the > -2Φ (4 mm) and <4Φ (0.0625 mm) fractions dominating the samples. The percent of sample weight ranged from 5.8 to 40.6% for > -2Φ size, and 10.5 to 45% for the <4Φ size. Intervening grain size classes tended to have similar percentage by weight values in each sample. Cumulative graphs of the sample weight exhibit a roughly linear trend (Appendix E).

Minor amounts of sorted sediment occurred as lenses of normally graded to massive openwork gravel and coarse sand (Figure 4.14). These concave lenses always mirrored the underside of clasts and pinched out towards clast edges. Lens thickness was proportional to clast size and varied between a few millimetres and >10 cm thick. Boulder lines occurred at 10 of the 26 sites, and consisted of single rows of aligned similarly-sized clasts (Figure 4.15). Striations were not observed on the boulder tops, but they were usually underlain by openwork gravel that extended the length of the boulder line.

Figure 4.14 Photograph of a typical deposit within exposures on the Avalon Peninsula. Openwork gravel lenses are outlined. Each division on the scale bar is 1 cm.

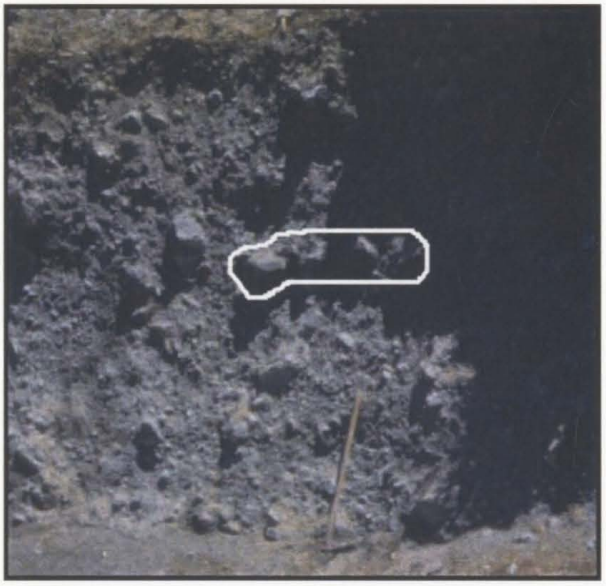

Figure 4.15 Horizontal boulder line (outlined in white) 4 clasts long. The pick axe is approximately 80 cm.

Boulder lines were overlain by silt caps, the thickness of which increases proportionally with the size of the underlying clast, varying from a few mm to 5 cm thick (Figure 4.16). Thin layers (no more than 5 mm thick) of sand occasionally overlie the silt caps.

Figure 4.16 The remnant of a silt cap lining a cavity from which a clast was removed.

The following are descriptions of two typical exposures, examined in this study. Site 1 and 9 like 75% of the exposures, are composed of a single diamicton.

Site 1 was a 7 m high exposure cut into the southeast slope, near the top of a moraine ridge (Figure 4.17). It was composed of a coarse, highly compact, olive grey (5Y 4/2) diamicton (>50% stoniness), with a predominantly silty sand matrix. Clast lithologies were composed of local sandstones and siltstones of the Conception and Signal Hill groups. Clasts were commonly angular, striated and faceted. Grain size analysis revealed that the matrix was predominantly silty sand (Figure 4.18). Openwork gravel beneath individual boulders and boulder lines was common throughout the exposure.

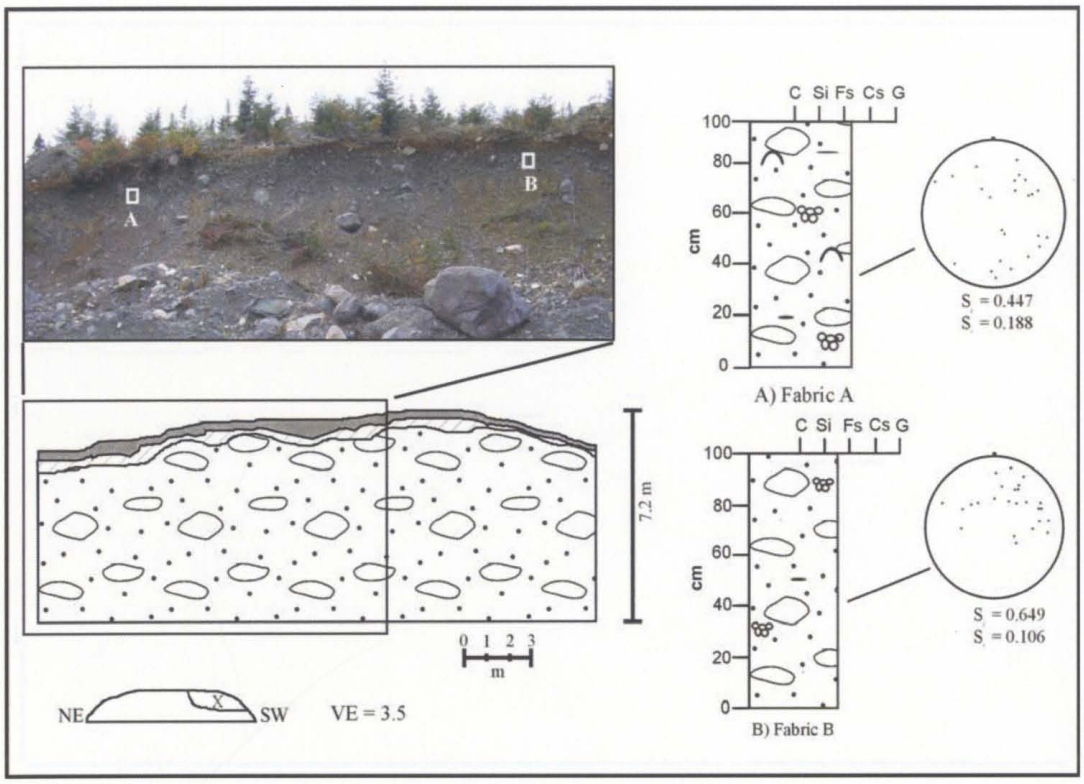

Figure 4.17 Site 1 exposure sketch, including site photograph, sedimentary log and clast fabric diagrams. Refer to Appendix C for legend.

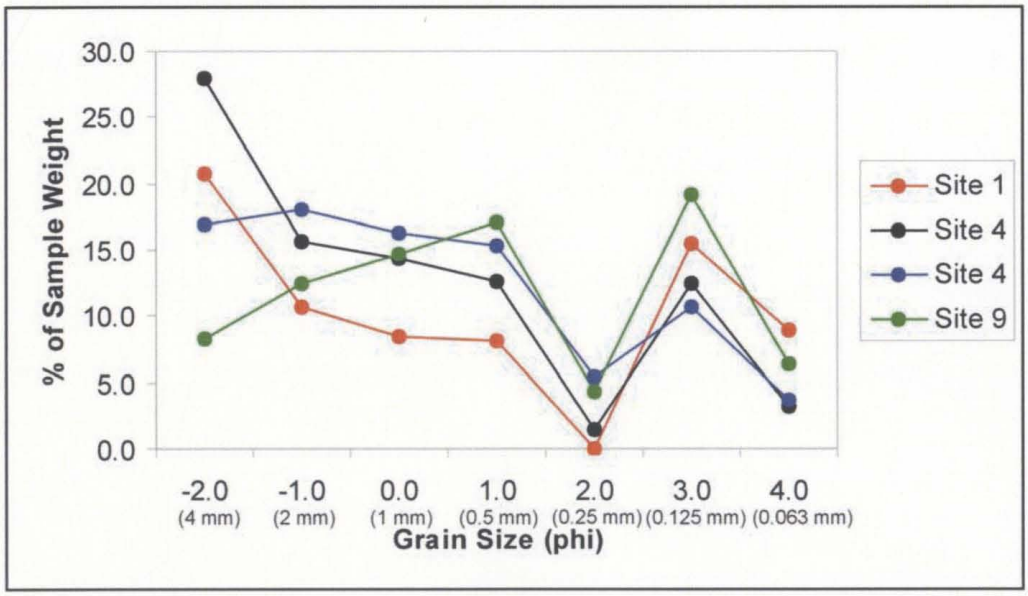

Figure 4.18 Graph of grain size against percent sample weight for diamicton matrix samples from sites 1, 4 and 9.

Site 9 is a 6 m high exposure in the top of the eastern face of a moraine ridge (Figure 4.19). The exposure was composed of a coarse-grained, compact diamicton. Stone content was greater than 50% and clast lithologies were local sandstone and siltstone. Clasts were angular to sub-angular, striated and faceted. The diamicton matrix was predominantly fine sand. Openwork gravel lenses beneath clasts, and silt caps overlying clasts were present throughout the diamicton.

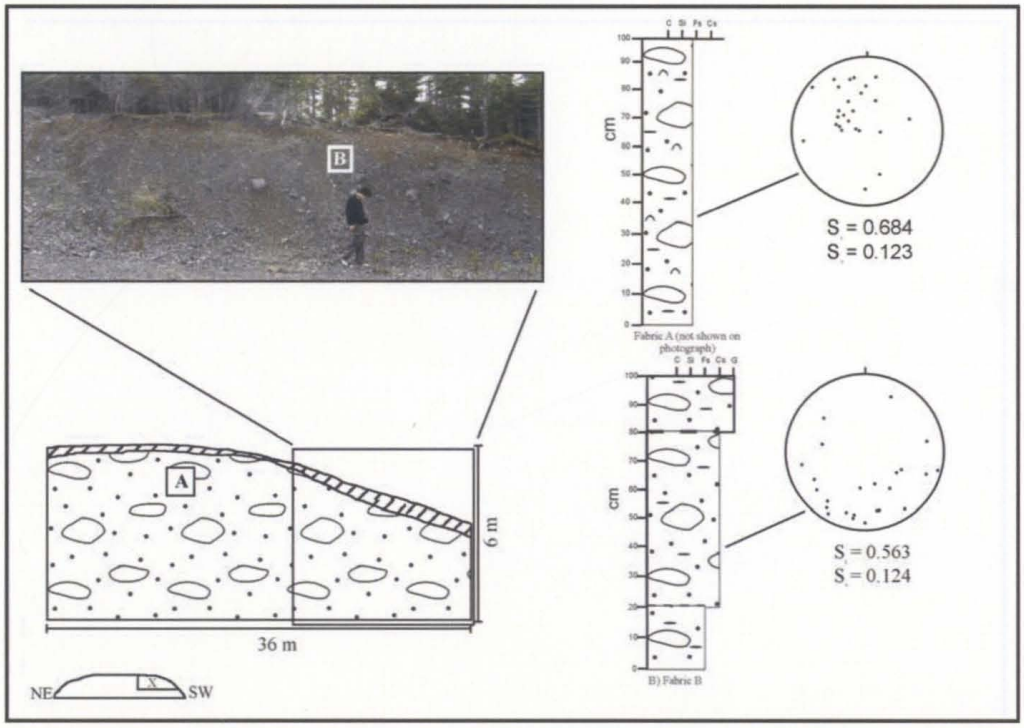

Figure 4.19 Site 9 exposure sketch including site photograph, sedimentary log and clast fabric diagrams.

4.4.2 Upper and lower diamictons

At 9 of the 26 sites two different diamicton units were identified, distinguished on the basis of matrix texture and stoniness. Seven of the nine exposures were located within

Rogen moraine, and two in hummocky moraine. The thickness of the upper unit varies between 1 and 4 m, and had a gradational contact with the lower diamicton. The upper of the two diamictons is consistent with observations of the single diamicton observed at the other 20 sites (described above). The matrix of the upper diamicton is generally coarser than that of the lower diamicton. Grain size analysis revealed that the upper diamicton contained a greater proportion of pebble-sized (-2Φ) particles compared to the lower diamicton (ranges of 13 to 32 % and 5 to 26 % respectively. Relative proportions of the intermediate grain sizes (from 0 to 3Φ) were similar for both the upper and lower diamictons in almost every case. These grain-size relationships were similar for both the hummocky and the ridged moraine.

Site 4 was a 6 m high exposure cut into the upper part of a hummock (Figure 4.19). It was composed of two coarse, matrix-supported, olive grey (5Y 6/1) diamictons. Stone content was approximately 50%, and clasts were sandstone and siltstone from the local bedrock. Clast sizes ranged from pebble to large boulders (approximately 1 m in diameter). Individual clasts were commonly faceted and striated. The matrix was dominated by coarse sand. Silt caps, openwork gravel lenses underlying clasts and boulder lines were observed throughout the diamicton.

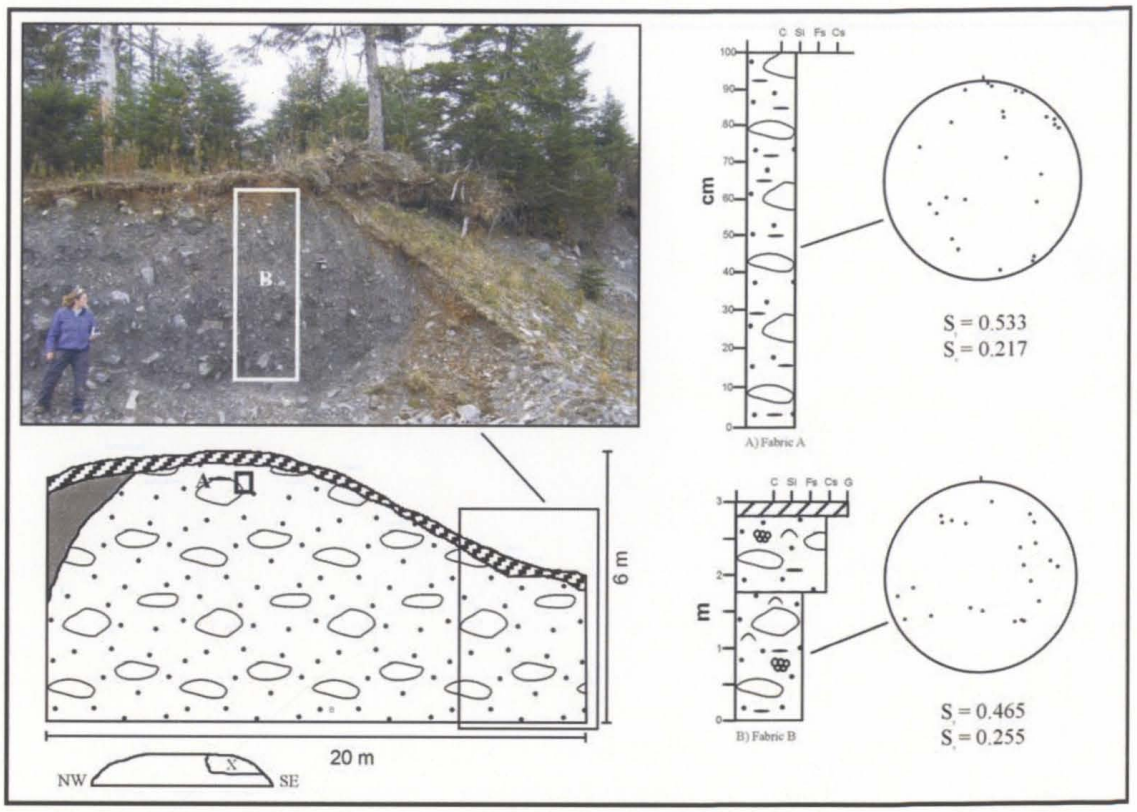

Figure 4.20 Site 4 exposure sketch including site photograph, sedimentary log and clast fabric diagrams.

4.4.3 Clast fabrics

A total of 56 clast fabrics were measured, with at least two clast fabrics measured at each of the 26 exposures. Thirty-nine clast fabrics were measured in moraine ridges, and seventeen in hummocky moraine. The clast fabrics are typically weak girdles or clusters. Of the 56 clast fabrics measured 31 were clusters (K<1), one of which was a strong cluster (K>3 and C= 3.9) and 25 were moderate to weak girdles (K>1) (Figure 4.21). There is large variability in clast fabric shape and mean direction, even amongst those measured at the same site (Appendix F).

Clast fabrics measured within hummocky moraine (n=16) had S_1 values raging from 0.43 to 0.92 with an average value of 0.64, whereas clast fabrics measured within ridged moraine (n=39) had S_1 values ranging from 0.4 to 0.8, but averaged 0.56.

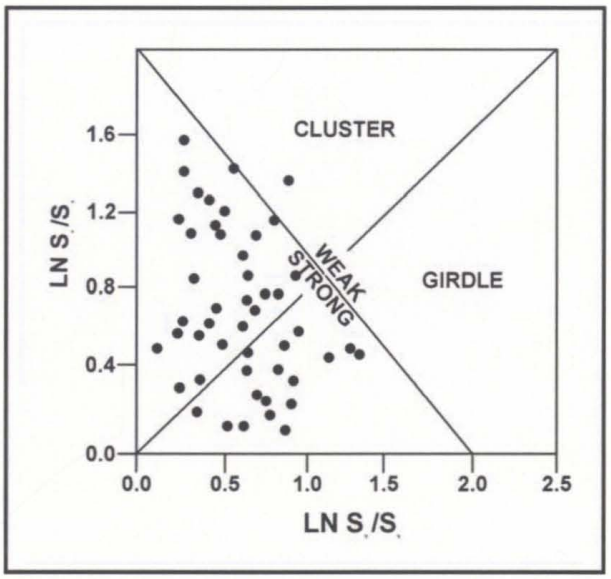

Figure 4.21 Shape of clast fabrics from diamictons within landforms of the central Avalon Peninsula. Note that the fabrics are either weak clusters or girdles (Modified from Woodcock, 1977).

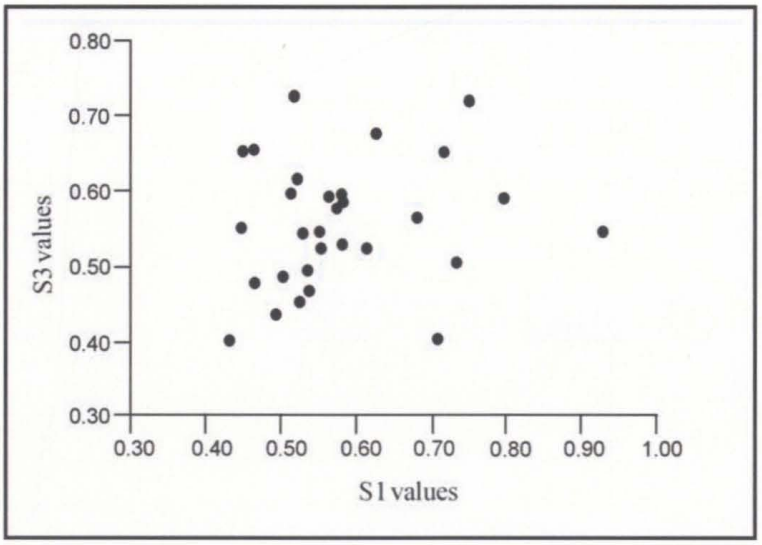

Figure 4.22 Plot of S_1 versus S_3 Eigenvalues from diamictons within the Avalon Peninsula. Each point represents the S1 and S3 values from fabrics measured at a single site. Note that the points are randomly arranged indicating that the S1 and S3 values differ in fabrics measured at the same site.

Mean clast fabric directions and girdle plane directions (from ridge exposures only) were compared to ridge crest orientations, and were found to be either oblique or tangential to one another (Appendix G). Clast fabric mean direction values ranged from 5 to 349°, but averaged 143°. The girdle plane direction values ranged from 29-332°, and they deviated from the ridge crest orientations by 28° to 75° (Appendix G).

Twelve sites in the northern portion of the study area (Sites 1, 2, 6, 7, 8, 12, 14, 15, 17, 18, 20 and 21) were located close to observed striation data (within 3 km). Only fabrics with an S_1 value greater than 0.6, K values greater than 1, and C values greater than 3 were selected for comparison with the striation data because they were the most likely to reflect former ice movement (Woodcock, 1977; Hicock *et al.*, 1996; Larsen and Piotrowski, 2003). A total of 9 clast fabrics from 7 sites were considered moderately strong clusters and were compared to nearby striation data. The mean directions of these clast fabrics were mostly oblique (27° to 130°) to the striation orientation. Only one fabric measurement appeared to mimic the adjacent ice flow direction (Appendix H; Appendix I).

Clast fabrics measured within hummocky moraine (n=16) had S_1 values ranging from 0.429 to 0.922 with an average value of 0.640, whereas clast fabrics measured within ridged moraine (n=39) had S_1 values ranging from 0.402 to 0.796, but averaged at 0.557.

4.4.3.1 Upper and lower diamictons

There is no marked difference between clast fabrics measured in the upper diamicton versus the lower diamicton. At the 9 sites where two diamictons were observed 12 clast

fabrics were measured in the upper diamicton, and 11 in the lower diamicton. For the upper diamicton, 10 of the 12 clast fabrics were clusters with K values ranging from 1.000 to 9.700 and S_1 values of 0.465 to 0.684.

Thirteen girdle fabrics (K= 0.160-0.960 and S_1= 0.402-0.617) were measured in the two diamictons, seven in the upper diamicton and six in the lower diamicton.

4.4.4 Interpretations of sedimentological data

4.4.4.1 Sedimentology

The diamicton exposed at each of the study sites had a clast content of at least 50% and a bimodal grain size distribution (-2Φ and 4Φ). The diamicton observed also has predominantly locally derived sandstone and siltstone clast lithologies. These lithologies are easily broken down over short transport distances in a glacial environment, which may explain the presence of a relatively fine-grained matrix in diamicton (c.f. Benn and Evans, 1998), despite a local bedrock origin. The combination of a stony diamicton with local lithologies and a fine-grained matrix therefore are best explained by transportation over a short distance within the subglacial environment.

Few sedimentary structures were observed within local diamictons, but those that were appeared consistently throughout all of the exposures. The gravel lenses under clasts are similar to those described by Fisher and Shaw (1992) which they interpreted as the remnants of sorted beds subsequently eroded by hyperconcentrated flows. Large clasts sitting above these beds apparently prevented erosion beneath them, and the lens therefore conforms to the shape of the clast. Alternatively, Shaw (1982a, 1982b)

interpreted similar gravel lenses as the product of melt-out during ice stagnation. He suggested that these lenses are formed when boulders and smaller clasts are held in the ice above a cavity, obstructing meltwater flow. The increased flow and turbulence caused by the boulder produces a scour beneath the boulder, and a gravel or sand lag to be deposited within the scour. As the ice continues to melt the boulder is let down onto the gravel lag.

Boulder lines are linear groupings of clasts that occur randomly in the diamicton. These structures are not interpreted as boulder pavements, because they are only one clast thick and wide, and they lack striations on their upper surface typical of boulder pavements (Dreimanis, 1991). These groupings of clasts may occur through lodgement or sediment gravity flow processes (Dreimanis, 1991; Hicock, 1991). Hicock (1991) suggested that boulder lines can develop in a viscously deforming till where similar sized clasts sink to a common level within the till. In sediment gravity flows larger particles are buoyed to the surface of the flow because of dispersive forces (Benn and Evans, 1998). Therefore these boulder lines are thought to be the result of sedimentary gravity flows.

The silt and fine sand caps found on clasts in the diamictons are likely similar to the draped beds observed by Shaw (1982) in the Sveg tills of central Sweden. These are a melt-out structures formed as ice melts and sediment is let down onto the underlying clasts, with the silt and fine sand being eroded away in areas between larger clasts by meltwater. Fine sand overlying silt caps may be a lag deposit resulting from very low energy meltwater flow that removed the silt. An alternative explanation for the caps is that they developed post-depositionally as meltwater percolated through the till and

deposited elluviated silt on large clasts. It is suggested here that the first of these ideas likely explains the formation of the observed silt caps. A post-depositional explanation for these structures would imply that there was a void in the diamicton, but the thickness of the silt caps (up to 5 cm thick) and the density of the diamicton make the presence of voids unlikely.

4.4.4.2 Upper and lower diamictons:

The progressive coarsening upwards of the diamictons where more than one diamicton occurs may indicate that the lower diamicton is slighter further travelled than the upper diamicton (c.f. Benn and Evans, 1998) or that the upper diamicton was transported slightly higher up in the ice, which was most likely the case.

4.4.4.3 Clast fabrics

Clast fabric data from stony diamictons may be difficult to interpret. Clast interaction during deposition of stony diamicton is common, and therefore the orientation of individual clasts represents those interactions rather than just the directions of ice flow in tills or slope aspect in gravity flow deposits (e.g., Benn and Evans, 1998). This may explain the within-site variability of clast fabric data. Also, clast lithology influences fabric measurements. Local bedrock of the central Avalon Peninsula produce clasts that break easily along fractures and bedding planes, thus elongated clast shards tend to develop. Measurement of these clasts may be problematic in that the clast orientation may not necessarily represent ice flow, but the fracture plane of the clast. A plot of S_1 against S_3 values for each of the 57 fabrics suggests that most are fabrics similar to those

measured for sediment gravity flow, lodgement, or deformation till deposits (Figure 4.23).

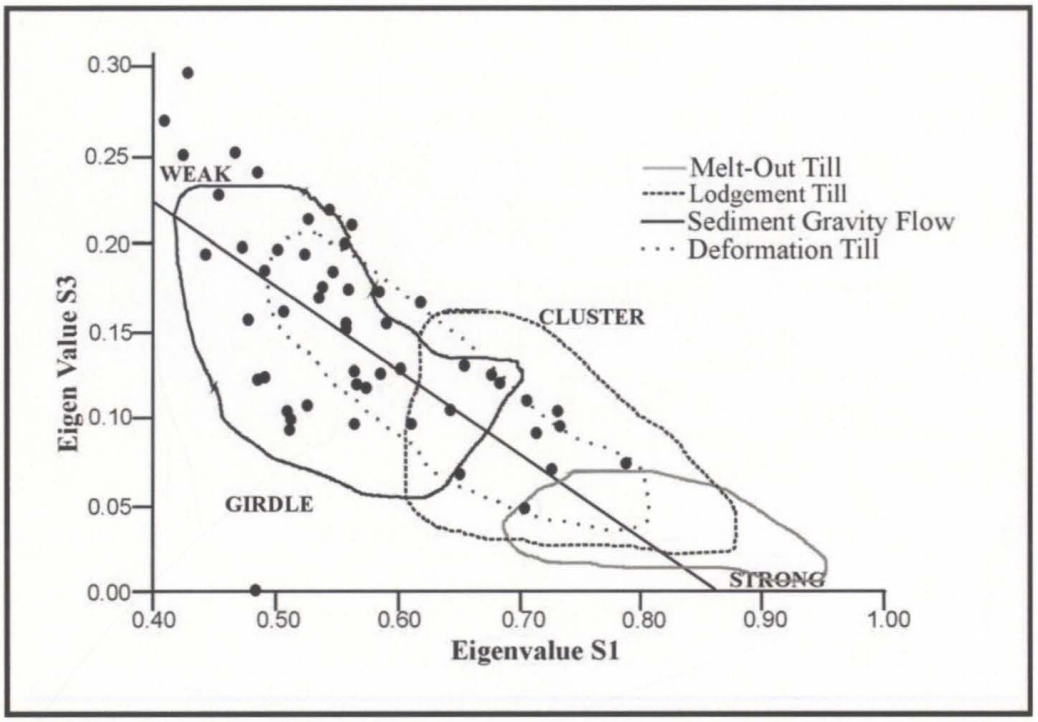

Figure 4.23 Plot of S_1 versus S_3 Eigenvalues from diamictons within the Avalon Peninsula. These envelopes are derived from clast fabrics measured from sediments deposited in known genetic environments, which was plotted on the conventional two-axis plot of S_1 vs S_3 (Woodcock, 1977).

4.4.4.4 Summary

The sediments within the moraine ridges and hummocks of the central Avalon Peninsula provide limited information pertaining to the depositional processes involved in the genesis of these landforms. Although the data is limiting, two processes were likely involved; melt-out and debris flows. Evidence for melt-out processes include the gravel lenses and silt caps, while the boulder lines and weak clast fabrics were the result of the

remobilization of sediment following deposition. The boulder lines were interpreted as debris flow structures rather than lodgement structures because the body of evidence suggests melt-out, and there was no evidence of lodgement within the diamicton.

Chapter 5 Discussion

This chapter discusses the results described in the previous chapter and is organized in such a way as to address the general research questions: (1) Are the moraine ridges true Rogen moraines; (2) what is the origin of the moraine ridges; and (3) what was the timing of events involved in moraine ridge formation? The various hypotheses of Rogen moraine formation are evaluated in the context of the moraine ridges on the central Avalon Peninsula.

5.1 Are the moraine ridges true Rogen moraines?

The moraine ridges resemble Rogen moraine described elsewhere (Hughes, 1964; Lundqvist 1969, 1981, 1987, 1997; Shaw, 1979; Bouchard, 1989; Hättestrand, 1997; Knight and McCabe, 1997; Dunlop, 2004). The parallel sets of evenly spaced, anastomosing and branching ridges, oriented perpendicular to the dominant ice flow direction, are analogous to those found in Ireland (Knight and McCabe, 1997; Dunlop, 2004), Sweden (Lundqvist, 1969, 1989; Shaw, 1997; Hättestrand, 1997), and Canada (Aylsworth and Shilts, 1989; Bouchard, 1989). Although a transition to drumlins is not observed on the Avalon Peninsula, many other Rogen moraine characteristics are identified and therefore the term "Rogen moraine" is applied to these moraine ridges. Both Rogerson and Tucker (1972) and Fisher and Shaw (1992) also classified the moraines on the Avalon Peninsula as Rogen moraines.

Henderson (1972) interpreted the moraines on the Avalon Peninsula as recessional moraines but the current evidence does not support this. For example, there is no evidence

of overprinting of moraine ridges, a characteristic that occurs in many areas of recessional moraine (Sharp, 1984; Krüger, 1995; Menzies, 2002). Typically, as a glacier recedes, there is ice marginal readjustments and re-advances that cause overriding and reworking of previously deposited recessional moraines. Overlapping of individual moraine ridges does not occur in the study area. Branching of ridges does occur, but should not be misconstrued as overprinted ridges because there is no evidence to suggest that different branches possess different sedimentologies or clast fabric orientations. A final argument against the recessional moraine interpretation is that it is difficult to trace a glacial margin by connecting adjacent moraine ridges on the Avalon Peninsula. The moraine ridges show no evidence of post-depositional dissection, which could indicate that the ridges were attached at one point in time. However it must be noted that Henderson's (1972) access to exposures in the interior of the moraine field was extremely limited, and access to new exposures has lead to better interpretations.

The moraines of the Avalon Peninsula may be argued to be De Geer moraines. The ridges, however, are generally taller than the 1-10 m height cited for De Geer moraines (Beaudry and Prichonnet, 1995) and most importantly they lack the fine-grained laminated sediments that indicate deposition within a post-glacial lake or shallow marine basin (King and Fader, 1986; Amos and Miller, 1990; Wellner *et al.*, 1993; Gipp, 1994). The moraines are well above Holocene marine limit (close to modern sea level in this area; Liverman, 1994) and no glaciolacustrine sediments have been mapped in the area (Catto and Taylor, 1998) and although running water plays a part in the deposition of some minor moraine deposits, there is no evidence to support widespread deposition in standing water.

The sediments of the Avalon Rogen moraines exhibit similar characteristics to those studied in Rogen moraine elsewhere. These characteristics include poor sorting, local provenance, with clasts ranging in size from pebbles to large boulders, matrix texture varying from silt to coarse sand, possessing a range of clast fabric orientations (Lundqvist, 1969, 1989, 1997; Shaw, 1979; Aario, 1987; Bouchard, 1989).

The diamictons within the Avalon Rogen moraines were likely deposited primarily through melt-out and sedimentary gravity flows, processes thought to be involved in Rogen moraine formation elsewhere. The minor sorted beds (gravel lenses under clasts, and silt caps) are similar to melt-out structures (Shaw, 1982, 1982a), whereas the boulder lines and the variable clast fabric values are typical of sediment gravity flow deposits (Dreimanis, 1991; Hicock, 1991).

5.2 Landform associations on the Avalon Peninsula

Glacial depositional landforms other than Rogen moraine occupy much of the study area and include hummocky moraine and flutes. Hummocky moraine possesses identical sedimentological characteristics to those of Rogen moraine. The irregular morphology of hummocks together with sedimentary structures that generally support melt-out processes suggest that this landform type was formed through ice stagnation and melt-out. The subglacial nature of the sediments indicates that differential melt-out at the glacier base is the most likely process. Uneven melting of stagnating ice can lead to irregular hills and depressions as well as the doughnut shaped mounds occasionally observed (c.f Johnson *et al.*, 1995; Andersson, 1998; Eyles *et al.*, 1999). Patches of hummocky moraine throughout the study area suggests that ice stagnation was a dominant process in the

formation of this landscape. Therefore the large amount of hummocky moraine on the central Avalon Peninsula strongly suggests significant ice stagnation during deglaciation.

Flutes are most numerous near the western margin of the study area where they are aligned north-south. These features occur most commonly beneath warm-based ice, and form parallel to the ice flow direction (Embleton and King, 1968; Hambrey, 1994; Bennett and Glasser, 1996; Benn and Evans, 1998). The flutes were therefore formed by northward flowing ice originating at the ice centre over St. Mary's Bay. The Rogen moraines on the other hand are oriented roughly perpendicular to the flutes. The flutes therefore predate the formation of the Rogen moraines, which were formed by northeastward flowing ice. Warm-based ice flowing in a northeastward direction has also been postulated from striations and streamlined bedrock features near the northeastern boundary of the study area (Catto, 1998; Batterson and Taylor, 2004).

The side-hill meltwater channels are indicative of the progressive southward and southwestward retreat of glacier margins confined within valleys draining into St. Mary's Bay. They suggest that these thin ice margins were predominantly cold-based, restricting meltwater to their surface margins. The meltwater channels also suggests that ice was actively retreating towards St. Mary's Bay in this particular area, in contrast to other areas farther north and west where ice stagnation was dominant.

5.3 What is the origin of Rogen moraine on the Avalon Peninsula?

This section addresses the question of Rogen moraine formation in the study area using available evidence from their sedimentology, morphology and association with other landforms.

The sedimentology of the moraine ridges and hummocks show they are composed of a coarse diamicton, with very few sedimentary structures. The faceting of clasts within the diamicton reflects the fracture planes within the rock. The clasts are derived from local sandstones, siltstones and volcanics, indicating that the diamicton was locally derived (Bennett and Glasser, 1996; Benn and Evans, 1998). Striated clasts were present in half of the exposures which suggests clast-to-clast or clast-to-bedrock interactions were occurring. This process occurs most commonly in the subglacial environment, within the debris-rich basal ice horizon or in a subglacial deforming layer (Hart, 1994). Therefore, short transport distances, coarse texture, poor sediment sorting, and faceted and striated clasts all suggest the sediments within Rogen moraines were transported subglacially.

Two dominant processes were involved in the deposition of the Rogen moraine sediments: melt-out and sediment gravity flows. Evidence for melt-out includes draped beds (silt caps) and openwork gravel lenses, whereas sediment gravity flow deposits are inferred from girdle clast fabrics, boulder lines, and minor sorted beds (Dreimanis, 1991; Hicock, 1991). Sediments were therefore likely deposited through melt-out and later partially reworked by sediment gravity flows. The sediments were not completely reworked by these flows; otherwise the sedimentary structures associated with melt out (e.g., openwork gravel lenses, and silt caps) would not have been preserved.

Both Rogen and hummocky moraines exhibit identical internal composition, suggesting the same depositional processes were involved in their formation. Therefore the difference in morphological characteristics between these two landform types is likely a result of differential accumulation of sediment beneath the ice imposed by local topographical conditions, which occurred prior to deposition. In the northern two-thirds

of the moraine field there is a distinct pattern of Rogen moraine in valleys and hummocky moraine on the uplands. In the southern portion (mainly in the southeast) the topography becomes more subdued, hummocky moraine dominates and Rogen moraines are much less well-developed, with disconnected and poorly-oriented ridges.

Since the Avalon Peninsula ice cap was relatively thin (between 400 and 500 m; Catto, 1998) during deglaciation the difference in elevation between the uplands and the troughs (between 15 and 30 m) and the distance between them (a kilometre or two) may have been adequate to affect debris accumulation in the active ice. For example, it may have caused ice flow to be focussed in the valleys, and therefore ice stagnation would be dominant on the intervening ridges. The compressive active ice flow caused preferential accumulation/shearing of debris within the ice in the valleys which, upon stagnation simply was deposited on the valley floors. In contrast, the debris in ice on the uplands did not undergo preferential orientation to the same degree, therefore when it was deposited it created hummocks and disoriented ridges.

Thicker sediment accumulations would be expected within the localized valleys than the uplands if ice was more active in these areas (Bennett and Glasser, 1996). It appears from field observations that Rogen moraines are composed of a larger volume of sediment than the hummocky moraines, and therefore the areas with thicker sediment accumulations are more likely to contain Rogen moraine. If the study area was located on flat terrain, or even on a gentle slope, the sediment may have accumulated as a till blanket rather than sets of Rogen moraines and hummocks.

5.3.1 What was the direction of ice movement during Rogen moraine ridge formation?

The alignment of Rogen moraine ridge crests suggests that the ice was flowing northeastward at the time of their formation; if the relationship between ice flow direction and ridge orientation is assumed to be perpendicular (e.g. Lundqvist, 1969, 1981, 1987, 1997; Shaw, 1979; Bouchard, 1989; Fisher and Shaw, 1992; Dunlop, 2004). Striation data and alignment of streamlined bedforms, and ice flow patterns reconstructed by Henderson (1972), Rogerson and Tucker (1972), and Catto (1998) all correspond to this ice flow direction. The clast fabrics from sediments exposed in ridges and hummocks were unreliable indicators of ice flow.

5.3.2 What was the timing of events that lead to the formation of Rogen moraine on the Avalon Peninsula?

Rogen moraine formation is not likely to have occurred during glacial maximum. Although precise chronology is lacking, at the last glacial maximum in Newfoundland, ice extended out towards the continental shelves and in order for that to occur a large ice divide is thought to have extended across the central Avalon Peninsula, extending eastward from the Great Northern Peninsula (Shaw *et al.*, in press). This idea differs from that of Catto (1998) who suggested that the ice dispersal centre during glacial maximum was situated over St. Mary's Bay. Perhaps Catto's (1998) glacial maximum ice configuration occurred later than he suggests, and this configuration was more likely deglacial. If the Rogen moraines are LGM in age, they would have been situated directly beneath the ice divide, where very little sediment accumulation or erosion occurs (c.f.

Bennett and Glasser, 1996; Benn and Evans, 1998). The alignment of Rogen moraine ridge crests reflects a northeastward ice flow, one which would not have been the case if the ice dispersal centre was located over the study area. On either side of the ice divide there are areas of extremely slow, or non-flowing ice and therefore landforms forming under the ice dispersal centre would not reflect an ice flow direction (Bennett and Glasser, 1996; Benn and Evans, 1998). Therefore the moraines likely formed during deglaciation.

Final deglaciation of the Avalon Peninsula occurred through ice stagnation and subsequent meltout of glacially entrained debris. The Avalon Peninsula ice cap was cut off from the remainder of Newfoundland ice, and the outlets to the large bays were no longer filled with ice, and ice stagnated and melted *in situ*. The coastal bays around the Bonavista Peninsula were ice-free by 13.0 ka based on radiocarbon dates of marine shells from Bonavista Bay (Cumming, 1992; Batterson and Taylor, 2001). Therefore, the Avalon Peninsula ice cap became independent at approximately this time. Final deglaciation occurred shortly after 10.1 ka (Macpherson, 1996). Therefore the Rogen moraines must be older than 10.1 ka BP.

5.4 Examining the alternative hypotheses for Rogen moraine formation.

5.4.1 The subglacial meltwater hypothesis

Rogen moraines on the Avalon Peninsula are thought to have been the result of a massive subglacial meltwater flood (Fisher and Shaw, 1992). Fisher and Shaw (1992) cited several pieces of sedimentological evidence to validate their hypothesis including sorted

beds of sediment beneath perched clasts, horizontal stratified beds, and clast fabrics indicative of fluvial and debris flow deposits.

Sedimentological evidence alone is not sufficient to accept that a subglacial meltwater flood deposited the Avalon Rogen moraines. In their paper, Fisher and Shaw (1992) describe sorted beds of sediment beneath perched clasts, as well as horizontal stratified beds. The former was observed throughout the exposures examined in this study, although a different interpretation is provided. Rather than suggesting that these beds are the remnants eroded by hyper-concentrated meltwater flows (Fisher and Shaw, 1992), here they are interpreted as melt-out structures resulting from flow obstruction by overhanging boulders (c.f. Shaw, 1982). Fisher and Shaw (1992) also cite the presence of a surface boulder lag as evidence of meltwater flow. Munro (1999) uses a similar argument to explain the formation of hummocky moraine in Alberta. This lag is completely absent on Rogen moraines and hummocks examined in this study, and there is no concentration of boulders, other than rare lines, within the sedimentary profile. Large boulders were found within almost every section, but no distinct pattern or arrangements of those boulders were observed. The absence of striated clasts in ridge exposures was cited by Fisher and Shaw (1992) as evidence opposing a subglacial depositional origin. In this study, however, 50% of the 26 exposures logged contained striated clasts. It is possible that Fisher and Shaw's (1992) sample size was too small (5 exposures) or that the location of their exposures (all on the boundary of the moraine field) was too restrictive to encompass the full range of sediment characteristics.

Sedimentological evidence that may be used to support the subglacial meltwater hypothesis is the presence of debris flow deposits, but such deposits are not diagnostic of

subglacial meltwater floods. Debris flows are likely to occur within the meltwater-scoured subglacial cavities once they are infilled with sediment, and later reworked under the influence of gravity (Fisher and Shaw, 1992; Shaw, 2002). Debris flows may occur subaerially or subaqueously (Benn and Evans, 1998), and Fisher and Shaw (1992) suggest this occurred subaerially on the Avalon Peninsula.

There are several major theoretical and empirical arguments opposing the subglacial meltwater hypothesis (Benn and Evans, 1998; Hättestrand, 1999; Dunlop, 2004; Clarke *et al.*, 2005). One such argument that is important in relation to these Rogen moraines is the source of meltwater for these large discharges (Hättestrand, 1999; Dunlop, 2004; Clarke *et al.*, 2005). Fisher and Shaw (1992) do not discuss a potential source of the meltwater. This is a major fault for their hypothesis because the Avalon Rogen moraine field likely formed during a late restricted stage of the Avalon ice cap when potential subglacial reservoirs of meltwater would have been limited in extent.

It is difficult to explain the pattern of alternating tracts of Rogen moraines and hummocky moraine that are topographically controlled using the meltwater hypothesis. According to their hypothesis, variations in the turbulence can create forms similar to ripples (i.e., Rogen moraine) and hummocky moraine (Fisher, University of Toledo, personal communication, 2005). Perhaps the variation in the underlying topography affects the way in which the sheet of meltwater flows, with increasing turbulence occurring along the uplands. However, on the basis of this study the subglacial meltwater hypothesis of Rogen moraine formation seems unlikely.

5.4.2 The bed deformation hypothesis

The bed deformation hypothesis explains Rogen moraines as the precursors to the drumlinization of transverse ridges (Boulton, 1982). This hypothesis requires landforms produced by a previous glacial event that possess alternating bands of weak and resistant sediments, and a change in ice flow direction that deforms the previously deposited landforms.

The bed deformation hypothesis cannot currently be used to explain the formation of the Avalon Peninsula Rogen moraines, due to several considerations:

1. On the Avalon Peninsula there was one dominant ice flow direction (northeastward) as reconstructed from striation data and streamlined bedform orientation (Henderson, 1972; Rogerson and Tucker, 1972; Catto, 1998; Batterson and Taylor, 2004).

2. The Avalon Rogen moraines do not possess any form of drumlinization on their surface or a transitional form to drumlins. It is possible that drumlins or drumlinised ridges exist offshore, but there is no evidence for a transitional phase to Rogen moraine in coastal areas.

3. The internal composition of the Rogen moraines revealed a consistently compact coarse diamicton, a material that is difficult to deform.

4. Hummocky moraine also occupies many areas between belts of Rogen moraine, yet the bed deformation hypothesis is currently unable to explain their formation.

Until the association of hummocky moraine and Rogen moraine can be explained with this hypothesis it cannot be used to explain the formation of Rogen moraine on the Avalon Peninsula.

5.4.3 Shattered till sheet hypothesis

Hättestrand's (1997) shattered till sheet hypothesis suggests that a large portion of the ice sheet margin undergoes extreme extensional stresses to produce a series of transverse crevasses. The hypothesis also requires that as the ice advances crevasses are continually produced, and the ice margin moves "en masse". The blocks of ice between crevasses subsequently melt *in situ* forming the Rogen moraine ridges.

Although Hättestrand (1997) has little sedimentary evidence for this hypothesis the jigsaw puzzle fit of adjacent Rogen moraines was suggested as evidence for this type of ice sheet motion. This is not the case for the Avalon Peninsula, where adjacent ridges rarely appear to fit together. Also it is unclear how some crevasses would continue to form at the ice sheet margin, while others would not expand dramatically or completely close as the ice sheet margin advances.

This hypothesis attempts to explain the wide range of sediments found within Rogen moraine, as well as the fact that Rogen moraine is commonly composed of material similar to the surrounding landscape. Hättestrand (1999) used this as a general model for Rogen moraine formation under large ice sheets, where the moraines are found near the former ice centre, as in Sweden (Lundqvist, 1969; Hättestrand, 1997). To produce Rogen moraine ridges of the appropriate size (10-30 m high, 50-100 m wide, 300-1200 m long) the ice sheet must have been large (continental in scale) and under extreme extensional stresses. The ice mass on the Avalon Peninsula was a small ice cap, and was predominantly warm-based (Catto, 1998; Batterson and Taylor, 2004), therefore the basal conditions for such extreme extensional stresses would not likely have been

possible. Also, sediments exposed to high amounts of internal stress tend to deform and as a result deformation structures should be found within them. No evidence of deformational processes was observed within the Avalon Rogen moraine. As well, the shattered till sheet hypothesis does not predict the association of Rogen moraine and hummocky moraine that occurs commonly on the Avalon Peninsula.

Dyke and Evans (2003) suggest that an up-ice migrating boundary between cold- and warm-based ice during deglaciation would preserve Rogen moraines near the final deglacial margin. They make this suggestion after observing the Rogen moraines on Prince of Wales Island in the Canadian Arctic, and around the Labrador Ice Divide. There may have been a migrating boundary between cold- and warm-based ice on the Avalon Peninsula, but there are too many issues with the shattered till sheet hypothesis to apply it to the Avalon Rogen moraines.

5.4.4 Subglacial meltout and basal thrusting.

The suggestion has been made by several researchers (Shaw, 1979; Aylsworth and Shilts, 1989; Bouchard, 1989) that Rogen moraines form as a result of thrusting of slabs of basal ice followed by meltout. This process occurs most effectively where an ice sheet is sitting within a topographic basin, whereby the down-ice edge of the basin acts to restrict ice flow. The obstruction slows flow and causes an increase in the compressional stresses at the margin leading to the production of thrust slabs of ice. Observations cited as evidence for this hypothesis included the fact that Rogen moraines occur at the down ice edge of the basin whereas hummocky moraine occurs further up ice, and adjacent Rogen moraine ridges are similar in height. Also, sediments are highly deformed and show

evidence of shear planes, and subsequent melt-out. The first of these observations does not occur on the Avalon Peninsula. Rogen moraine and hummocky moraine are found adjacent to one another, with no apparent relationship to the ice margin. Second, adjacent ridges are not necessarily the same height, and this has been found in other areas including Labrador, Ireland, and Sweden (Dunlop, 2004). Third, again there is no evidence of deformation within the Rogen moraine sediments, and no shear planes indicating the boundaries between individual thrust blocks of ice. There is some limitation to the observations made in this study because most of the exposures examined were through the top or sides of ridges; therefore, the evidence for shear planes may not have been uncovered, but no other evidence to support this hypothesis is available, and it is excluded as an explanation for the Avalon Rogen moraines.

5.4.5 Bed Ribbing Instability Explanation (BRIE)

Although the BRIE has not been explicitly tested in the current research, the wavelengths between Rogen moraine ridges measured within the study area (between 200 and 300 m) are consistent to the wavelengths predicted by the model (a maximum of 300 m; Dunlop, 2004). The BRIE hypothesis has been suggested by Dunlop (2004) as a general model for Rogen moraine formation, irrespective of the underlying topography. On the Avalon Peninsula there is a strong link between glacial landforms and the bedrock topography. Since the sediments within Rogen moraine and hummocky moraine are similar and likely formed contemporaneously, then there was a factor that altered the way in which the sediment accumulated within the ice to form Rogen moraine ridges, and hummocky moraine respectively.

Since Dunlop (2004) has been able to calculate Rogen moraine wavelengths that occur naturally with the BRIE, it is likely that this model can be applied to wide areas of Rogen moraine, but until an in-depth review of this hypothesis with respect to the Avalon Rogen moraines is completed it cannot be used to explain their formation.

5.5 Summary of Major Findings and Conclusions

This thesis has re-examined the field of Rogen moraine on the central Avalon Peninsula, Newfoundland, and the following has been determined:

1. The field of moraine ridges on the central Avalon Peninsula are Rogen moraines. These moraines have similar morphologies to Rogen moraines described in Sweden, Ireland, and elsewhere in Canada, although there is no association with drumlins or drumlinization of the Rogen moraine ridges
2. Rogen moraines postdate the deposition of flutes in the study area; they appear to be contemporaneous with hummocky moraines;
3. The sediment within the Rogen moraines and hummocky moraines is a coarse-grained-compact diamicton, derived from the local bedrock, and possessing structures indicative of melt-out and sediment gravity flows.
4. The alignment of Rogen moraine ridges is perpendicular (northwest-southeast) to the ice flow direction (northeast-southwest) in the central Avalon Peninsula during deglaciation
5. The field of Rogen moraines on the Avalon Peninsula was formed during the last deglacial phase on the peninsula. If the moraines had been formed earlier in the

glacial cycle the melt-out and sediment gravity flow structures would not have been preserved.

6. Currently, it is difficult to use any of these previously developed ideas of Rogen moraine formation to explain the formation of Rogen moraine on the Avalon Peninsula.

Table 5.1 summarizes the landform descriptions from this study.

This research has provided new information pertaining to the formation of Rogen moraines. Data acquired through this project has emphasized that Rogen moraines are the result of several processes, occurring under differing conditions. On the Avalon Peninsula the association of Rogen moraines and hummocky moraine has become a major influence in developing ideas of Rogen moraine formation for the area. The consistent alternating tracts of Rogen moraines in localized valleys with hummocky moraines on the uplands in the northern portion of the study area is replaced with poorly-developed Rogen moraines where the topography becomes more subdued in the southern portion of the study area. The apparent transition between Rogen moraines in valleys and hummocky moraines on uplands along with sedimentological evidence suggests that both landform types were formed at the same time. It is therefore concluded that the underlying topography has a strong effect on their formation. Hummocky moraine in the central Avalon Peninsula has been interpreted to be the result of melt-out from stagnating ice; therefore the Rogen moraines were also formed during a late deglacial stage of the Avalon ice cap. Perhaps then these landforms should be considered typical of deglacial

phases, and not associated with ice divides as previously thought (Lundqvist, 1969; 1989; 1997; Aario, 1987; Hättestrand, 1997). One question arises if these landforms were developed in a deglacial phase - why are there no eskers in the area? Eskers are typical of many deglacial landscapes yet none have been found on the Avalon Peninsula. Ice over the central Avalon Peninsula underwent regional stagnation, while the formation of eskers would require retreat of the ice margin in order to preserve the tunnel channels near the margin. Any such channels forming in the stagnating ice would have collapsed preventing the formation of an esker. Also, there may not have been an adequate supply of debris entrained in the ice to form eskers. The Avalon Peninsula ice cap did not transport material over long distances, therefore little debris would have migrated upwards through the ice. Despite the lack of eskers, the body of evidence obtained through this study suggests the moraines were formed during deglaciation. This idea may then be extended to potential areas of Rogen moraine elsewhere in the province, with the locations of Rogen moraine being interpreted as deglacial ice margins.

5.6 The formation of the Avalon Peninsula Rogen moraines

The following outlines a potential hypothesis for the formation of the Avalon Peninsula Rogen moraines. During glacial maximum, ice over the Avalon Peninsula was flowing radially from an ice centre located over the central part of the peninsula (Shaw *et al.,* in press). Ice flowing northward into Trinity Bay was focussed in the Whitbourne Trench, and flowed faster than ice flowing into Conception Bay, which was slowed by the series of bedrock ridges along the eastern coast of the bay. The ice flowing northward into Trinity Bay formed the flutes, and the northeastward flow into Conception Bay eroded,

polished, and streamlined the bedrock ridges. Between glacial maximum and the onset of deglaciation, the ice centre shifted southwards towards St. Mary's Bay. During this time, sediment was eroded and incorporated into the base of the ice. Sediment was eroded around the bedrock ridges and transported into the valleys leading to a thicker accumulation of sediment than on the uplands. Also, there would be greater erosion in the valleys than on the uplands because of thicker and warmer-based ice. The Rogen moraine ridges could be a result of the faster flowing ice in the valleys, which increased the compressional stress in the ice. On the uplands the ice was fairly unaltered. This variation in the speed of ice motion with respect to topographic variations may explain the difference in morphology, and transitions between the Rogen moraines and hummocky moraines. In the southern portion of the study area where Rogen moraines are poorly-developed, and have some similar characteristics to hummocky moraine, ice flow was slower than that in the valleys, but faster than on the uplands. Here ice flow was unconfined by topography and therefore a transitional type of landform (between Rogen moraine and hummocky moraine) similar to that on the upward edge of the bedrock valleys was developed.

Final deposition of the sediment would have occurred through melt-out, producing the hummocky moraines on the uplands and preserving the Rogen moraines in the valleys. Sediments on the slopes of the Rogen moraines may have subsequently been reworked through increased meltwater causing sediment gravity flows.

5.7. Further Research

Although this thesis has added to the body of knowledge pertaining to Rogen moraines and their formation, more work is required. Sedimentological data in this study was limited by the poor exposures through Rogen moraines and hummocky moraines, and it would be ideal to obtain cross-sections throughout the entire profile of a ridge or hummock to determine whether or not the observations made in this study were representative of the internal composition of the moraines. The digital technology used in this study was a substantial aid in the morphological description of both Rogen moraines and hummocky moraines, but was limited in that only a small portion of the study area was re-created in the model. A higher resolution DEM for the entire study area could be created from high-resolution satellite imagery such as LIDAR (LIght Detection and Ranging). Such a model would help to clarify some the relationships between the landform types.

As the interest in resource development continues within Newfoundland and Labrador opportunities may arise to re-examine this field of Rogen moraines at both the ground level and through improved remote sensing techniques. It is hoped that the data acquired in this study will provide any future researchers with a solid foundation to begin any new research endeavours.

Table 5.1 Summary of landforms examined in this study.

Landform	Topographic Setting	Description	Association with other landforms	Location within study area	Relationship to ice flow	Potential Formative Mechanism
Rogen Moraine	Well developed in valleys Poorly developed on uplands	Continuous, parallel, evenly spaced ridges Linear and sinuous Commonly branch on one end	Transition into hummocky moraine on uplands On occasion drape flutes	Better developed in the northern portion of the field Poorly developed in the southeastern portion of study area	Perpendicular	
Hummocky Moraine	Well developed on uplands	Rounded, knob-like hills, elongate to circular mounds and short, randomly-oriented hills Some doughnut shaped mounds	Transition to Rogen moraines in valleys	Throughout study area, but greatest concentration in NE portion		Melting of stagnating debris rich ice
Flutes	Occur on higher ground at the edge of a valley	Fairly straight linear ridge like features Occur in groups and are sub-parallel to one another	Overprinted by Rogen moraines Perpendicular to Rogen moraine	Occur predominantly along the western edge of the Whitbourne Trough	Parallel	Fast flowing ice, and deformation of sediments around obstacles on the bed
Meltwater Channels	Occur along upper edge of river valleys	Channels cut into bedrock	Perpendicular to valley in which they occur	Northern Points of St. Mary's Bay	Perpendicular	Stagnant ice melting
Streamlined Bedforms		600 –3000 m wide Widest at NE end Trend NE-SW Between 2 and 7 km long 25- 100 m above surrounding landscape		Northeastern portion of the study area near Conception Bay	Parallel	Erosion by advancing glacier

References

Aario, R, 1987. Drumlins of Kuusamo and Rogen-ridges of Ranua, northeast Finland. In: Menzies, J., Rose, J. (Eds.), Drumlin Symposium, A.A. Balkema, Rotterdam, 87-101.

Amos, C.L., Miller, A.A.L. 1990. The Quaternary stratigraphy of southwest Sable Island Bank, Eastern Canada. Geological Survey of America, Bulletin 102: 915-934.

Andersson, G., 1998. Genesis of hummocky moraine in the Bolmen area, southwestern Sweden. Boreas 27, 55-67.

Aylsworth, J. M., Shilts, W. W, 1989. Bedforms of the Keewatin Ice Sheet, Canada. Sedimentary Geology 62, 407-428.

Batterson, M., 1980. Contemporary frontal moraine formation in the Yoho Valley, British Columbia. MSc Thesis. Memorial University of Newfoundland, St. John's, Newfoundland, Canada, 150 pages.

Batterson, M. J., Taylor, D. M., 2004. Regional till geochemistry and surficial geology of the central Avalon and Bay de Verde peninsulas. In: Pereira, C. P. G., Walsh, S. J. (Eds.), Current Research 04, 93-106.

Beaudry, L. M., Prichonnet, G., 1995. Formation of De Geer moraines deposited subglacially, central Quebec. Geographie Physique et Quaternaire 49, 337-361.

Bell, T., Liverman, D. G. E., Batterson, M., Sheppard, K., 2001. Late Wisconsinan stratigraphy and chronology of southern St. George's Bay, Newfoundland : a re-appraisal. Canadian Journal of Earth Science 38, 851-869.

Benn, D. I., Evans, D. J. A, 1998. Glaciers & Glaciation. Arnold, London, UK, 734 pages.

Bennett, M. R., Glasser, N. F., 1996. Glacial Geology: Ice Sheets and Landforms. John Wiley & Sons, Chichester, 364 pages.

Blair, C. L., Day, E. E. D, Frid, B. R., 1990. The Canadian Landscape: Map and Air Photo Interpretation. Copp Clark Pittman, Toronto, 340 pages.

Bouchard, G. S., 1989. Subglacial landforms and deposits in central and northern Quebec, Canada, with emphasis on Rogen Moraines. Sedimentary Geology 62, 293-308.

Bouchard, M. A., Ignatius, H. G., Konigsson, L.-K., 1989. Ribbed moraines of North America- a historical account. Geologi 41, 75-79.

Boulton, G. S., 1982. Subglacial processes and the development of glacial bedforms. In: Davidson-Arnott, R., Nickling, W., Fahey, B. D. (Eds), Research in glacial, glacio-fluvial, and glacio-lacustrine systems, Geo Books, 1-31.

Boulton, G. S., Caban, P., 1995. Groundwater flow beneath ice sheets: Part II - its impact on glacier tectonic structures and moraine formation. Quaternary Science Reviews 14, 563-587.

Boulton, G. S., 1996. Theory of glacial erosion, transport and deposition as a consequence of subglacial sediment deformation. Journal of Glaciology 42, 43-62.

Boulton, G. S., Dobbie, K. E., Zatsepin, S., 2001. Sediment deformation beneath glaciers and its coupling to the subglacial hydraulic system. Quaternary International 86, 3-28.

Burgess, D. O., 1994. Morphometric comparisons between Rogen terrain and hummocky terrain. MSc. Thesis. University of Alberta, Edmonton, Alberta, Canada, 39 pages.

Burgess, D. O., Shaw, J., 2003. Morphometric comparisons between Rogen terrain and hummocky terrain. Physical Geography 24, 319-336.

Burrough, P.A., McDonnell, R.A., 1998. Principles of Geographical Information Systems. Oxford University Press, Oxford, UK, 333 pages.

Carl, J. D., 1978. Ribbed moraine-drumlin transition belt, St. Lawrence Valley, New York. Geology 6, 562-566.

Catto, N. R., 1998. The pattern of glaciation on the Avalon Peninsula of Newfoundland. Geographie Physique et Quaternaire 52, 23-45.

Catto, N. R., Taylor, D. M., 1998. Landforms and Surficial Geology of Holyrood, St.Catharines, Placentia, Argentia, NL. Map 98-69, Newfoundland Department of Mines and Energy, St.John's, Newfoundland.

Chamberlin, T. C., 1895. Notes on the glaciation of Newfoundland. Bulletin of the Geological Society of America 6, 467 pages.

Clarke, G. K. C., Leverington, D. W., Teller, J. T., Dyke, A. S., Marshall, S. J., 2005. Correspondence. Quaternary Science Reviews 24, 1533-1541.

Coleman, A. P., 1926. The Pleistocene of Newfoundland. Journal of Geology 34, 193-223.

Cumming, E. H., Aksu, A. E., Mudie, P. J., 1992. Late Quaternary glacial and sedimentary history of Bonavista Bay, northeast Newfoundland. Canadian Journal of Earth Science 29, 222-235.

Davis, J. C., 1986. Statistics and Data Analysis in Geology. John Wiley & sons, New York, 646 pages.

Dreimanis, A., 1989. Tills: their genetic terminology and classification. In: Goldthwait, R. P, Matsch, C. C. (Eds), Genetic Classification of Glacigenic Deposited, A.A. Balkema, 17-83.

Dunlop, P., 2004. The characteristics of ribbed moraine and assessment of theories for their genesis. PhD. Thesis. University of Sheffield, UK, 363 pages.

Dyke, A.S., Evans, D.J.A. 2003. Ice marginal terrestrial landsystems: Northern Laurentide and Innuitian ice sheet margins. In: Evans, D.J.A. (Ed), Glacial Landforms. Arnold, London, UK: 143-203.

Eastman, J.R., 2003. IDRISI Kilimanjaro Version 14.02 Manual. Clark Labs, Worchester, 328 pages.

Embleton, C., and King, C. A. M. 1968. Glacial and Periglacial Geomorphology. Edward Arnold, London, UK, 608 pages.

Eyles, N., Boyce, J. I., Barendregt, R. W., 1999. Hummocky moraine: sedimentary record of stagnant Laurentide Ice Sheet lobes resting on soft beds - reply. Sedimentary Geology 129, 169-172.

Fisher, T. G., 1989. Rogen moraine formation: examples from three distinct areas within Canada. Queen's University, Kingston, Ontario, Canada, 195 pages.

Fisher, T. G., Shaw, J., 1992. A depositional model for Rogen Moraine, with examples from Avalon Peninsula, Newfoundland. Canadian Journal of Earth Science 29, 669-686.

Fisher, T. G., Spooner, I., 1994. Subglacial meltwater origin and subaerial meltwater modifications of drumlins near Morley, Alberta, Canada. Sedimentary Geology 91, 285-298.

Fisher, T. G., Taylor, L. D., Jol, H. M., 2003. Boulder-gravel hummocks and wavy basal till contacts: products of subglacial meltwater flow beneath the Saginaw Lobe, south-central Michigan, USA. Boreas 32, 328-336.

Gale, S. J., Hoare, P. G., 1991. Quaternary Sediments. Wiley, New York, 323 pages.

Gipp, M.R. 1994. Late Wisconsinan deglaciation of Emerald Basin, Scotian Shelf. Canadian Journal of Earth Sciences 31:554-566.

Grant, D. R., 1989. Quaternary geology of the Atlantic Appalachian region of Canada. In: Fulton, R. J. (Eds), Quaternary Geology of Canada and Greenland, Geological Survey of Canada, 393-440.

Hambrey, M.J. 1994. Glacial Environments. UCL Press Ltd. Frome, England, 296 pages.

Hambrey, M.J., Huddart, D., Bennett, M. R., Glasser, N. F., 1997. Genesis of "hummocky moraines" by thrusting in glacial ice: evidence from Svalbard and Britain. Journal of the Geological Society, London 154, 623-632.

Hart, J. K., 1994. Till fabric associated with deformable beds. Earth Surface Processes and Landforms 19, 15-32.

Hart, J. K., Roberts, D. H., 1994. Criteria to distinguish between subglacial glaciotectonic and glaciomarine sedimentation: deformation styles and sedimentology. Sedimentary Geology 91, 191-213.

Hart, J. K., 1997. The relationship between drumlins and other forms of subglacial glaciotectonic deformation. Quaternary Science Reviews 16, 93-107.

Hart, J. K., Boulton, G. S., 1991. The inter-relation of glaciotectonic and glaciodepositional processes within the glacial environment. Quaternary Science Reviews 10, 335-350.

Hart, J. K., Roberts, D. H., 1994. Criteria to distinguish between subglacial glaciotectonic and glaciomarine sedimentation: deformation styles and sedimentology. Sedimentary Geology 91, 191-213.

Hättestrand, C., 1997. Ribbed moraine in Sweden - distribution pattern and palaeoglaciological implications. Sedimentary Geology 62, 41-56.

Hättestrand, C., Kleman, J., 1999. Ribbed moraine formation. Quaternary Science Reviews 18, 43-61.

Henderson, E. P., 1959. A glacial study of central Quebec-Labrador. In: Geological Survey of Canada, Department of Mines and Technical Surveys, Report 50, 1-94.

Henderson, E. P., 1972. Surficial geology of Avalon Peninsula, Newfoundland. In: Department of Energy, Mines and Resources, Canada, Report, 1-121.

Hicock, S. R, 1991. On subglacial stone pavements in till. Journal of Geology 99, 607-619.

Hicock, S. R, Goff, J. R., Lian, O. B., Little, E. C., 1996. On the interpretation of subglacial till fabric. Journal of Sedimentary Research 66 (5), 928-934.

Hindmarsh, R., 1997. Deforming beds: viscous and plastic scales of deformation. Quaternary Science Reviews 16, 1039-1056.

Hindmarsh, R., 1998. Drumlinization and drumlin-forming instabilities: viscous till mechanisms. Journal of Glaciology 44, 293-314.

Hindmarsh, R., 1998. The stability of a viscous till sheet coupled with ice flow, considered at wavelengths less than the ice thickness. Journal of Glaciology 44, 285-292.

Hindmarsh, R. C. A., 1998a. Ice-stream surface texture, sticky spots, waves and breathers: the coupled flow of ice, till and water. Journal of Glaciology 44, 589-614.

Hoppe, G., 1959. Glacial morphology and inland ice recession in northern Sweden. Geografiska Annaler 35, 105-115.

Hughes, O. L., 1964. Surficial geology, Nichicun-Kaniapiskau map-area, Quebec. In: Geological Survey of Canada, Department of Mines and Technical Surveys, Report 106, pp. 1-20.

Ives, J. D., 1956. Till patterns in central Labrador. Canadian Geographer 1, 25-33.

Jensen, J. R., 1996. Introductory Digital Image Processing: A Remote Sensing Perspective. Prentice Hall, Upper Saddle River, New Jersey, 318 pages.

Johnson, M. D., Mickelson, D. M, Clayton, L., Attig, J. W, 1995. Composition and genesis of glacial hummocks, western Wisconsin, USA. Boreas 24, 97-116.

King, A. F., 1988. Geology of the Avalon Peninsula, NL. Map 1K, 1L, 1M, 1N, 2C, Newfoundland Department of Mines, Mineral Development Division, St.John's, Newfoundland, Canada.

King, A. F., 1989. Geological evolution of the Avalon Peninsula, Newfoundland. Newfoundland Journal of Geological Education 10, 17-32.

King, L.F., Fader, G.B. 1986. Wisconsinan glaciation of the Atlantic continental shelf of southeast Canada. Geological Survey of Canada, Bulletin, 363.

Knight, J., 2002. Bedform patterns, subglacial meltwater events, and Late Devensian ice sheet dynamics in north-central Ireland. Global and Planetary Change 35, 237-253.

Knight, J., McCabe, A. M., 1997. Drumlin evolution and ice sheet oscillations along the NE Atlantic margin, Donegal Bay, Western Ireland. Sedimentary Geology 111, 57-72.

Kor, P. S. G., Cowell, D. W., 1998. Evidence for catastrophic subglacial meltwater sheetflood events on the Bruce Peninsula, Ontario. Canadian Journal of Earth Science 35. 1180-1202.

Krüger, J., 1995. Origin, chronology and climatological significance of annual-moraine ridges at Murdalsjökull, Iceland. The Holocene 5, 420-427.

Kumler, M.P., 1994. An intensive comparison of triangulated irregular networks (TINs) and digital elevation models (DEMs). Cartographica 31, 1-99.

Larsen, N. K., Piotrowski, J. A., 2003. Fabric pattern in a basal till succession and its significance for reconstructing subglacial processes. Journal of Sedimentary Research 73 (5), 725-734.

Liverman, D.G.E. 1994. Relative sea-level history and isostatic rebound in Newfoundland, Canada. Boreas, 23:217-230.

Lundqvist, J., 1969. Problems of the so-called Rogen moraine. Sveriges Geologiska Undersokning Series C NR 648, 3-32.

Lundqvist, J., 1981. Moraine morphology: terminological remarks and regional aspects. Geografiska Annaler 63A, 127-138.

Lundqvist, J., 1989. Rogen (ribbed) moraine - identification and possible origin. Sedimentary Geology 62, 281-292.

Lundqvist, J., 1997. Rogen moraine - an example of two-step formation of glacial landscapes. Sedimentary Geology 111, 27-40.

MacClintock, P., Twenhofel, W. H., 1940. Wisconsinan glaciation of Newfoundland. Bulletin of the Geological Society of America 51, 1729-1756.

Macpherson, J. B., 1996. Delayed deglaciation by downwasting of the northeast Avalon Peninsula, Newfoundland: an application of the early postglacial pollen record. Geographie Physique et Quaternaire 50, 210-220.

Marich, A. S., Batterson, M., Bell, T., 2005. The morphology and sedimentological analyses of Rogen moraines, central Avalon Peninsula, NL. In: Current Research, Geological Survey Branch, Newfoundland Department of Mines and Energy, Report 05-1, 1-14.

Mawdsley, J. B., 1936. Washboard moraines of the Opawica-Chibaugamau District. Transactions of the Royal Society of Canada 3, 30, 9-12.

Menzies, J. (Ed). 2002. Modern & Past Glacial Environments. Butterworth Heinemann, Oxford, 543 pages.

Möller, P., 2005. Rogen moraine: An example of glacial reshaping of pre-existing landforms. Quaternary Science Reviews 25 (3-4), 362-389.

Munro, M., Shaw, J., 1997. Erosional origin of hummocky terrain in south-central Alberta, Canada. Geology 5, 1027-1030.

Murray, A., 1883. Glaciation in Newfoundland. Proceedings and Transactions of the Royal Society of Canada 1, 55-76.

Murray, T., 1997. Assessing the paradigm shift: deformable glacier beds. Quaternary Science Reviews 16, 995-1016.

Prest, V. K., Grant, D. G., Rampton, V. N., 1968. Glacial Map of Canada. Map 1253A, Geological Survey of Canada, Ottawa, Canada.

Rogerson, R. J., Tucker, C. M., 1972. Observations on the glacial history of the Avalon Peninsula. Maritime Sediments 8, 25-31.

Sharp, M., 1984. Annual moraine ridges at Skalafellsjökull, south-east Iceland. Journal of Glaciology 30, 82-93.

Sharpe, D. R., 2005. Correspondence. Quaternary Science Reviews 24, 1529-1532.

Shaw, J., 1979. Genesis of the Sveg tills and Rogen moraines of central Sweden: a model of basal melt out. Boreas 8, 409-426.

Shaw, J., 1982a. Forms associated with boulders in melt-out till. INQUA Symposia on the Genesis and Lithology of Quaternary Deposits.

Shaw, J., 1982b. Melt-out till in the Edmonton area, Alberta, Canada. Canadian Journal of Earth Science 19, 1548-1569.

Shaw, J., 1983. Drumlin formation by subglacial meltwater erosion. Journal of Glaciology 29, 461-479.

Shaw, J., 2002. The meltwater hypothesis for subglacial bedforms. Quaternary International 90, 5-22.

Shaw, J., Kvill, D., Ruins, R. B, 1989. Drumlins and catastrophic subglacial floods. Sedimentary Geology 62, 177-202.

Shaw, J., Rains, B., Eyton, R., Weissling, L., 1996. Laurentide subglacial outburst floods: landform evidence from digital elevation models. Canadian Journal of Earth Science 33, 1154-1168.

Shaw, J., Stea, R. R., Fader, G. B., Todd, B. J., Courtney, R. C., Bell, T., Batterson, M., In Press. A conceptual model of the deglaciation of Atlantic Canada.

Shoemaker, E. M., 1992. Water sheet outburst floods from the Laurentide Ice Sheet. Canadian Journal of Earth Science 29, 1250-1264.

Shoemaker, E. M., 1995. On the meltwater genesis of drumlins. Boreas 24, 3-10.

Shoemaker, E. M., 1999. Subglacial water-sheet floods, drumlins and ice-sheet lobes. Journal of Glaciology 45, 201-212.

Shoemaker, E. M., 2003. Effects of bed depressions upon floods from subglacial lakes. Global and Planetary Change 35, 175-184.

Shoemaker, E. M., Walder, J. S., 2001. Reply to comments on "Subglacial floods and the origin of low-relief ice-sheet lobes". Journal of Glaciology 40, 201-200.

Summers, W., 1949. Physical geography of the Avalon Peninsula of Newfoundland. McGill University, Montreal, Canada.

Tucker, C. M., Leckie, D. A., McCann, S. B., 1982. Raised shoreline phenomena and postglacial emergence in south-central Newfoundland. Geographie Physique et Quaternaire 36, 165-174.

Van der meer, J. J. M., Menzies, J., Rose, J., 2003. Subglacial till: the deforming glacier bed. Quaternary Science Reviews 22, 1659-1685.

Wellner, R.W., Ashley, G.M., Sheridan, R.E. 1993. Seismic stratigraphic evidence for a submerged middle Wisconsinan barrier: Implications for sea level history. Geological Survey of Canada, 21, 109-112.

Wolf, P. R., 1983. Elements of Photogrammetry, with Air Photo Interpretation and Remote Sensing. McGraw-Hill, New York, 628 pages.

Woodcock, N. H., 1977. Specification of fabric shapes using an eigenvalue method. Geological Society of America Bulletin 88, 1231-1236.

Appendix A Ridge orientation calculations

An ArcView shapefile was created showing the location of ridge crests interpreted from the 1:50 000 air photos. Several steps were then completed in order to calculate the orientation of each ridge. Individual ridges are composed of multiple line segments that in turn have a specific orientation. Ridge crests are commonly curved, therefore the orientation for each ridge had to be calculated by averaging the orientation values for each of the individual line segments. This process required several steps: Each line representing a single ridge crest required a unique id value, and then three scripts (Output, Bearing, Explode) (Schultz, 2003; Chasan, 2000) were used to calculate the bearing of the line segments. The sine and cosine were calculated for each segment using the following equations:

sin_a = (Angle of segment in radians).sin

cos_a = (Angle of segment in radians).cos

The values were then summarized for each line, and the sum of the sine and the sum of the cosine for each ridge crest was calculated.

The mean direction was calculated for each line using:

$$Avg\_dir = ((\Sigma\ sina/Sum\_cosa).Atan)*180/\pi \qquad \text{where } 180/\pi = 57.29578$$

The actual orientation (angle) of the ridges was then calculated using the following relationships:

If $\text{Sin}\theta_i >= 0$ and $\text{Cos}\theta_i >= 0$ Then angle = angle

If $\text{Sin}\theta_i > = 0$ and $\text{Cos}\theta_i < 0$ Then angle = 180-(angle.ABS)

If $\text{Sin}\theta_i < 0$ and $\text{Cos}\theta_i <= 0$ Then angle = 180+(angle.ABS)

If $\text{Sin}\theta_i < 0$ and $\text{Cos}\theta_i >= 0$ Then angle = 360-(angle.ABS)

The resultant length was then calculated to determine the variability or the error in the orientation calculations:

$$R = \sqrt{(\Sigma \sin\theta_i)^2 + (\Sigma \cos\theta_i)^2}$$

And the mean resultant length:

$R = R/n$ where n is the number of segments in the line (Davis, 1986).

Large values of R indicate little variation or a straight line. R values near zero indicate that the line is curved.

Once the orientations for each of the ridge crest lines were calculated, the data were input into the GIS to examine the pattern of ridge crest alignments. Ridges were classified based on their orientations into four groups, 0-90°, 90-180°, 180-270°, and 270-360°. The orientation of ridges with respect to topographic and geologic trends within the landscape was also calculated.

Appendix B Location of landforms interpreted from aerial photographs

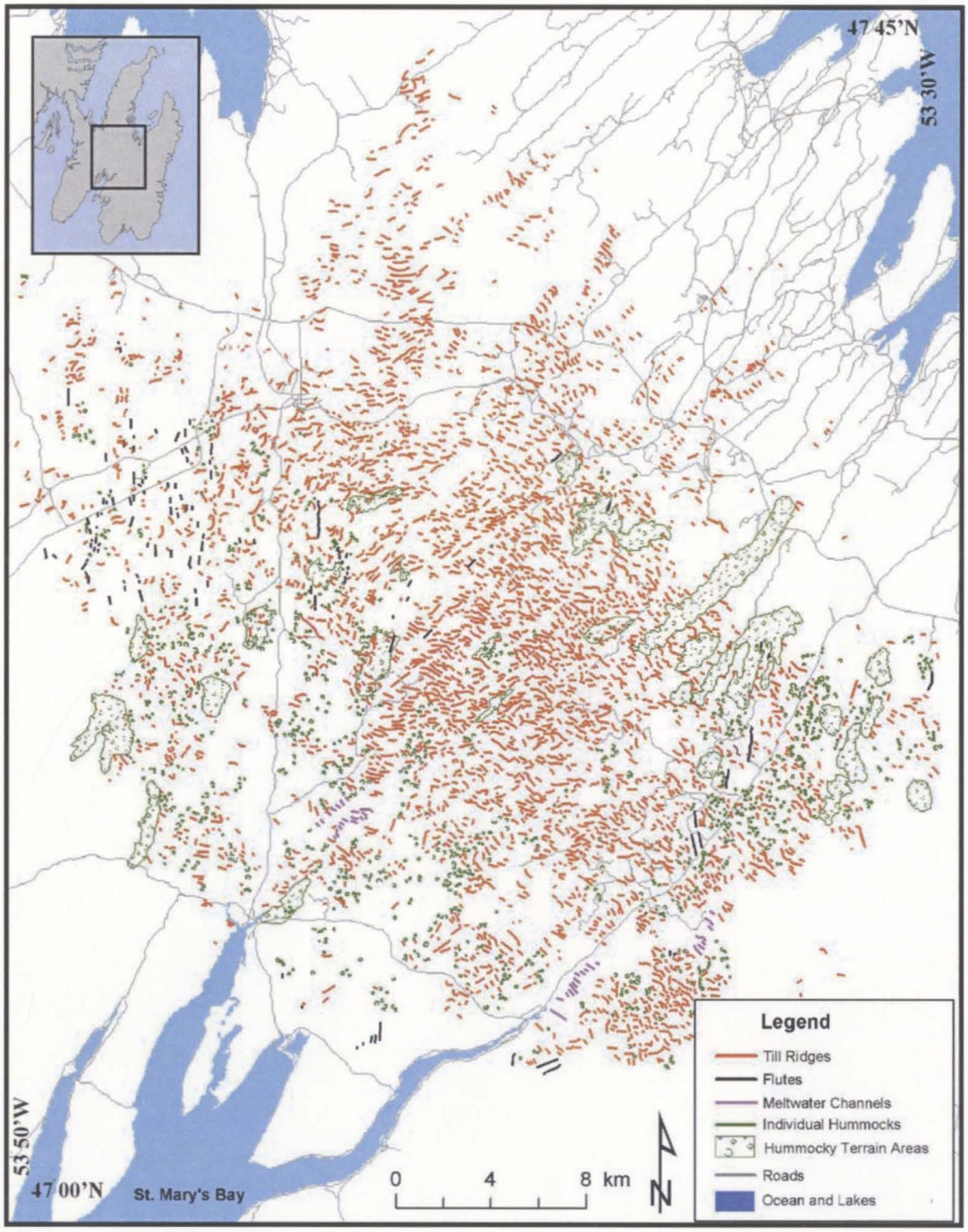

Figure B.1 Map showing the location of the landforms interpreted from the aerial photographs.

Appendix C Site Diagrams

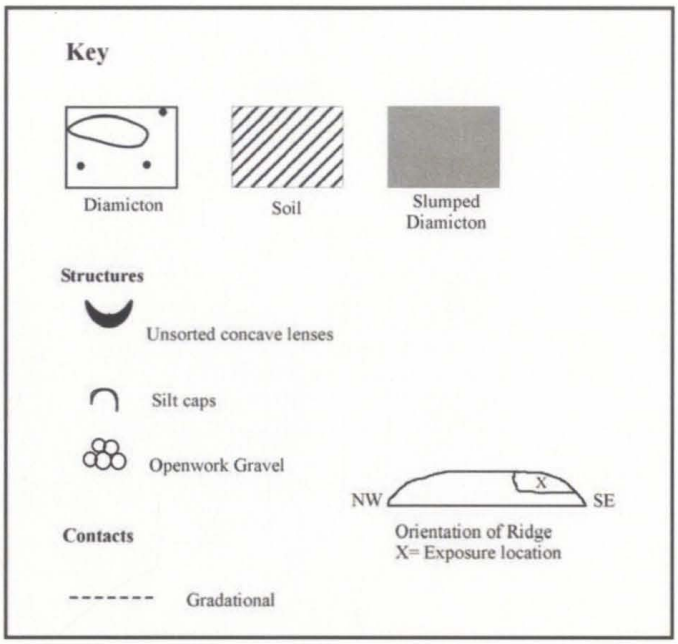

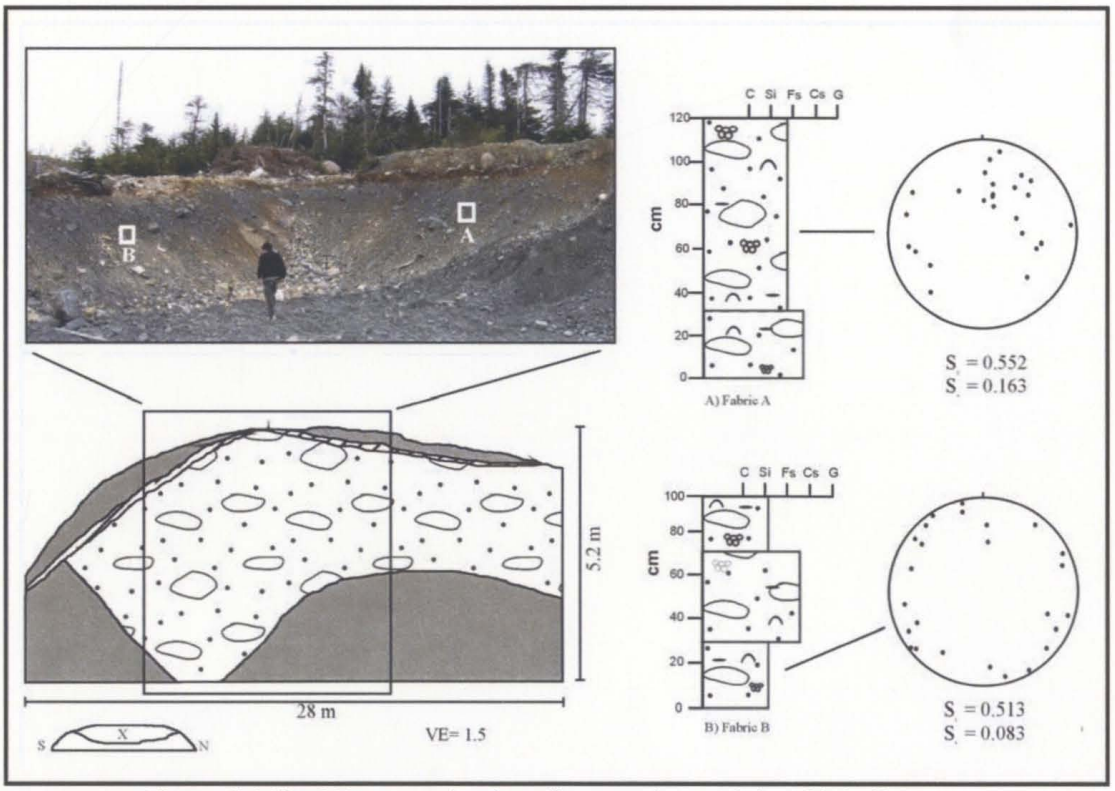

Figure C.1 Site 2 Exposure sketch, sedimentary logs and clast fabric diagrams.

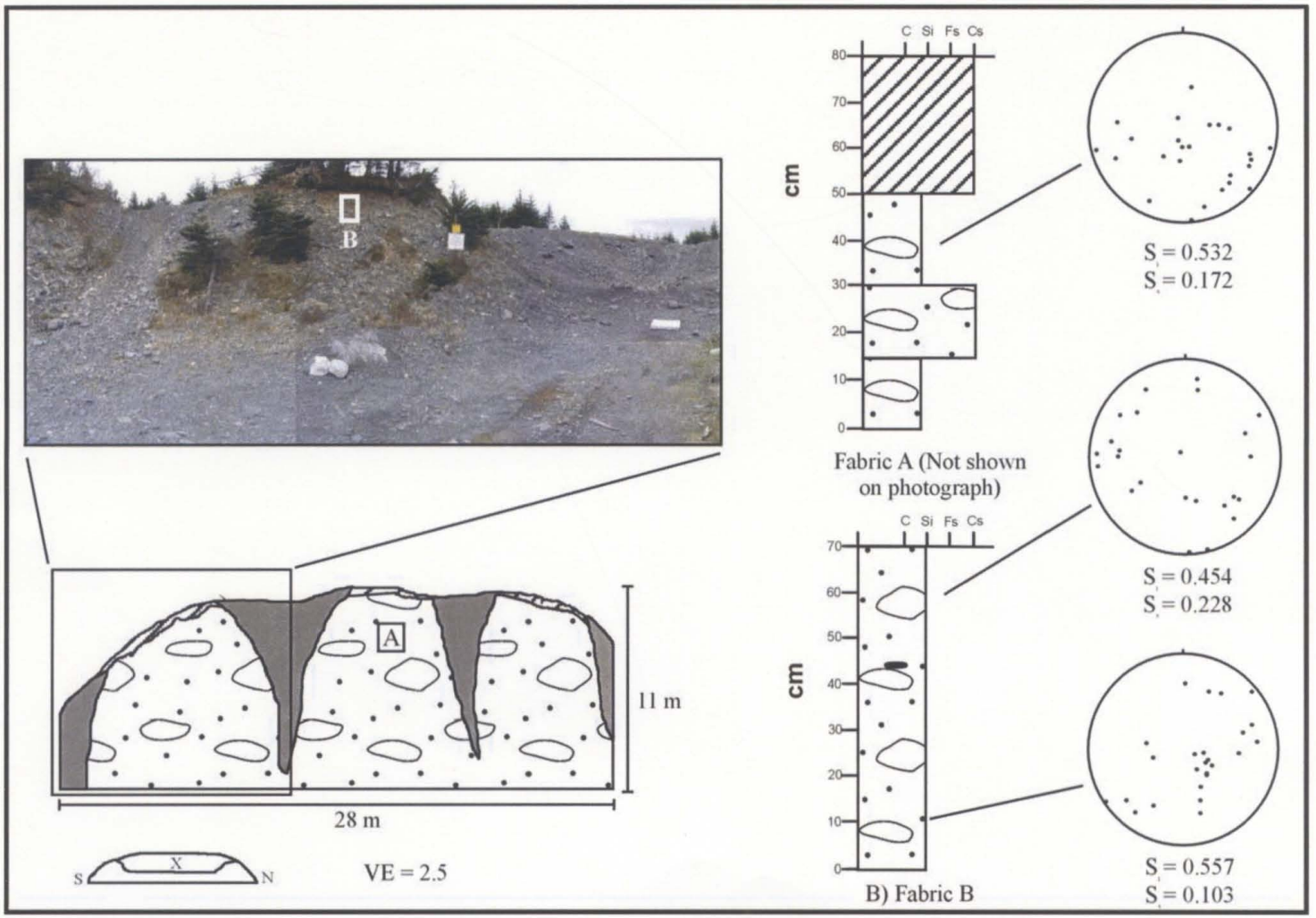

Figure C.2 Site 3 Exposure sketch, sedimentary logs and clast fabric diagrams.

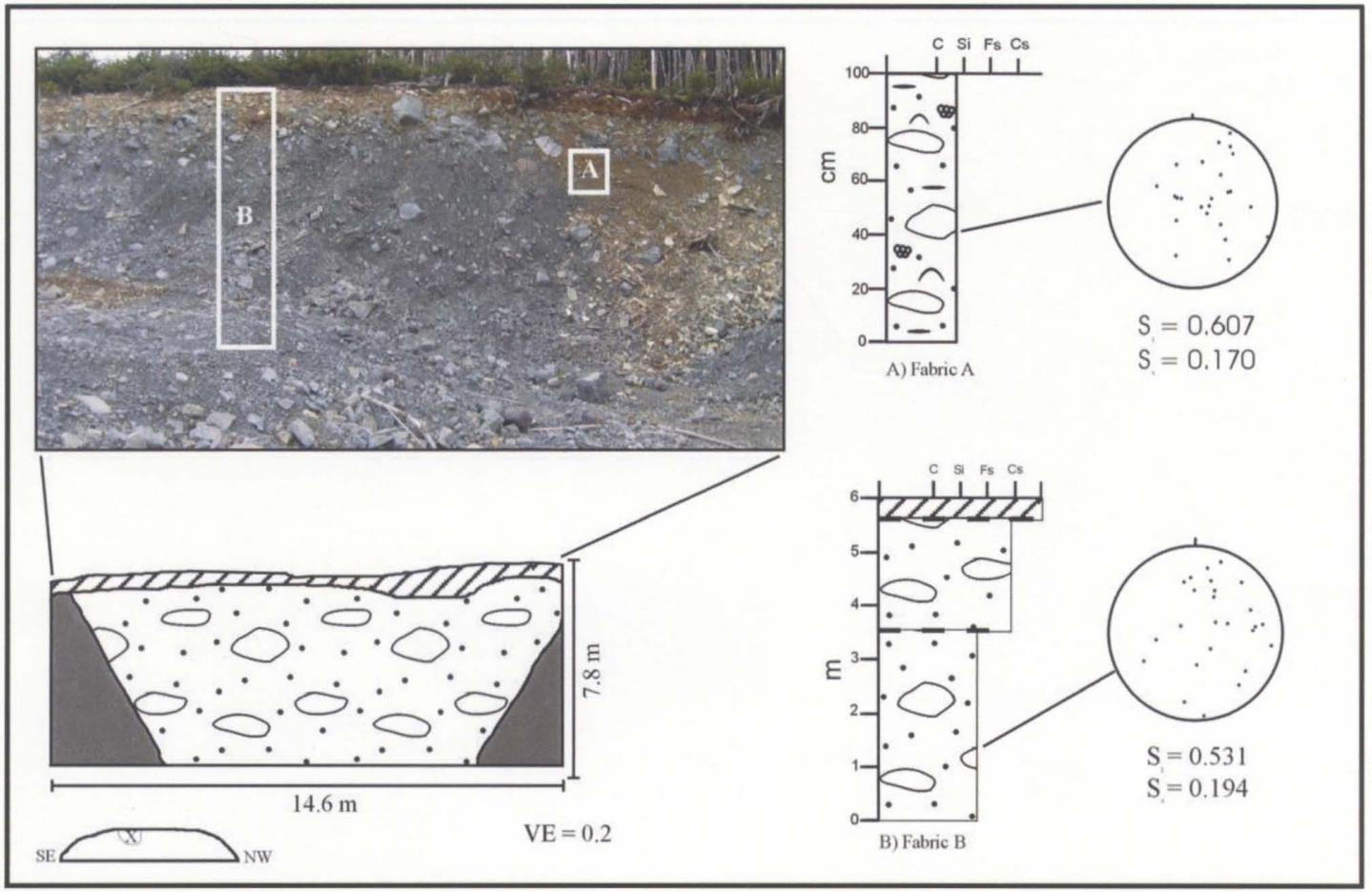

Figure C.3 Site 5 Exposure sketch, sedimentary logs and clast fabric diagrams.

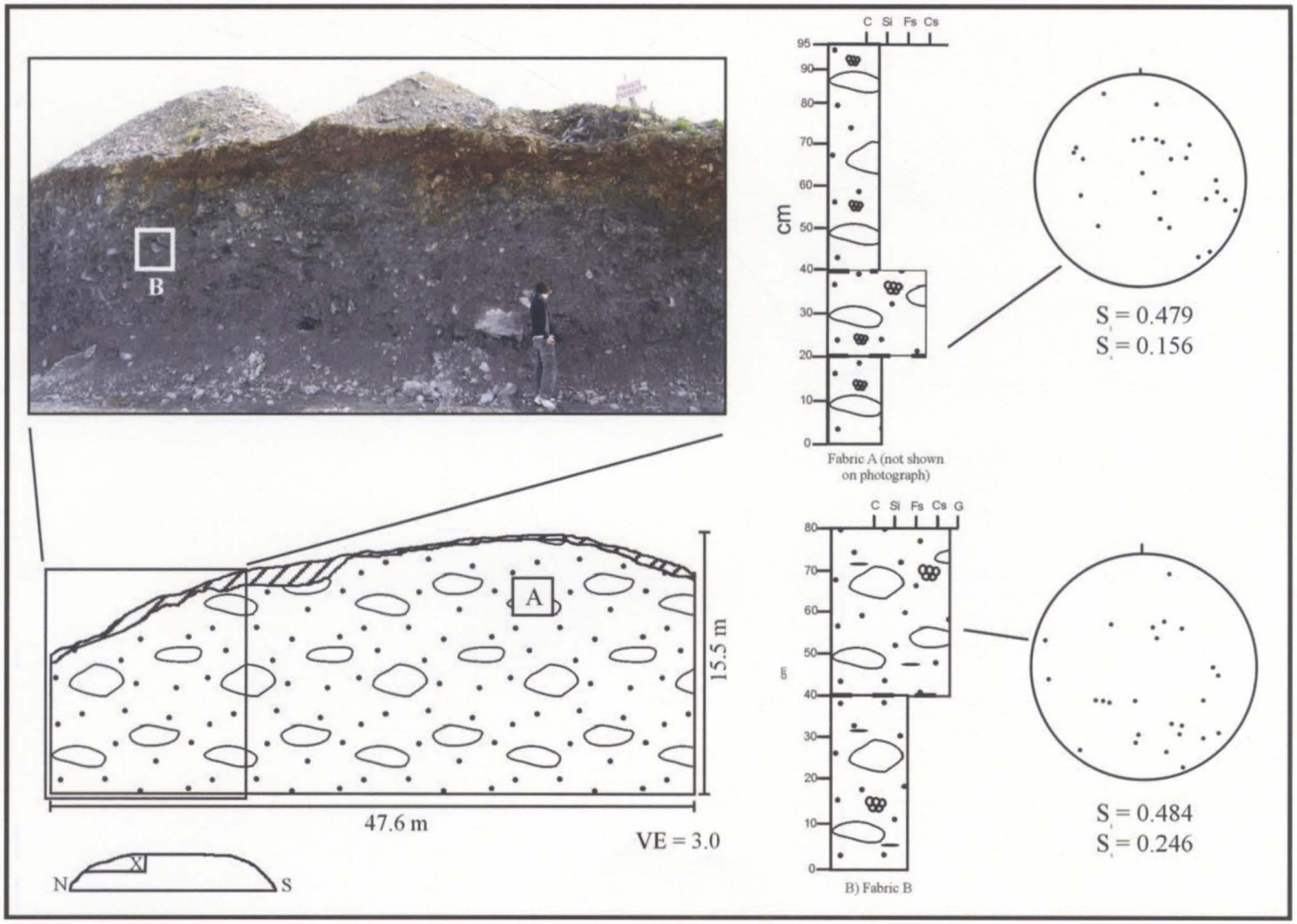

Figure C.4 Site 6 Exposure sketch, sedimentary logs and clast fabric diagrams.

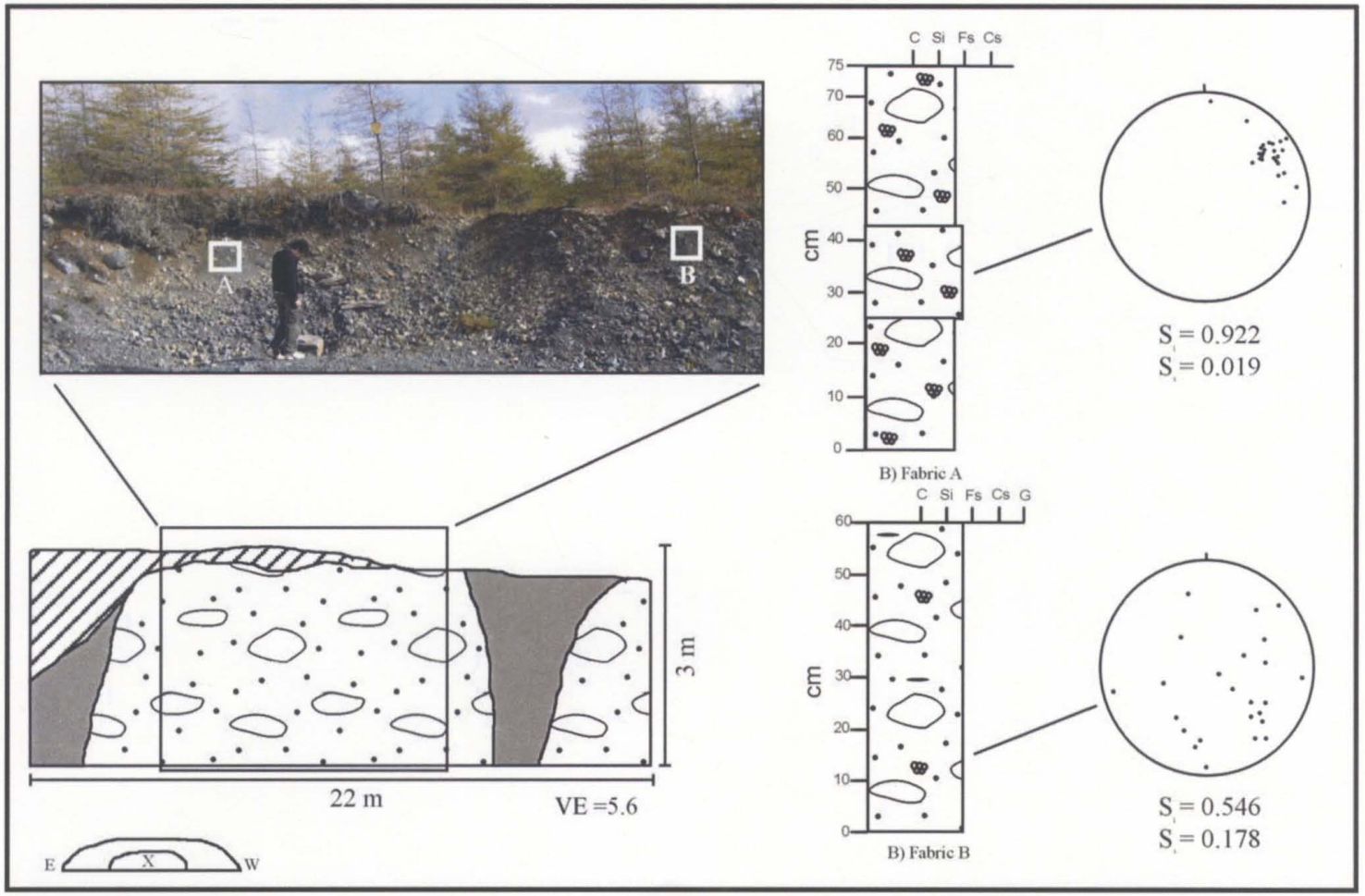

Figure C.5 Site 7 Exposure sketch, sedimentary logs and clast fabric diagrams.

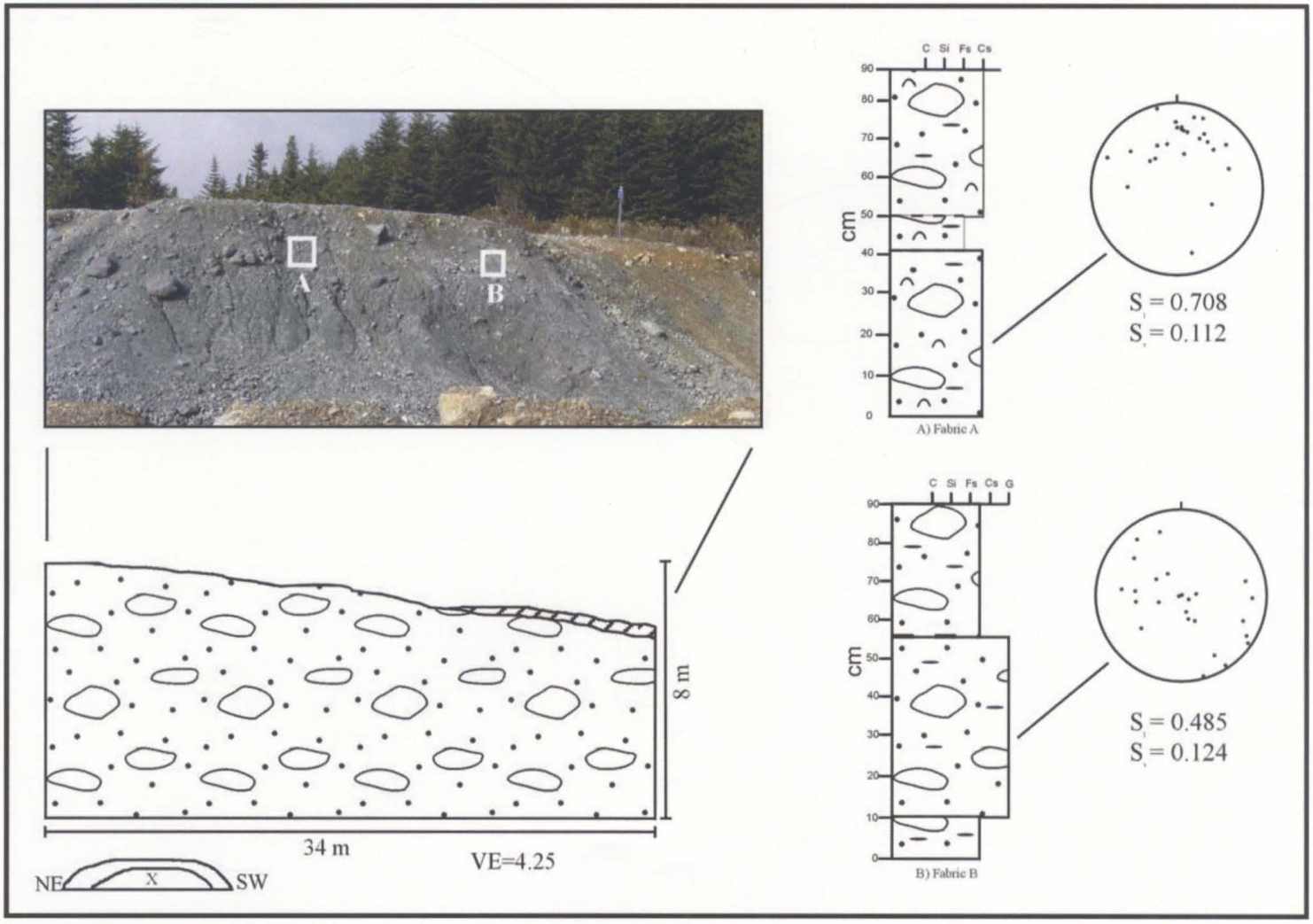

Figure C.6 Site 8 Exposure sketch, sedimentary logs and clast fabric diagrams.

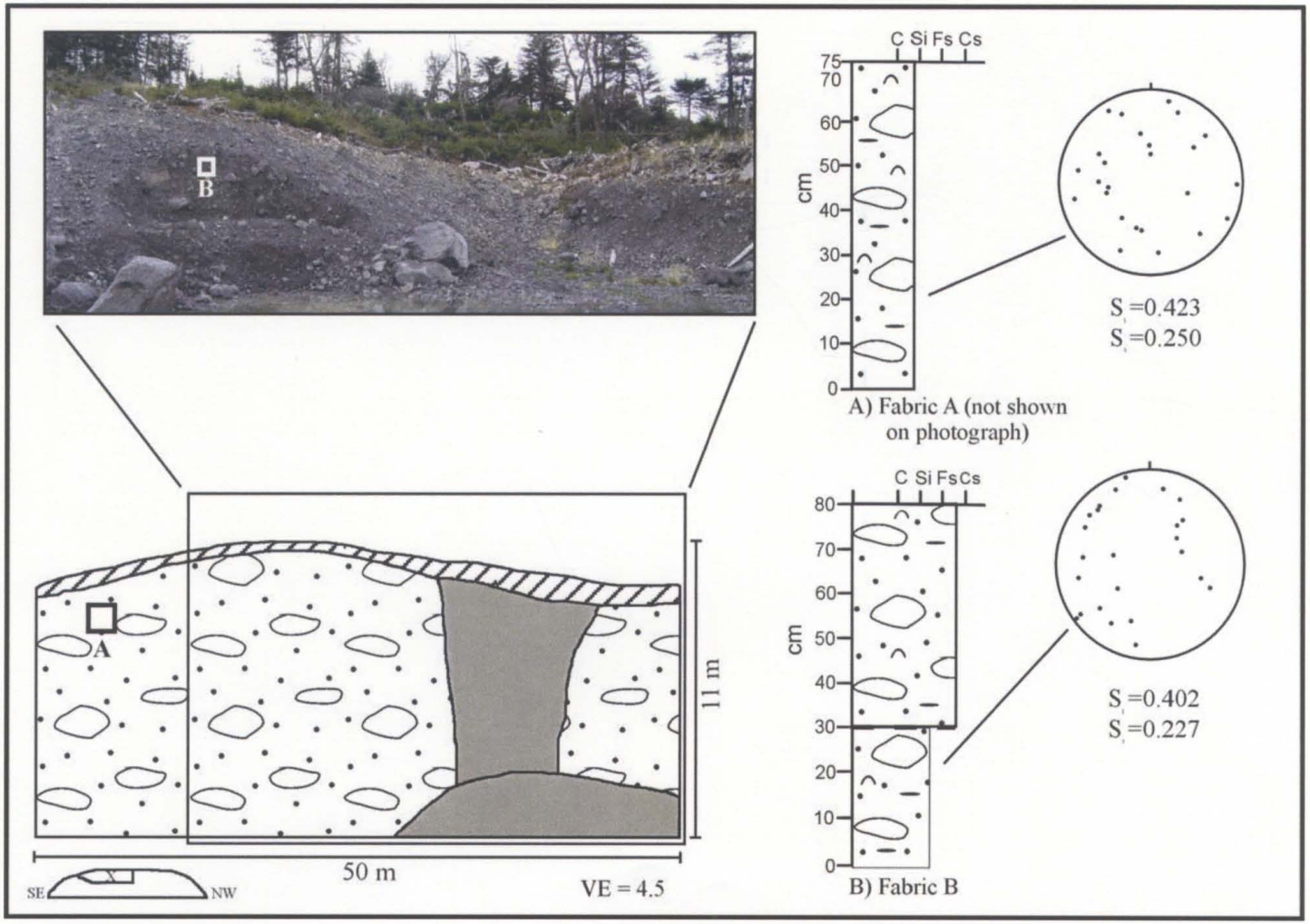

Figure C.7 Site 10 Exposure sketch, sedimentary logs and clast fabric diagrams.

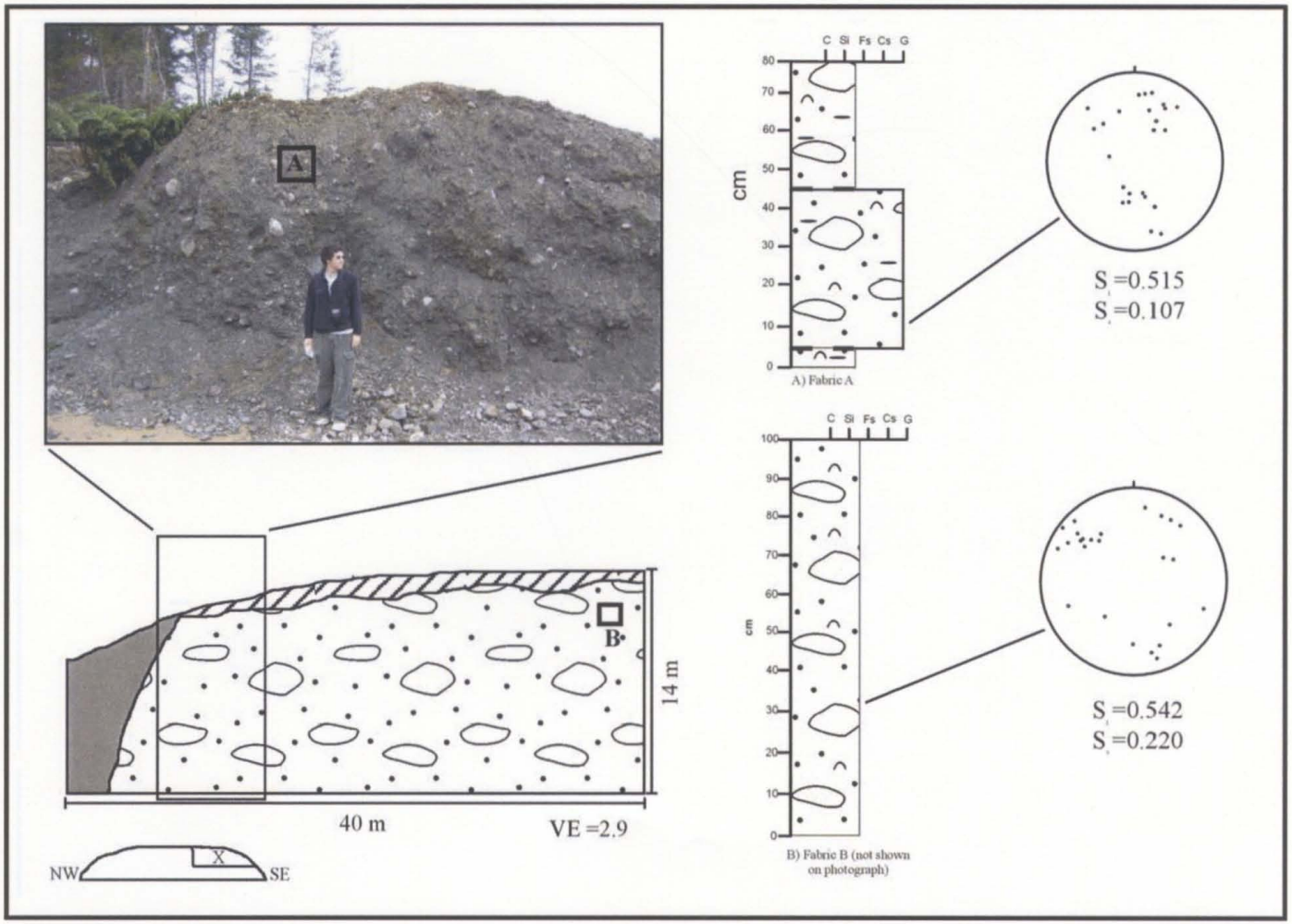

Figure C.8 Site 11 Exposure sketch, sedimentary logs and clast fabric diagrams.

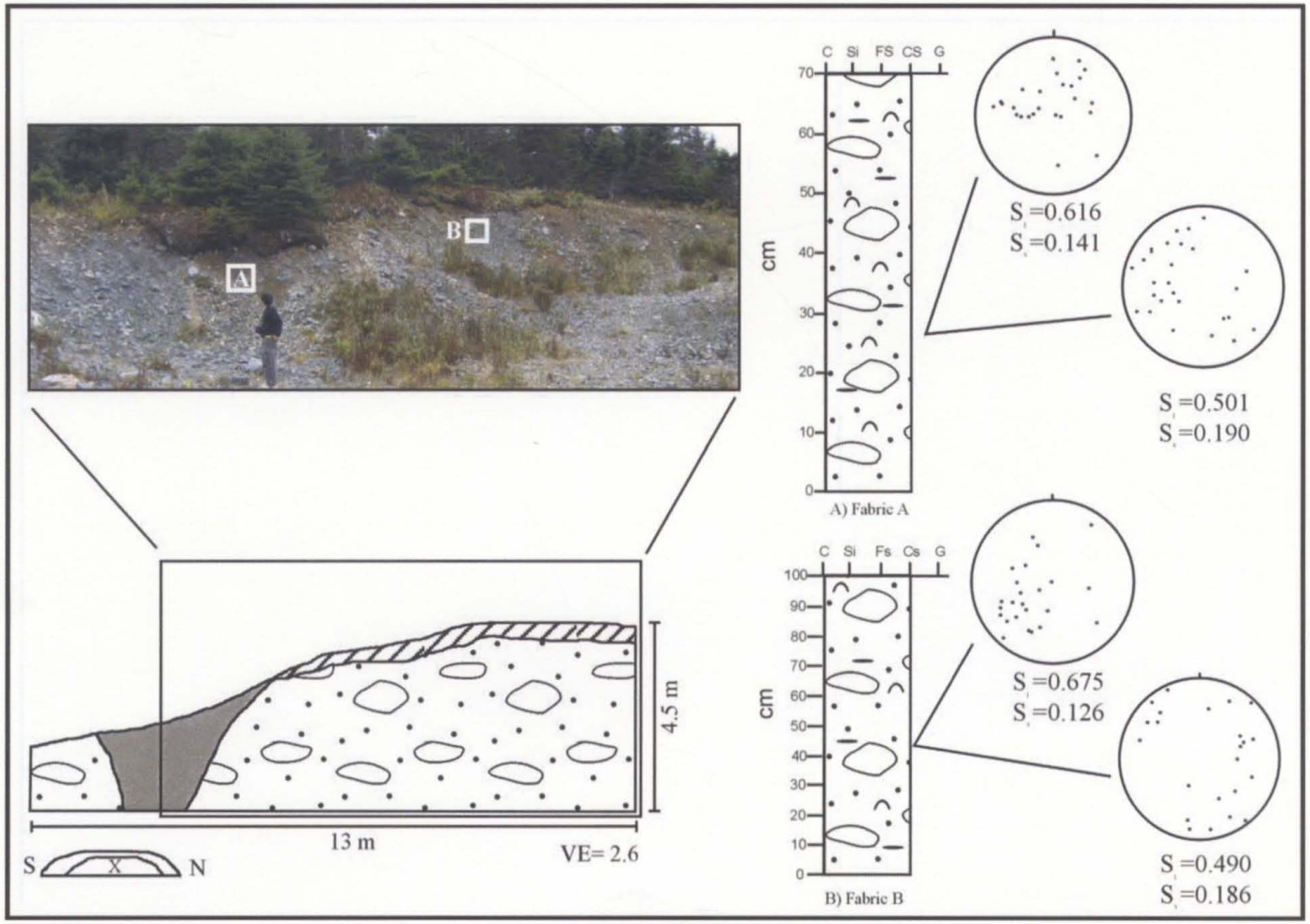

Figure C.9 Site 12 Exposure sketch, sedimentary logs and clast fabric diagrams.

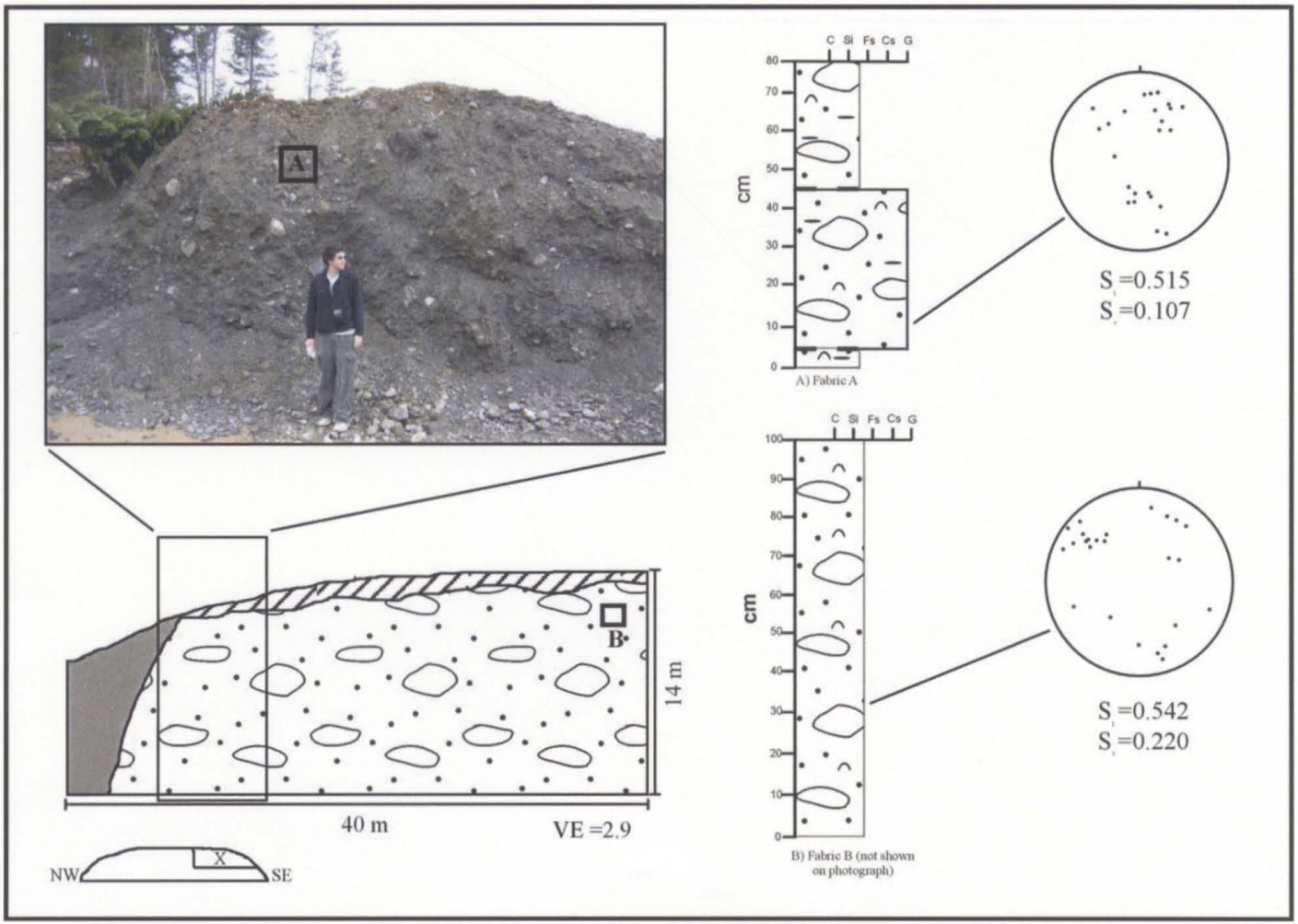

Figure C.10 Site 13 Exposure sketch, sedimentary logs and clast fabric diagrams.

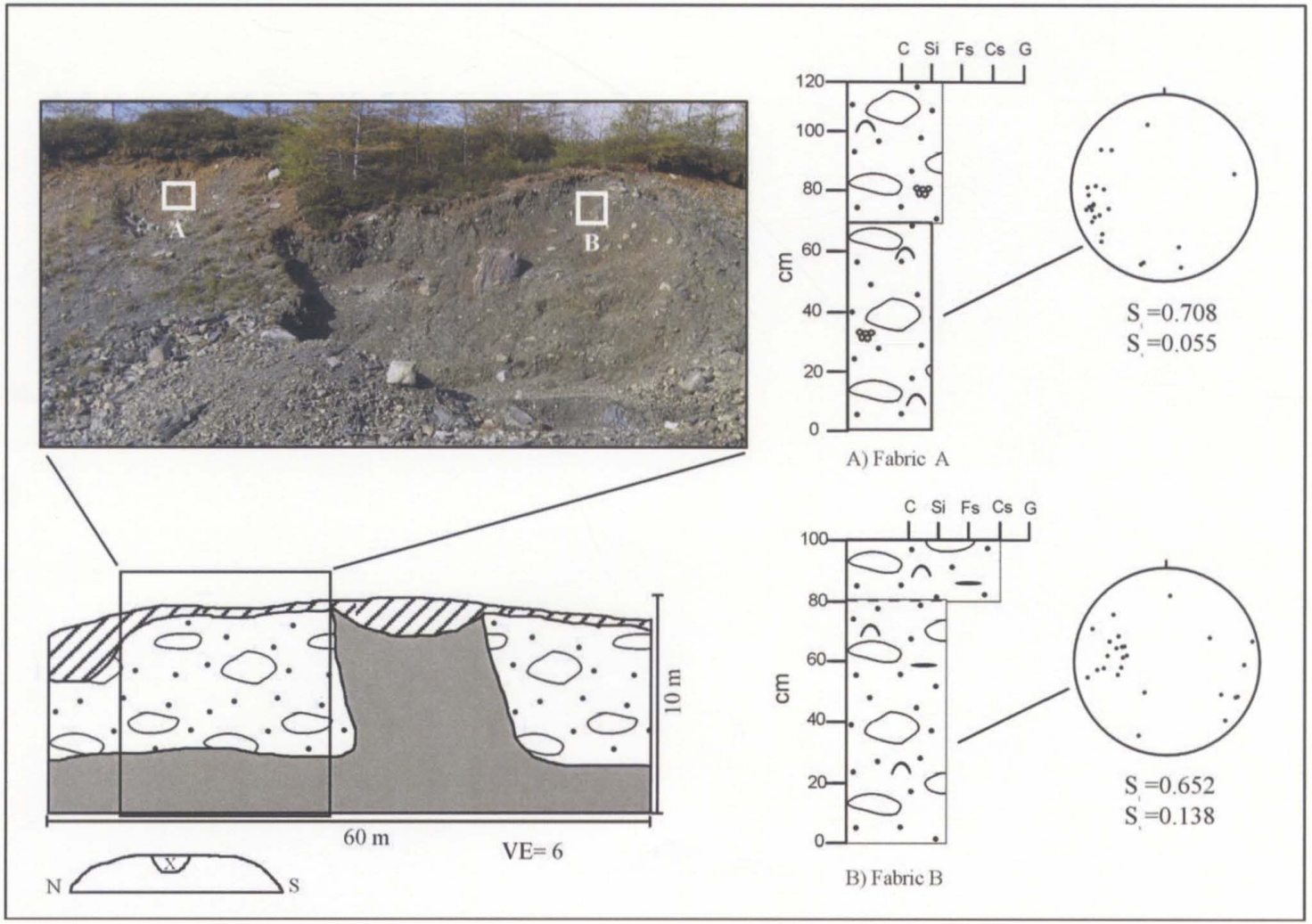

Figure C.11 Site 14 Exposure sketch, sedimentary logs and clast fabric diagrams.

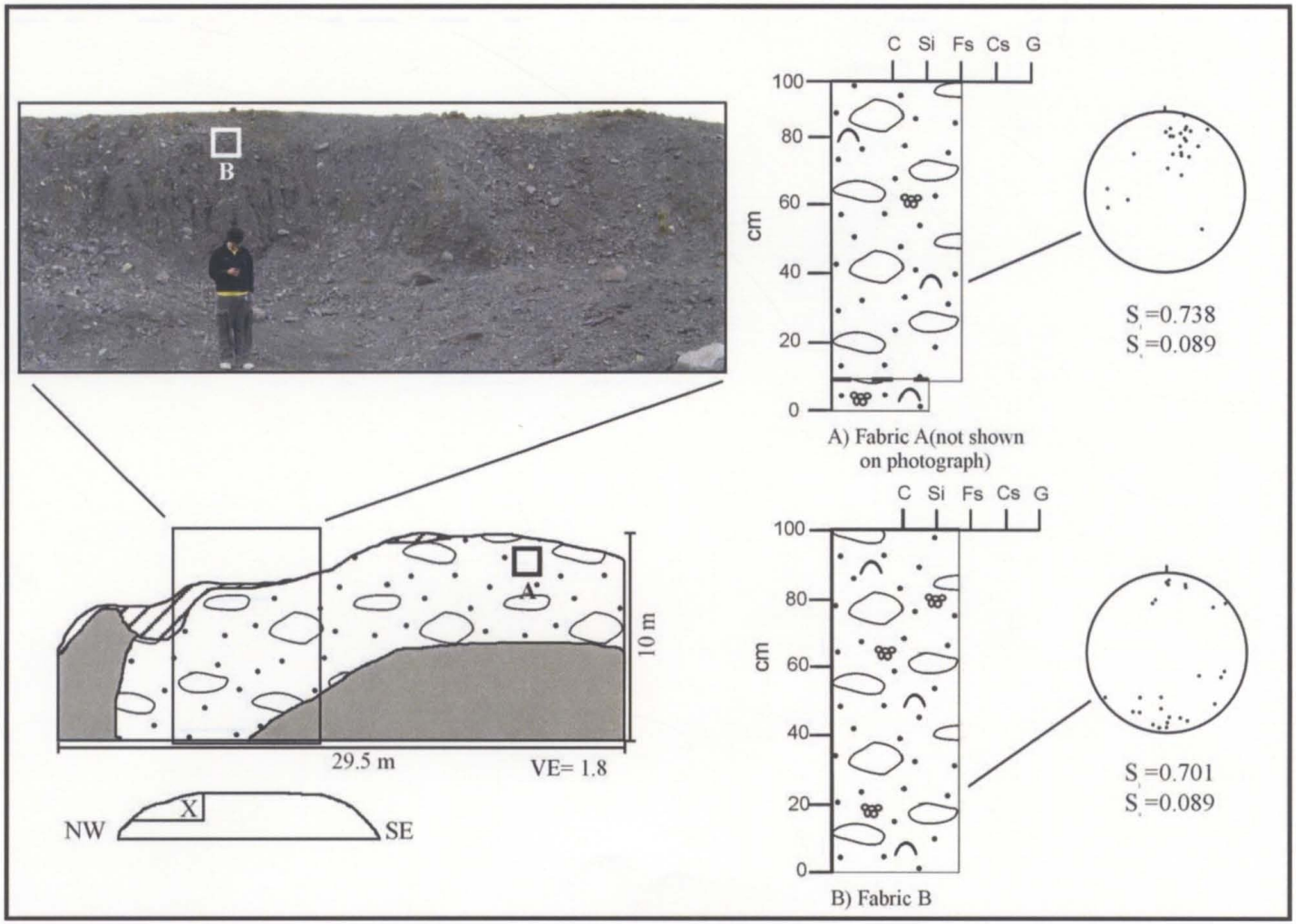

Figure C.12 Site 15 Exposure sketch, sedimentary logs and clast fabric diagrams.

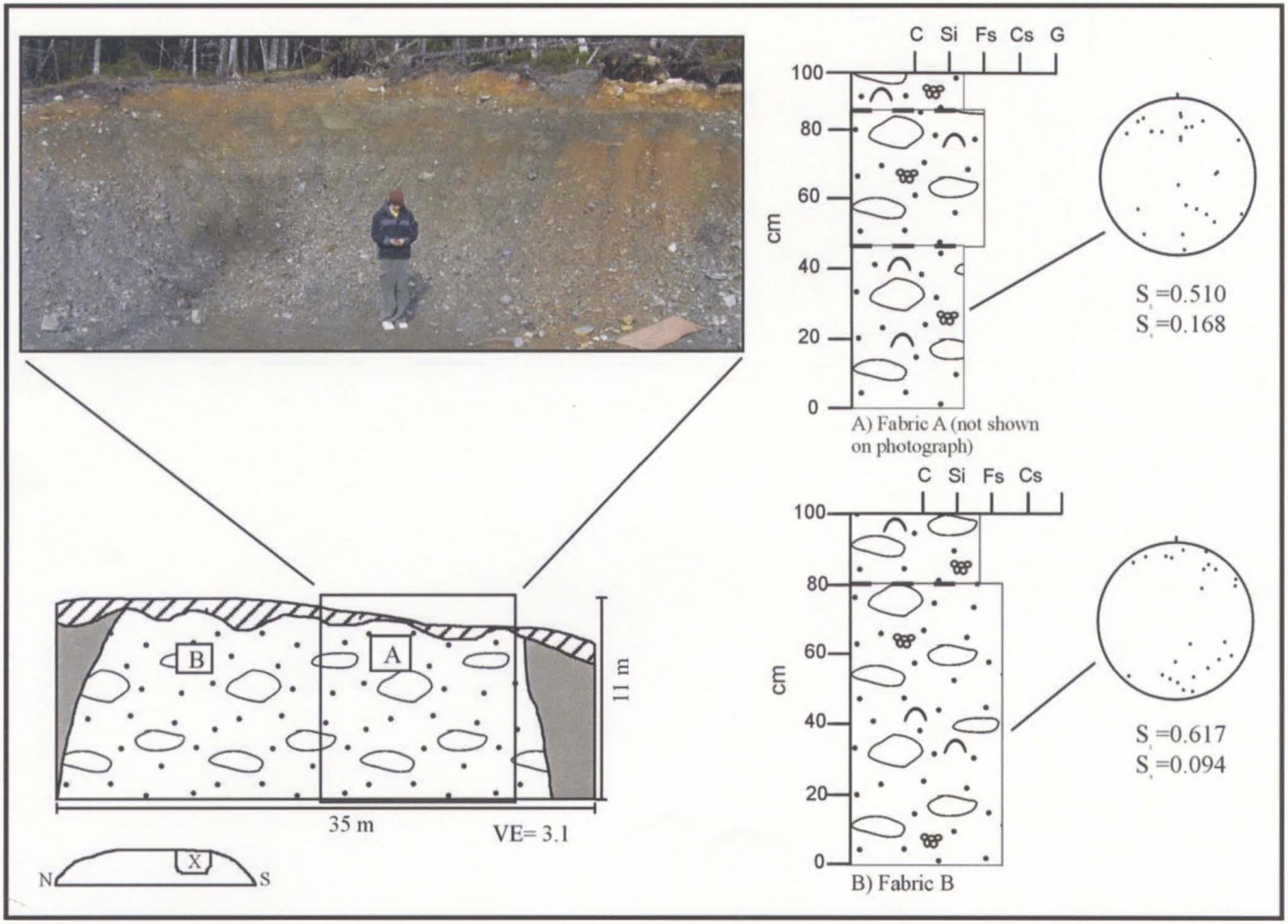

Figure C.13 Site 16 Exposure sketch, sedimentary logs and clast fabric diagrams.

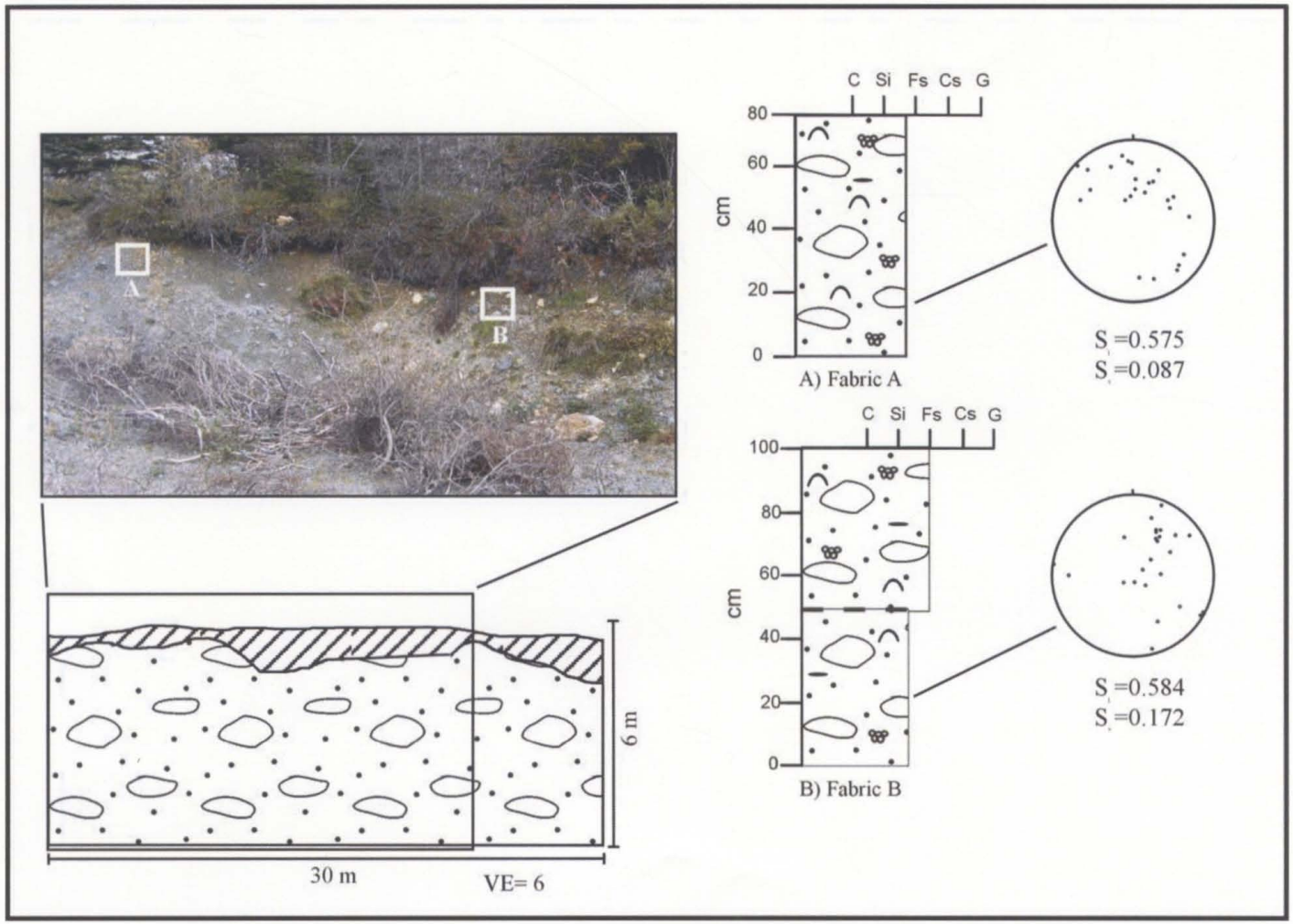

Figure C.14 Site 17 Exposure sketch, sedimentary logs and clast fabric diagrams.

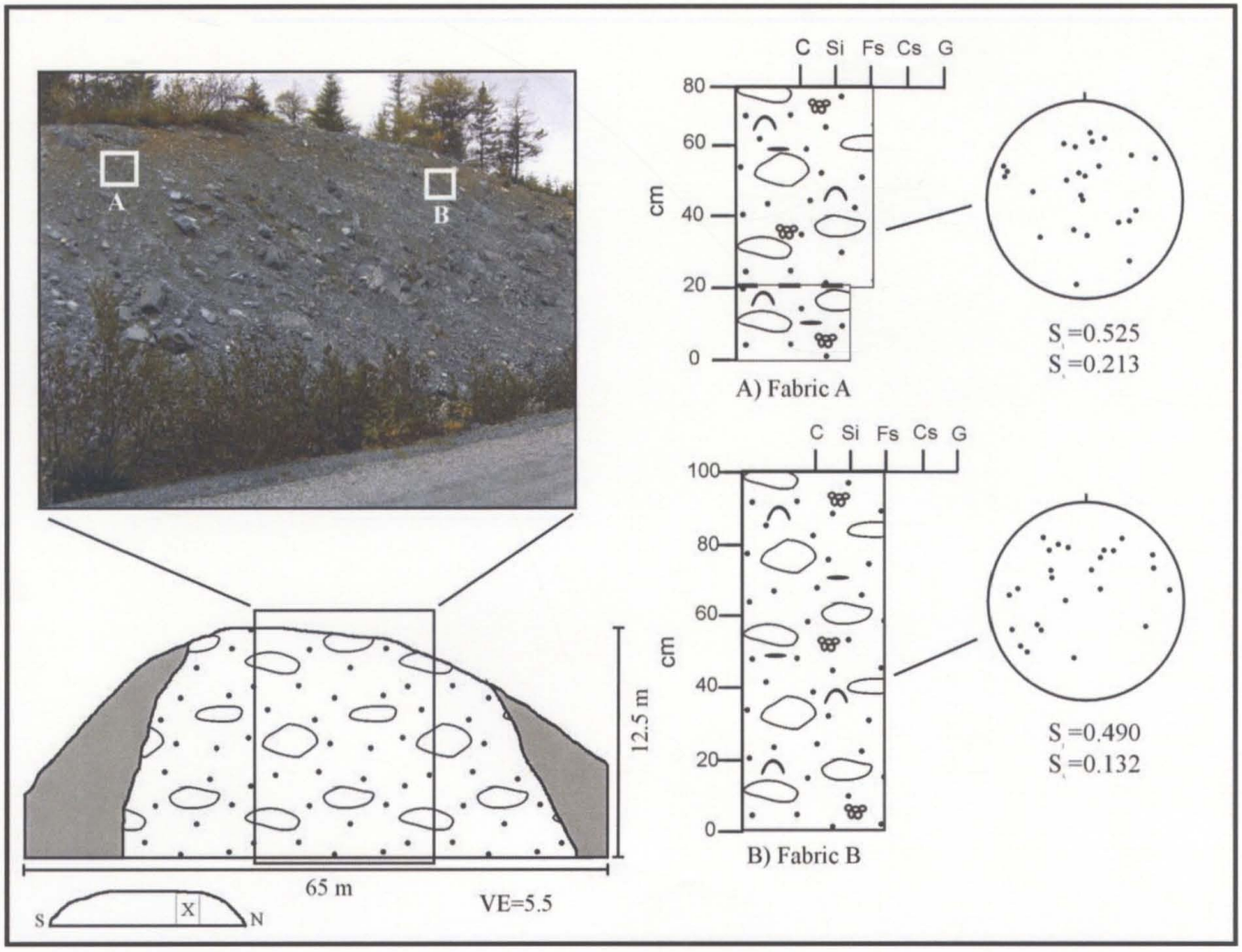

Figure C.15 Site 18 Exposure sketch, sedimentary logs and clast fabric diagrams.

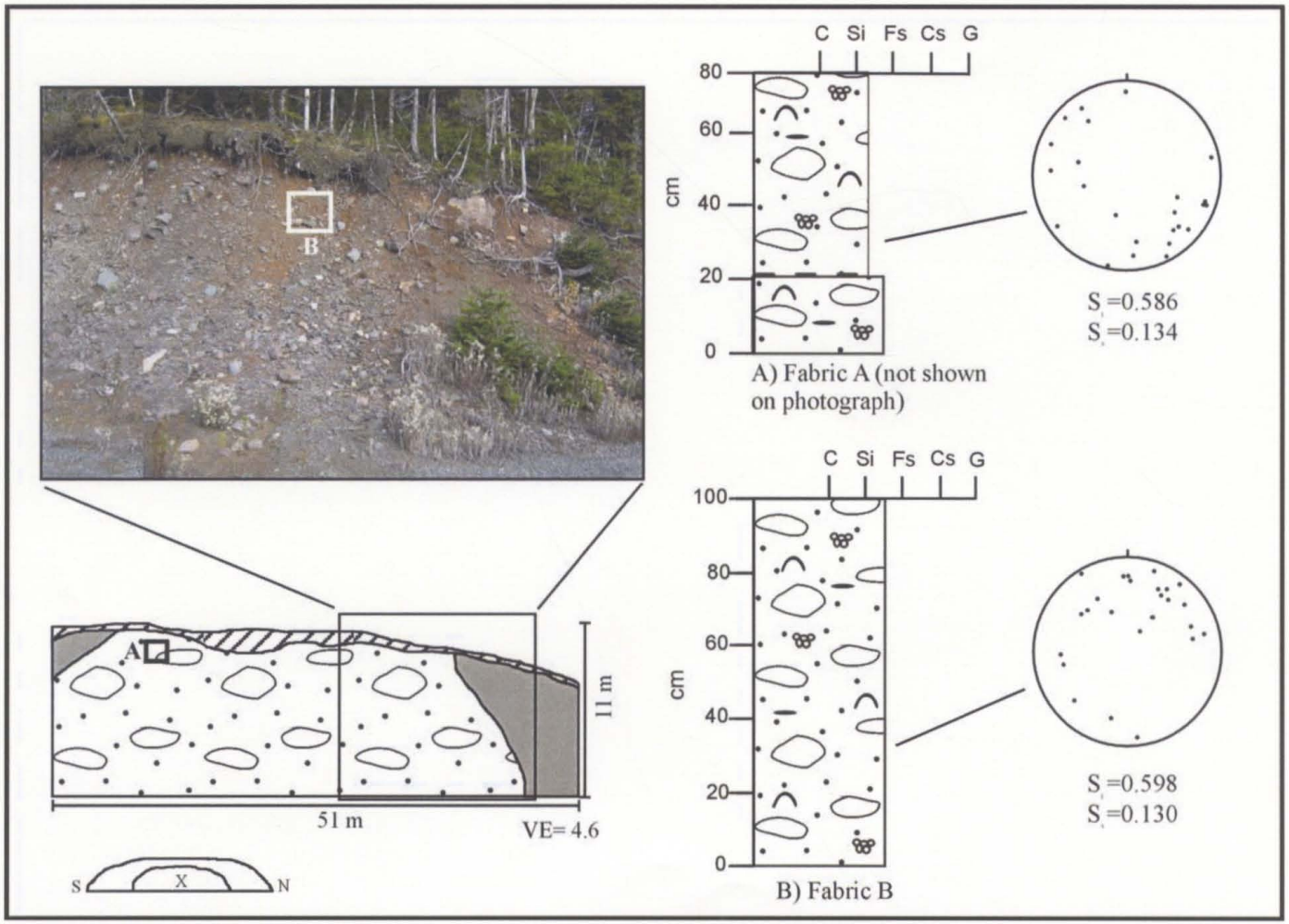

Figure C.16 Site 19 Exposure sketch, sedimentary logs and clast fabric diagrams.

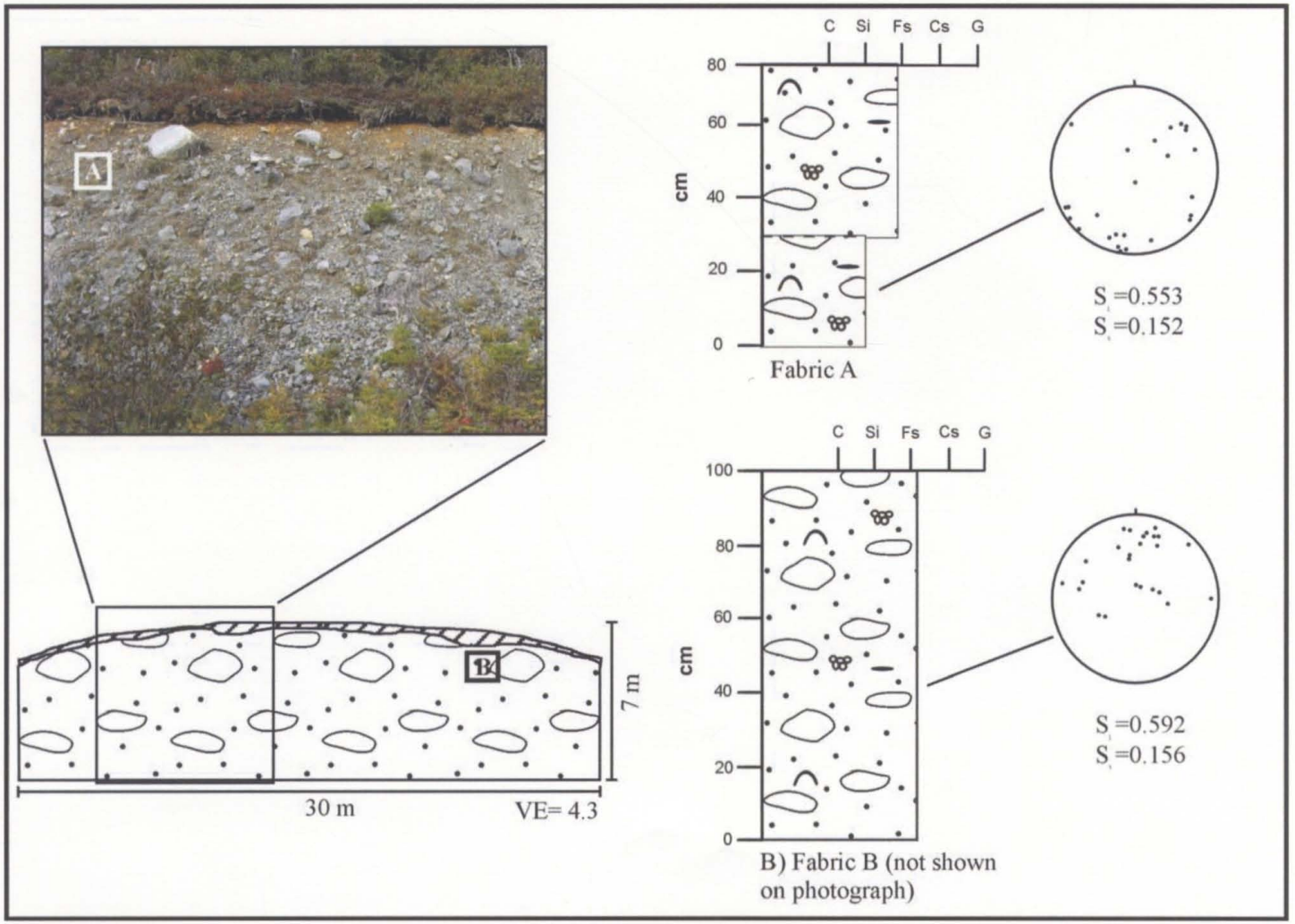

Figure C.17 Site 20 Exposure sketch, sedimentary logs and clast fabric diagrams.

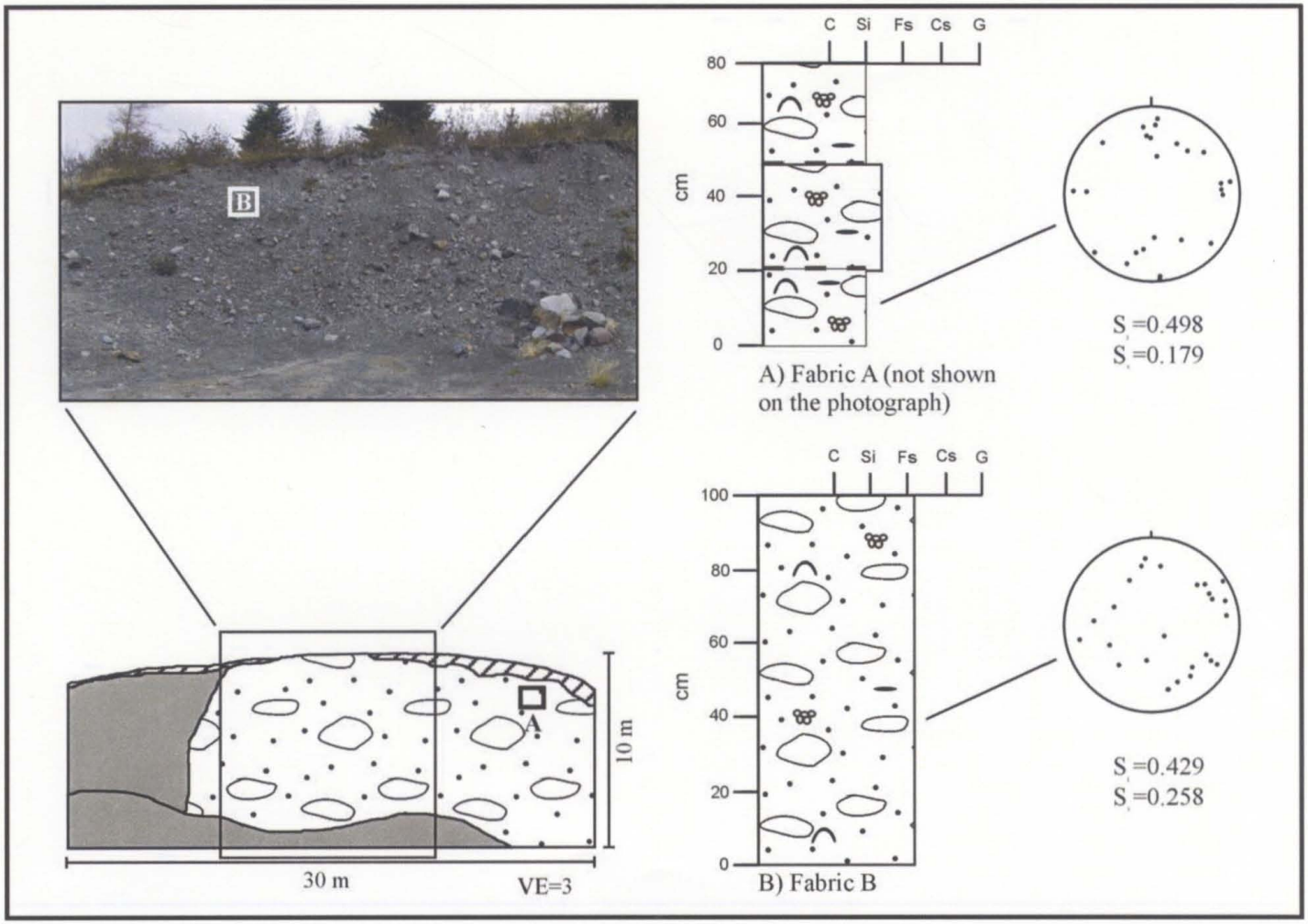

Figure C.18 Site 21 Exposure sketch, sedimentary logs and clast fabric diagrams.

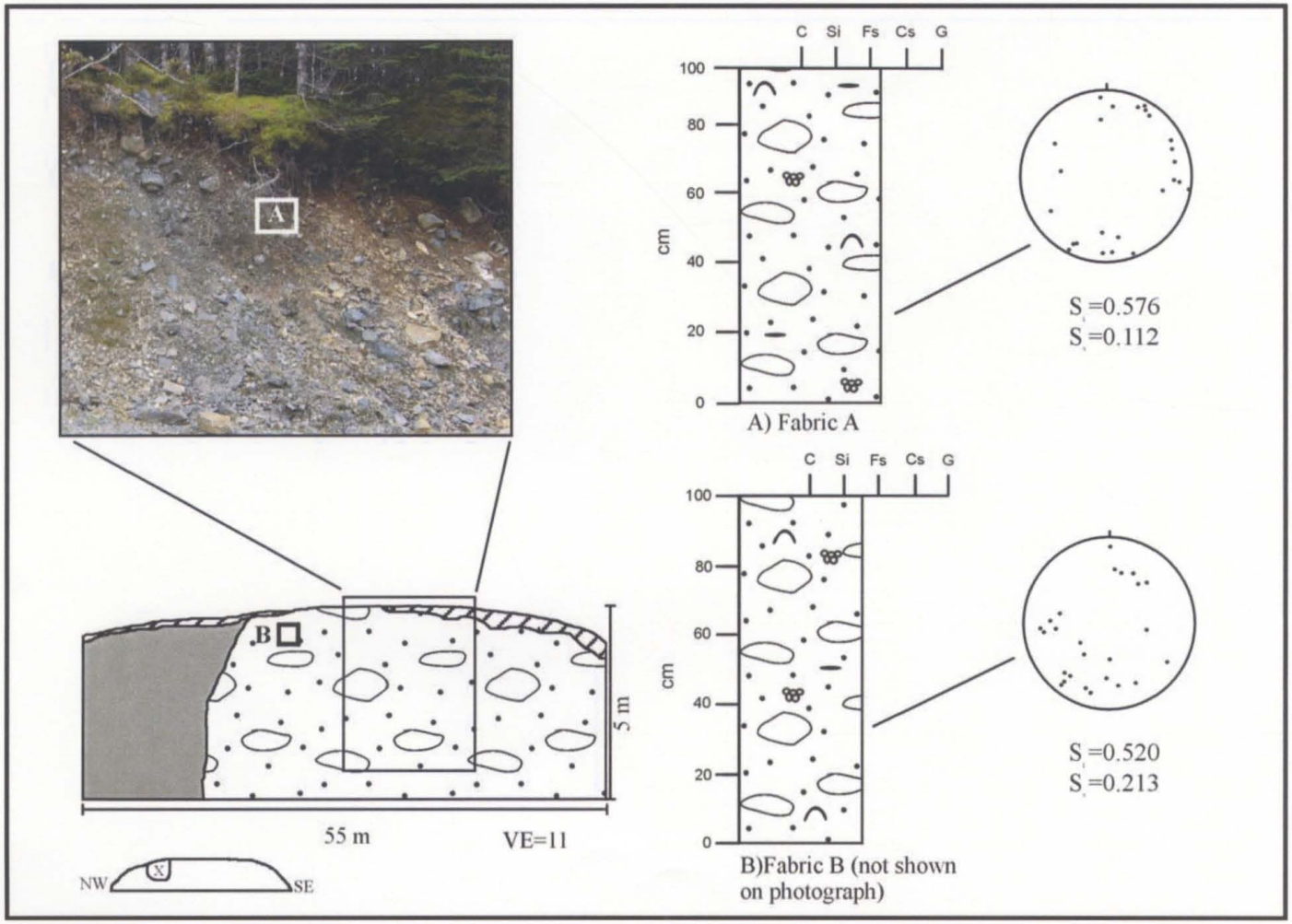

Figure C.19 Site 22 Exposure sketch, sedimentary logs and clast fabric diagrams.

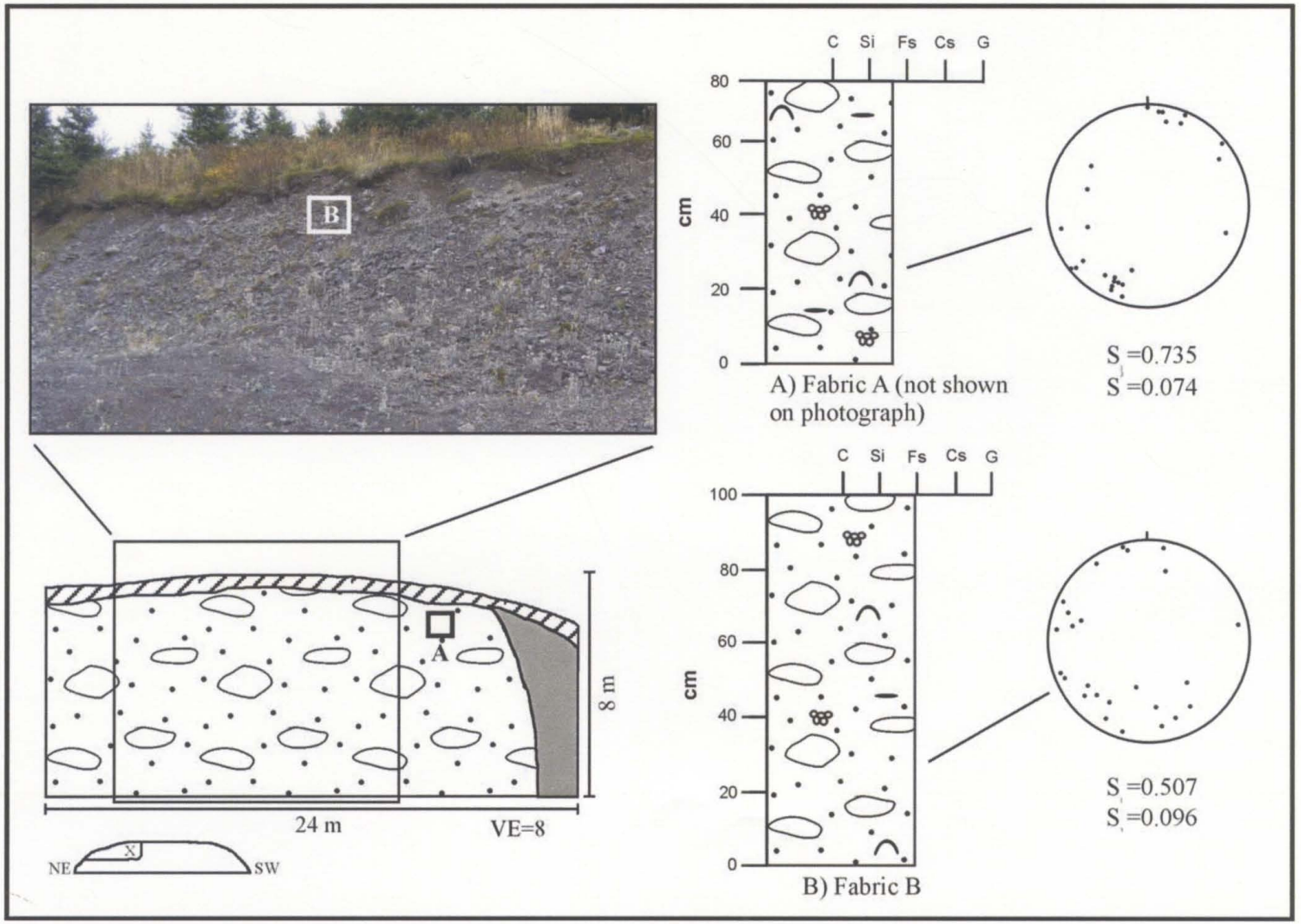

Figure C.20 Site 23 Exposure sketch, sedimentary logs and clast fabric diagrams.

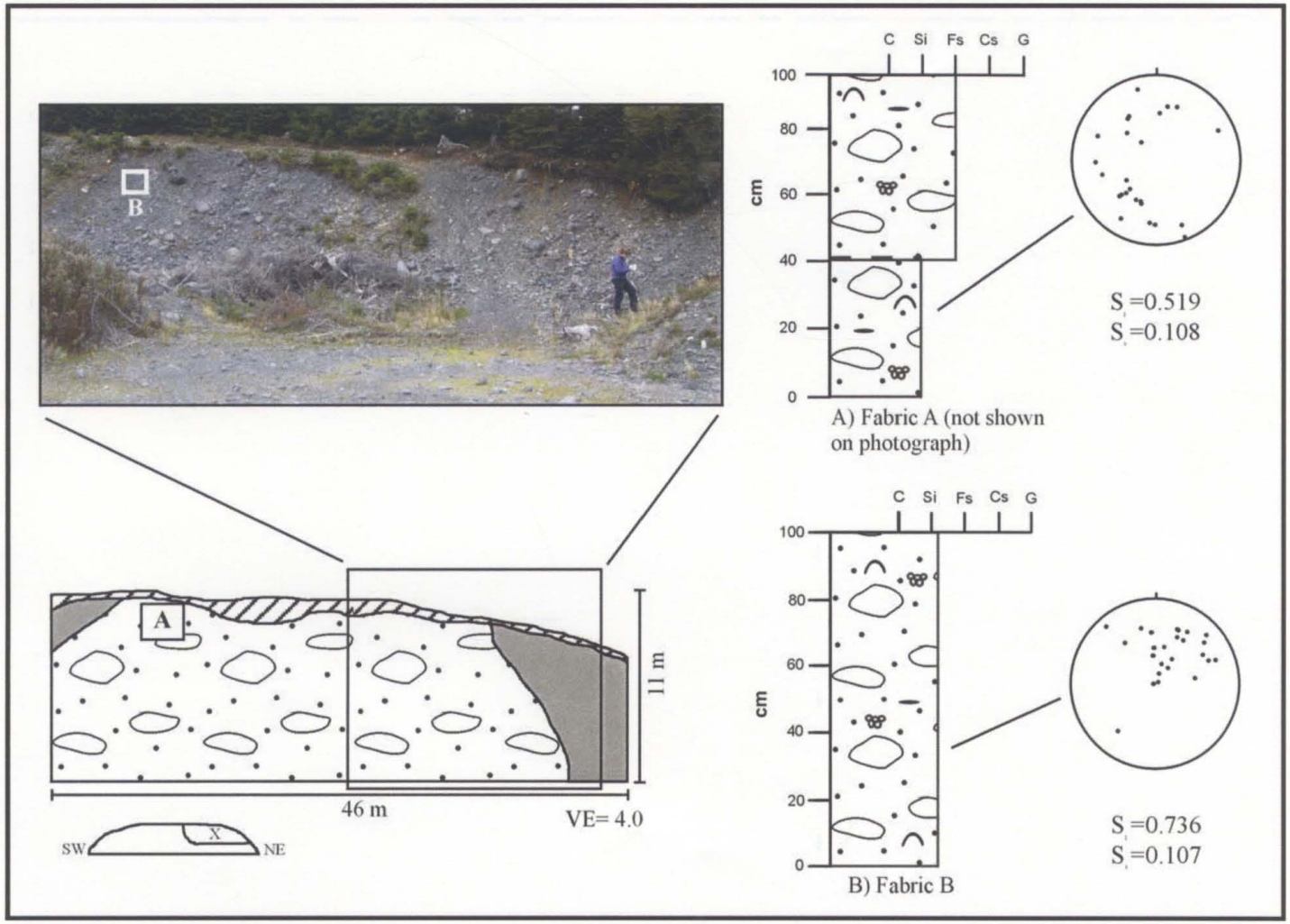

Figure C.21 Site 324Exposure sketch, sedimentary logs and clast fabric diagrams.

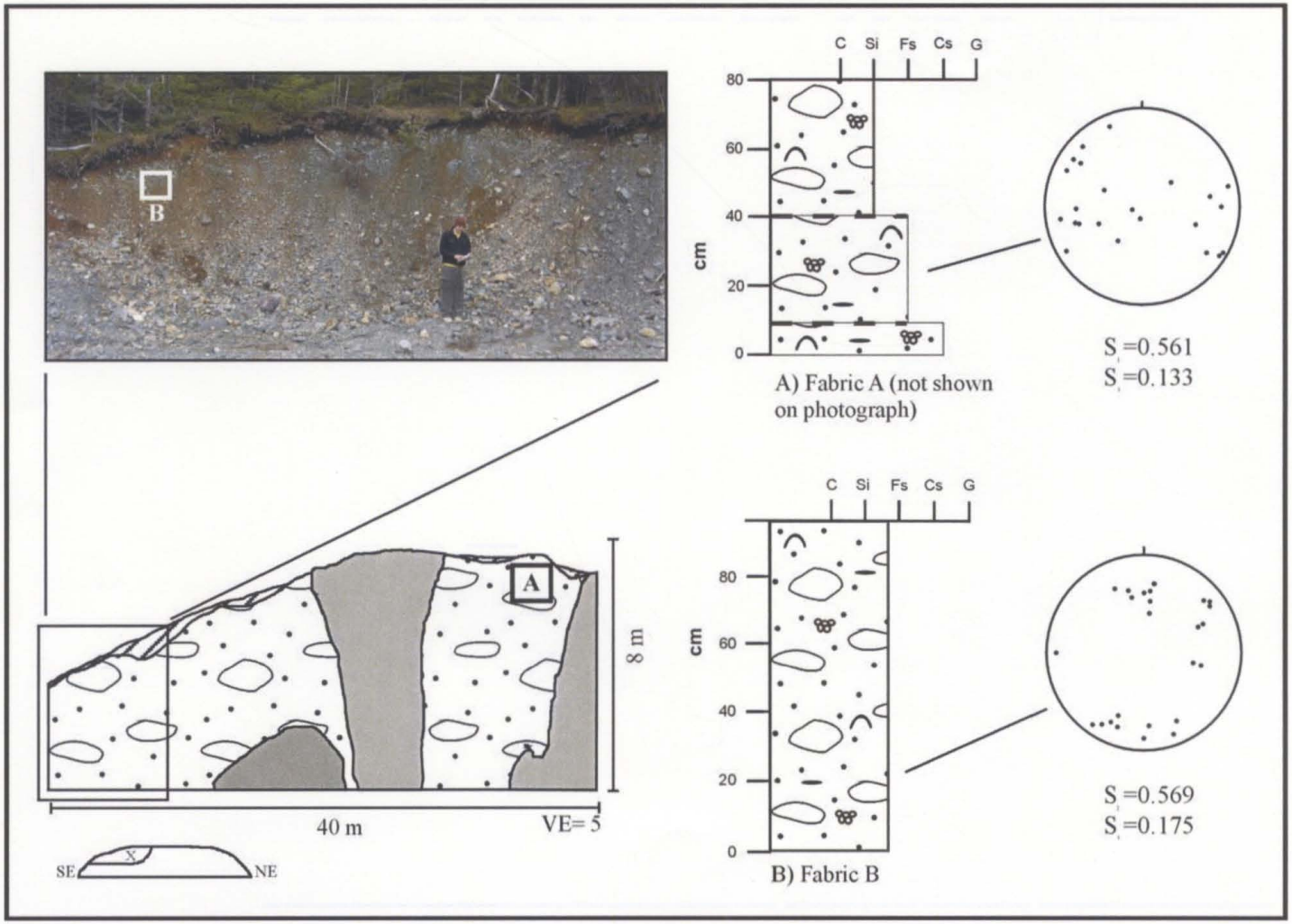

Figure C.22 Site 25 Exposure sketch, sedimentary logs and clast fabric diagrams.

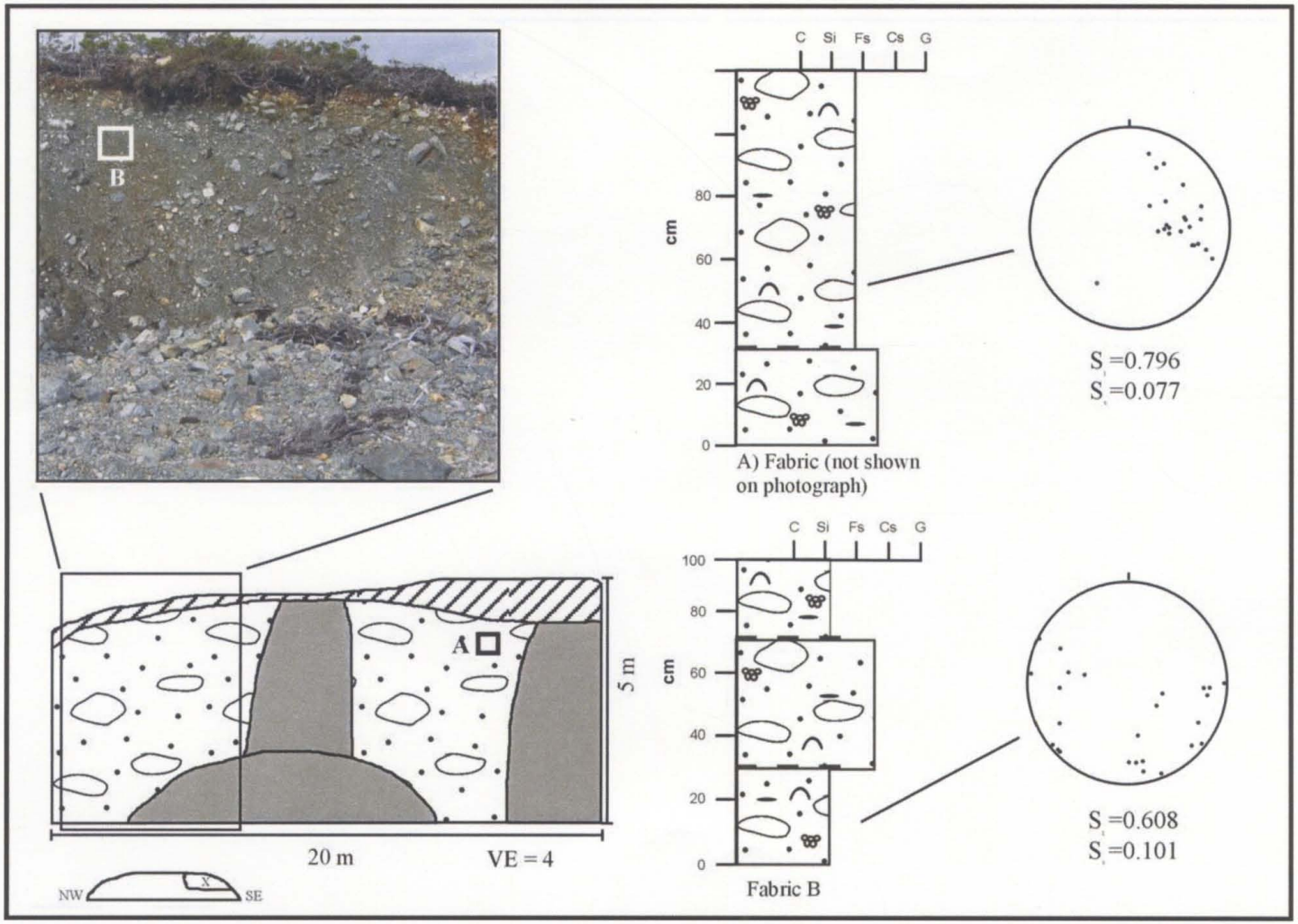

Figure C.23 Site 26 Exposure sketch, sedimentary logs and clast fabric diagrams.

Table D.1 Grain Size Analysis Results

Site #	Two Diamictons Observed	Upper or Lower Diamicton	Ridge or Hummock	% of Sample Weight (Φ Grain Size) (4 mm) -2.0	(2 mm) -1.0	(1 mm) 0.0	(0.5 mm) 1.0	(0.25 mm) 2.0	(0.125 mm) 3.0	(0.063 mm) 4.0	4.0100	Total
Site 1 matrix sample	N	U		20.8	10.7	8.4	8.1	0.0	15.5	8.9	28.3	99.9
Site 4 Exp A Fab A	Y	U	H	28.0	15.7	14.4	12.6	1.5	12.5	3.2	12.4	99.9
Site 4 Exp A Fab B	Y	L	H	16.9	18.1	16.2	15.3	5.4	10.7	3.6	13.8	99.8
Site 6 Fab B	N	L	H	22.7	11.3	10.1	9.4	7.5	5.9	4.3	28.8	99.8
Site 9 Sediment	Y	U	R	8.3	12.4	14.7	17.1	4.3	19.1	6.4	35.7	100.1
Site 10 Sediment	Y	U	R	22.6	13.4	14.2	12.9	0.0	14.4	3.2	20.1	100.5
Site 12	N	L	H	18.4	10.9	13.4	13.8	10.5	8.2	7.2	18.9	100.3
Site 12 Fab B	N	L	H	20.8	13.0	12.8	12.6	0.0	14.8	5.8	19.7	99.8
Site 12 Up	N	U	H	33.2	13.6	10.4	8.7	0.3	11.2	4.5	19.1	100.1
Site 12 Lower	N	L	H	15.9	11.4	10.5	10.0	7.6	8.2	7.4	29.5	99.8
Site 13 Fabric A Upper	Y	U	R	32.4	16.5	13.7	9.7	7.1	5.3	3.8	13.6	100.3
Site 13 Fabric A Lower	Y	L	R	26.6	10.2	8.1	8.5	7.9	6.6	4.6	27.5	99.8
Site 14 Upper	Y	U	R	28.4	11.2	9.8	9.1	2.9	10.0	4.9	24.2	99.8
Site 14 Lower	Y	L	R	5.8	12.8	17.7	18.7	0.9	19.5	5.5	20.0	100.2
Site 16 Fab A	Y	U	R	13.1	16.6	15.6	13.7	5.1	9.4	5.0	22.8	80.0
Site 16 Fab B	Y	L	R	12.1	8.0	8.2	8.7	4.1	10.7	7.6	41.6	100.4
Site 18 Fab A	N	U	H	17.0	12.1	11.0	10.2	0.8	14.4	5.2	29.8	99.7
Site 18 Fab B	N	L	H	25.0	11.9	10.8	10.6	8.8	6.9	5.4	21.4	99.3
Site 18 Fab B	N	L	H	18.4	13.3	12.0	11.7	8.7	8.4	5.2	22.6	99.2
Site 19 Fab A	N	L	R	14.0	12.8	11.8	11.3	4.1	12.1	7.1	27.0	99.4
Site 19 Fab B	N	U	R	40.6	17.0	9.6	7.1	2.5	5.3	3.2	13.8	98.6
Site 20 Fab B	Y	U	H	27.9	11.0	9.8	11.1	9.8	8.3	7.1	15.0	99.3

Table D.1 cont'd Grain Size Analysis Results

Site #	Two Diamictons Observed	Upper or Lower Diamicton	Ridge or Hummock	% of Sample Weight (Φ Grain Size)								
				(4 mm) **-2.0**	(2 mm) **-1.0**	(1 mm) **0.0**	(0.5 mm) **1.0**	(0.25 mm) **2.0**	(0.125 mm) **3.0**	(0.063 mm) **4.0**	**4.0100**	**Total**
Site 20 Fab A	Y	U	H	15.4	9.5	10.5	9.2	0.6	14.3	8.2	35.4	100.9
Site 21 Fab B	N	U	H	26.3	9.7	6.8	5.7	2.3	6.9	7.3	36.1	100.5
Site 21 Fab A	N	L	H	12.8	6.5	6.4	6.1	0.6	11.5	10.9	46.0	99.7
Site 23 Fab A	N	U	H	15.8	15.6	14.0	12.8	8.8	9.5	5.6	19.0	100.0
Site 23 Fab B	N	U	H	38.1	9.3	7.6	7.3	6.0	5.6	4.1	22.4	99.9
Site 24 Fab A	N	U	R	29.8	17.5	13.3	10.3	7.0	5.4	3.8	14.0	100.8
Site 24 Fab B	N	L	R	20.0	12.1	11.2	11.5	1.4	15.8	5.4	22.2	99.3
Site 25 Fab A	N	U	R	22.8	14.8	13.9	12.0	3.9	11.6	4.9	16.8	100.2
Site 25 Fab A	N	L	R	35.8	15.5	12.1	100.4	6.7	6.2	3.2	10.7	100.4
Site 25 Fab B	N	L	R	34.5	14.2	11.6	10.6	8.3	5.6	3.4	11.6	99.7
Site 26 Fab B	N	U	H	33.0	13.5	11.1	8.4	6.2	4.8	3.5	18.7	99.1

Appendix E Grain size distribution

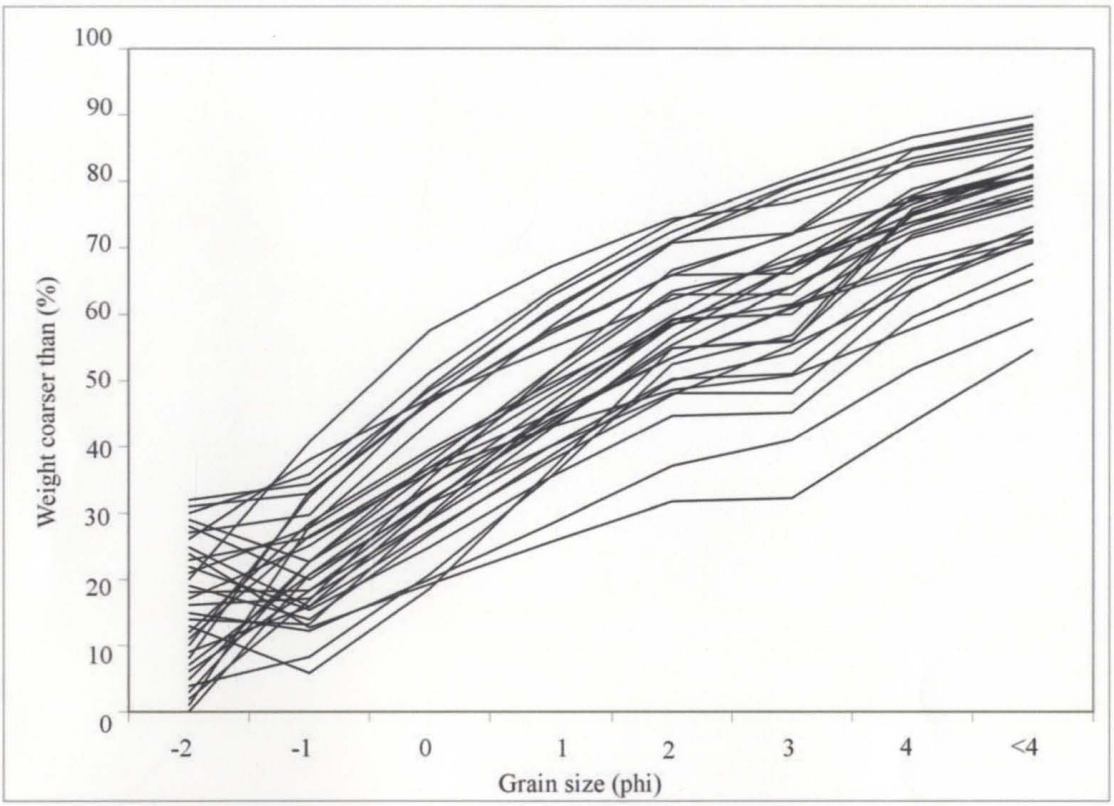

Figure E.10 Grain size distribution of diamicton matrix samples

Appendix F Comparison of example clast fabric plots

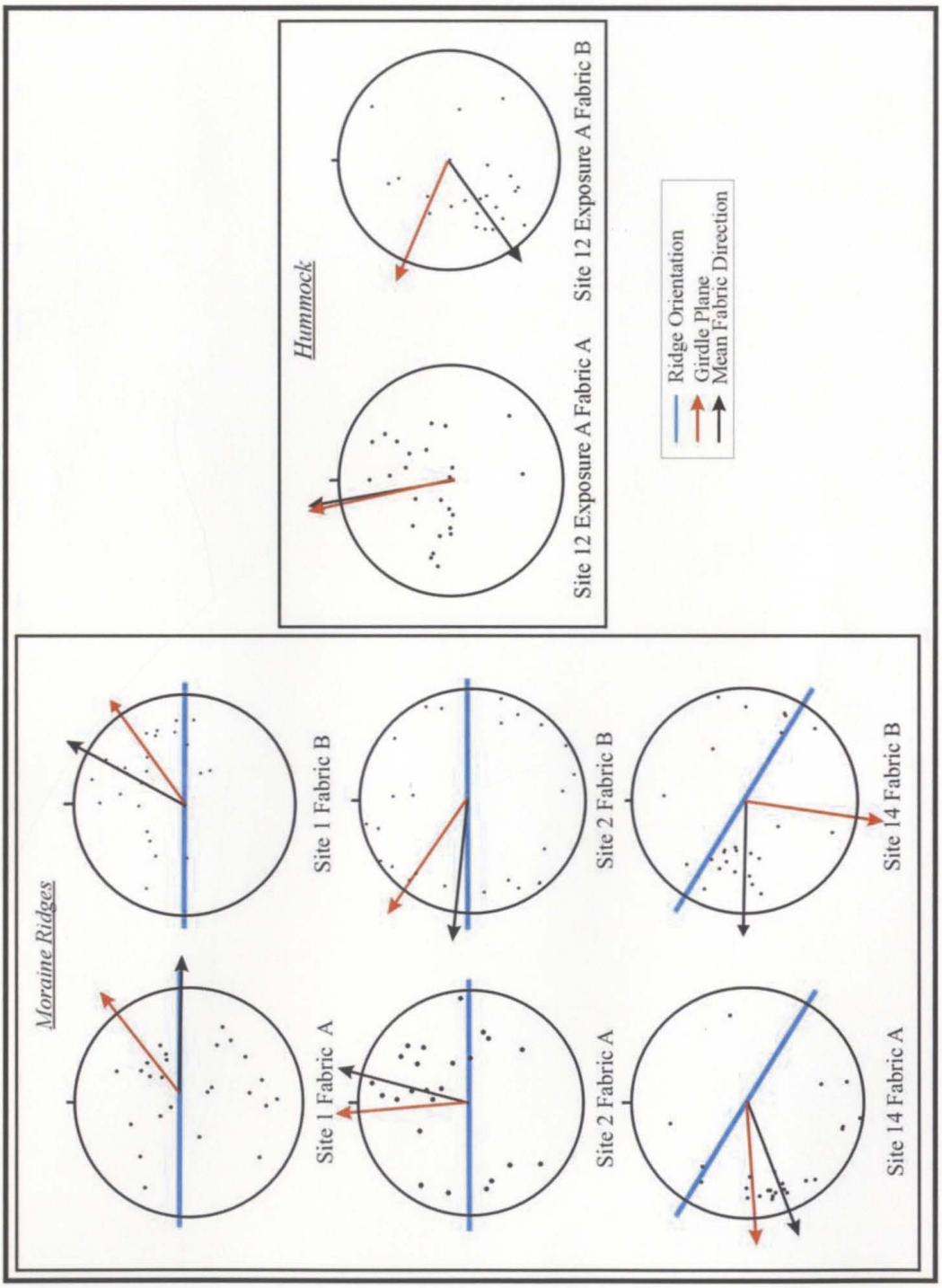

Figure F.1. Clast fabric plots showing the variation in clast fabric shape within a single site, and between several sites

Appendix G: Ridge crest orientations, girdle plane, and cluster orientations

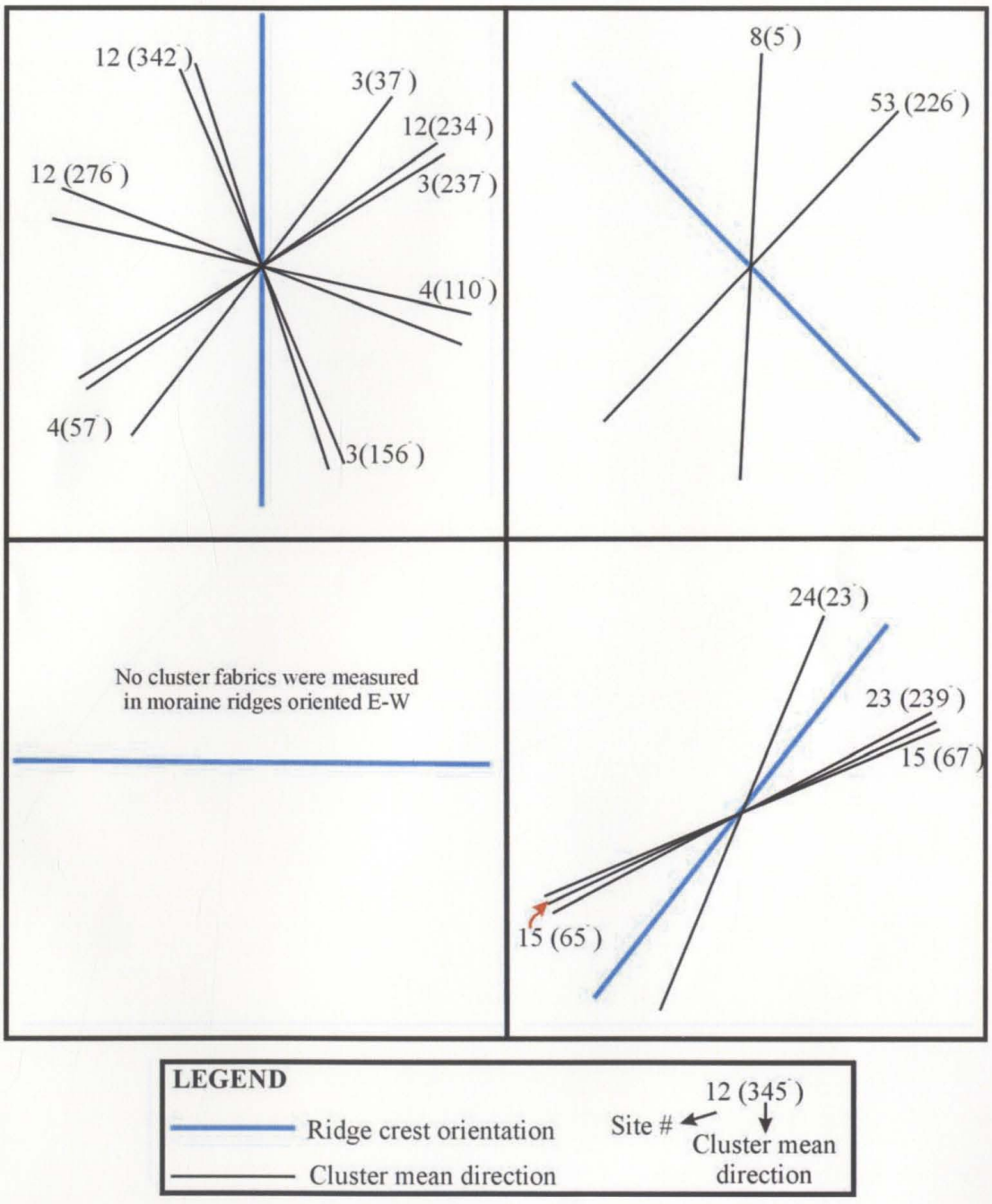

Figure G.1. Cluster mean directions and moraine ridge crest orientations. Cluster mean directions are predominantly oblique to ridge crest orientations.

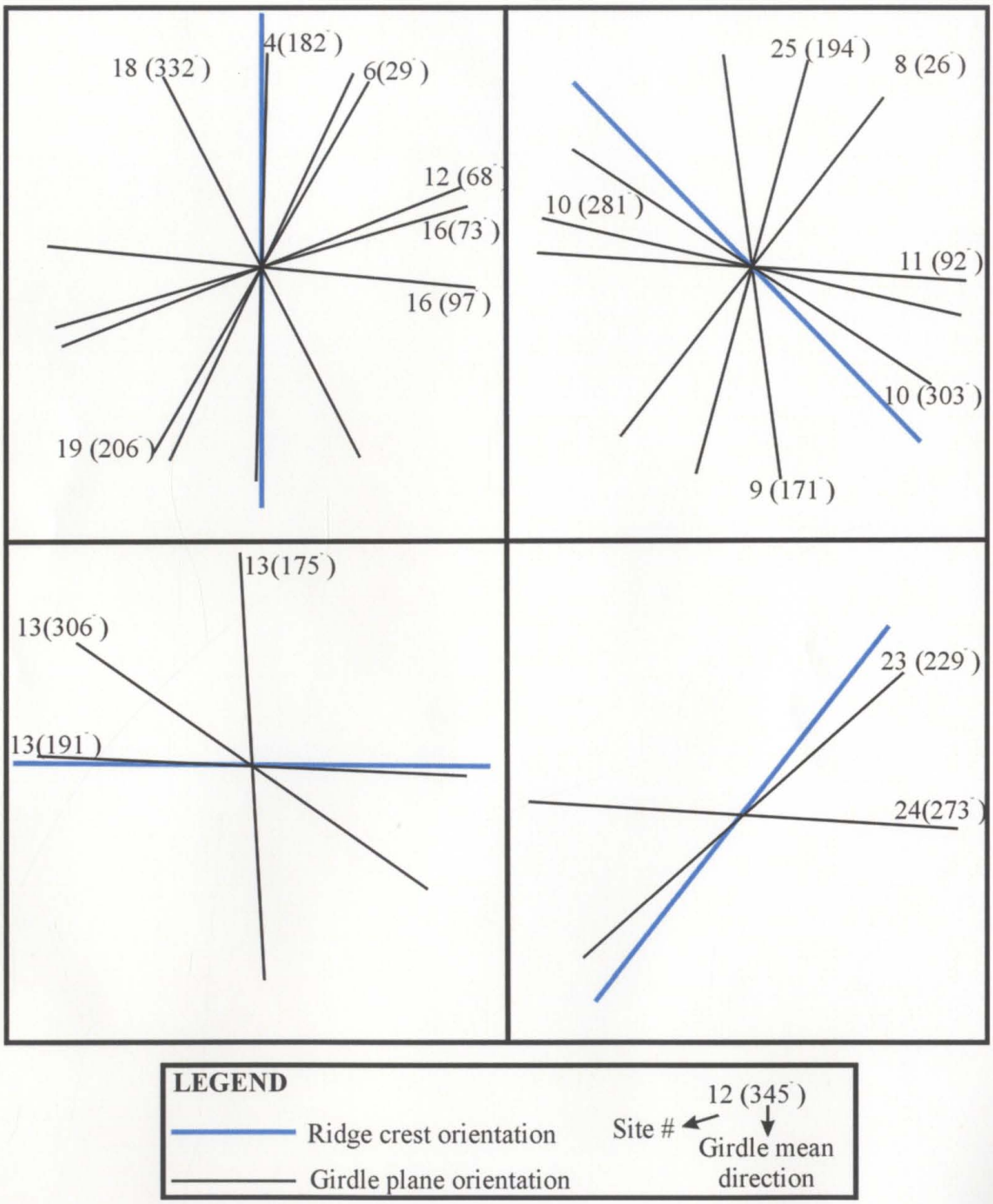

Figure G.2 Girdle plane orientation and moraine ridge crest orientation. Girdle plane orientations are predominantly oblique to ridge crest orientations.

Site #	S_1	K	C	Orientation (Degrees)	Orientation of Nearby Striations (Degrees)
14	0.652	2.7	1.55	273	22
15	0.738	2.19	2.12	11	
15	0.701	1.4	2.07	157	
12	0.616	1.72	1.47	342	40, 20, 322
12	0.675	2.64	1.68	234	
7	0.922	2.34	3.9	58	52
8	0.708	2.91	1.84	5	
26	0.796	3.58	2.34	81	
1	0.649	1.18	1.81	36	30, 27, 37, 356, 54, 10, 32, 30, 33

Table H.1 Comparisons of clast fabric orientations to nearby striations.

Appendix I Comparison of clast fabric and striation orientations

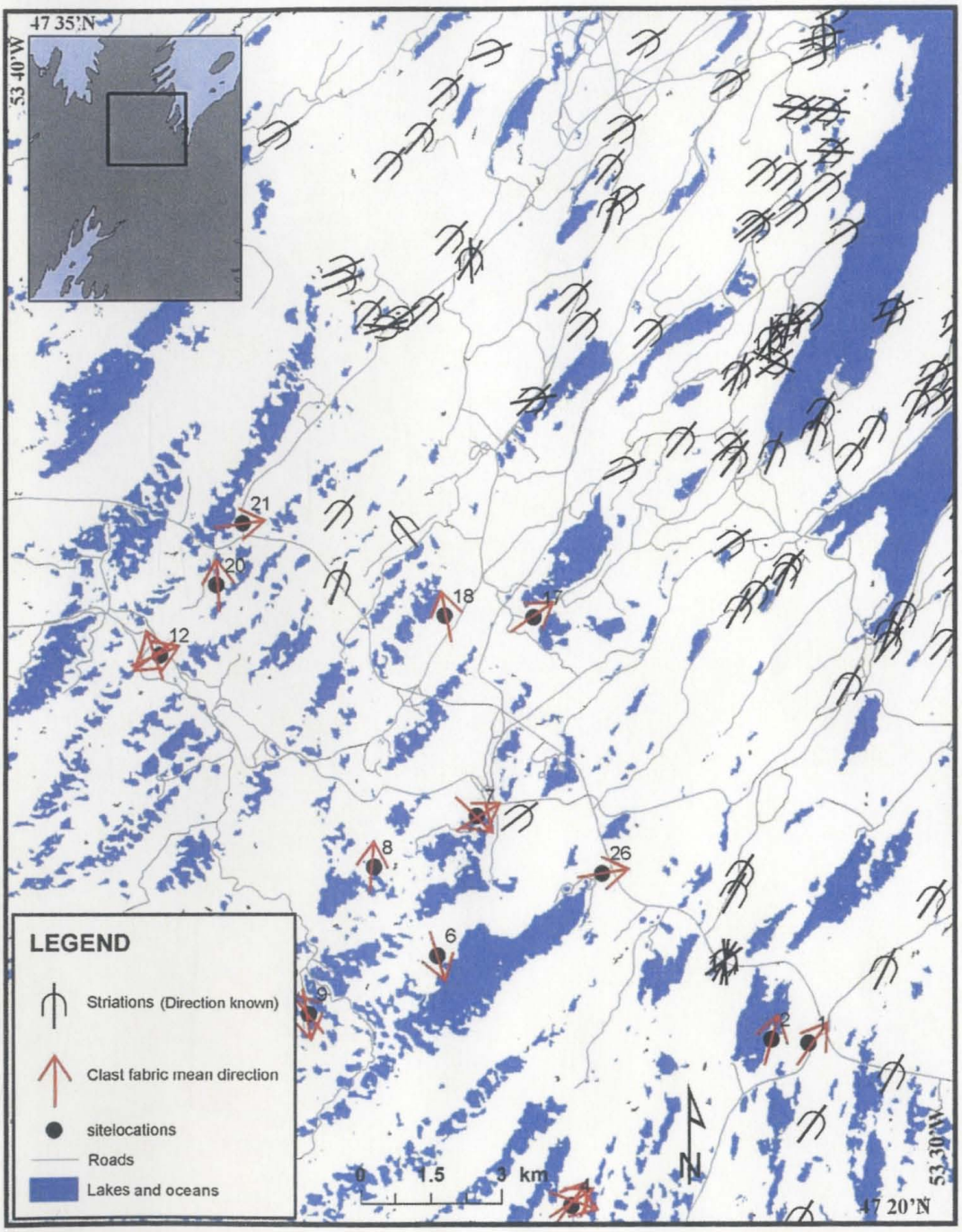

Appendix I.1 Exposure sites, clast fabric orientations, and striations. Striation data was acquired from the Newfoundland and Labrador Geological Survey.